# MAE 321 Wing Project
# Final Design Report

Wilson Moyer, Ella Simmons, Matthew McWeeney, Andrew Oliver, Joel Boon,
Timothy Seiferth, Ted McCormack

ABSTRACT

The objective of this project was to design, optimize, and manufacture a wing that can withstand a shear force of 97 lbs, 22 inches from the center of rotation. It was crucial the wing was both as light and as strong as possible, with additional points being assigned for relative mass and strength. To meet this objective, a design was chosen and manufactured. For each component, stress, buckling, and/or modal analysis were performed, in order to understand the strength and failure modes of specific geometries and configurations. Von Mises and buckling criteria were used as evaluation metrics. I-beam optimizations were centered around the truss design, corner fillets, and flange geometry. Bulkhead quantity and design were investigated, with the primary goal of reducing weight without losing preformation, and rivet placement and skin geometry were refined to minimize stress concentrations in the skin. In combination, these analyses showed that an I-Beam with holes and a rounded and thickened flange, ten bulkheads, and 1.25 rivets per inch, with more on the starting and ending bulkheads, is the most optimized wing design of the options analyzed. Once a design was finalized, the wing was manufactured using the shop tools and machines. The I-beam was cut with the CNC Mill, which was able to manufacture the unique and complex internal geometries. The end bulkheads were manufactured with the waterjet, while the rest were 3d printed, and the skin was cut using a band saw. Once all the individual pieces were machined, the wing was assembled using rivets. The final product, weighing in at 1 lb 11 oz., was then tested using the testing jig set up by Al and Glenn. The wing held the initial 97lbs, with 3 inches of deflection. More weight was placed on until the wing deflected 14.75” at 390 lbs.

*Prepared for Glenn Northey and Al Gaillard*
May 9, 2025

TABLE OF CONTENTS

I. Introduction..... 3
II. Background..... 4
III. Design Theoretical Analysis..... 5
A. I-Beam..... 6
B. Bulkheads..... 7
C. Skin..... 7
D. Rivets..... 8
IV. Material Selection and Bill of Materials..... 8
A. Bulkheads..... 8
B. Skin..... 10
C. Beam..... 10
D. Bill of Materials..... 10
V. Procedure..... 11
A. I-Beam..... 11
B. Bulkheads..... 12
C. Skin..... 12
D. Rivets..... 14
VI. Results and Discussion..... 15
A. I-Beam..... 15
B. Bulkheads..... 17
C. Skin..... 19
D. Rivets..... 20
VII. Conclusion..... 22
VIII. Appendix..... 26

# I. Introduction

The objective of this project was to design, optimize and construct a wing that is able to support 97 pounds without critical failure. The wing was required to have a surface area between 98 and 102 sq inches on the bottom of the wing and a length of 22 inches. Additional points were awarded for relative deflection and weight, as compared to the other group's wings. The wing is composed of four main elements: skin, beam, rivets, and bulkheads. The beam forms the core of the wing and is manufactured from aluminum. Per requirements, the beam is designed such that it extends 1.5 inches past the end of the wing, with a horizontal 3/16" hole exactly 23 inches from the securing end. Additionally, the beam must extend 2" from the securing end of the beam, with a ¾" solid square section. In this square section, a ¼" hole vertical drill is offset 1" from bulkhead one. These design specifications for the beam were mandated. Bulkheads are attached to the beam at regular intervals and are constructed in the geometry of the supplied airfoil, with the allowed materials limited to aluminum, 3d printed PLA or Nylon. Skin is wrapped around the bulkheads, attached by rivets. As dictated by the specifications, special attention was paid to workmanship.

In order to meet these constraints, Creo Parametric 11.0 was implemented to design within specification, and then optimize the remaining parameters to ensure the final product was both as strong and as light as possible. Each part of the wing was specifically analyzed, using stress, sensitivity, and modal simulation, which revealed the locations of failure and stress. The design for each component was then iterated, and the simulation was re-run.

After evaluating multiple designs, based on the analysis conducted, several designs emerged as the most efficient for our criteria. The holes were found to be effective, and decreasing distance from the holes to the edge proved to be an efficient use of material. Round and thickened flanges outperformed sharp, thin flanges. Bulkheads appeared to have little effect on the strength of the wing overall, but did have a significant effect on the location of buckling, allowing some control over the failure location. The most optimal layout of rivets, after analysis, was concluded to be 1.25 rivets per inch on the bulkheads, with most on the starting and ending bulkheads.

Manufacturing the parts involved a number of tools in the machine shop. The I-beam was cut using manual milling machines and CNC milling machines: the manual milling machines were used to provide places to hold the I-Beam during CNC manufacturing, and then the CNC mill was used to cut the complicated truss work into the beam. Bulkheads were made using both the waterjet and the 3d printer. The waterjet was used to cut the two end bulkheads out of aluminum, and the rest were made on a 3d printer. The 3d printer was able to make holes for the rivets, but since the waterjet is a 2d cutter, it was not, and the end bulkheads had to be drilled manually as

well. The skin was bent and rivet holes were manually drilled. Finally, everything was assembled, with rivets holding the pieces together.

Once everything was assembled, the wing was tested on the jig set up by Al and Glenn. The jig allowed a variable amount of weight to be placed on the wing, which started at 65 lbs. The wing was tested at 65, 97.5, 130, 195, 260, 325, and 390 pounds.

## II. Background

Since there are complex dynamics involved in the static wing system, an established understanding of several mechanical engineering concepts is key. All optimizations done involved stress, strain, deformation, and buckling. Stress is a measure of force over the area of a cross section. There are two types of stress: tensile stress (σ) and shear stress (τ). Tensile stress is calculated using the component of force normal to the surface, while shear stress is calculated using the component of force perpendicular to the surface. Strain (ε), is a non-dimensional number representing the deformation of a solid due to stress. Like stress, it can be either tensile or shear depending on the component of force used to calculate it. Stress and strain can be related using the following equation: $\varepsilon = \sigma/E$ , where E is Young's Modulus, or the Modulus of Elasticity. Young's modulus is a material specific measure of elasticity and can be found using a table or a graph. Often, the stress and strain relationship will be plotted for a given material. See image below:

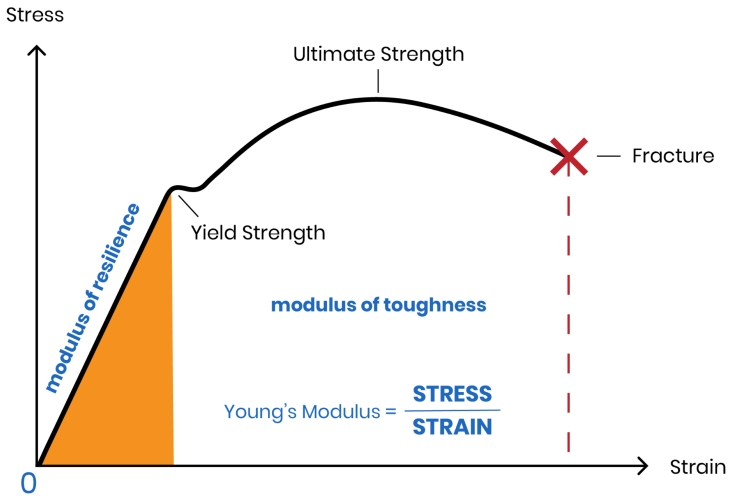


As the graph represents, the stress-strain relationship, as described by Young's Modulus remains constant until a material hits its Yield strength, after which any deformation is permanent. This

area of the graph is nonlinear, until eventually the material reaches its maximum strain possible and fractures. This is a prominent type of failure, and thus, was vital in the optimizations and simulations conducted. In order to determine this point of failure, a "yield condition" is necessary. Creo Parametric offers a number of possibilities when conducting analysis. The one selected for this project is the "von Mises" yield criteria. The software calculates von Mises stress from the principal stresses as compared to the material's yield strength. This yields the scalar "von Mises" strength.

Another important type of failure is buckling. Buckling occurs in beams with a small cross-sectional area compared to their length that are subject to tensile stress. Buckling is characterized by the equation $P_{cr} = \frac{\pi^2 EI}{L^2}$, where E is the Young's modulus, as discussed above, I is the second moment of the area, L is the effective length, and $P_{cr}$ is the critical buckling load. Critical buckling load is defined as the applied force at which any small disruption can cause the column to buckle. Buckling can be prevented by increasing the moment of inertia, which is mainly how we plan to mitigate the risk of buckling.

The next step is manufacturing, which includes concepts such as CNC machining and 3d printing. CNC machining is a type of machining where the tooling is designed and run by a machine. Creo Parametric 11.0 has a manufacturing program we will utilize to automatically generate the toolpaths. Creo writes the tooling in G-Code, which is a type of code the machine can easily convert into tooling. The milling machine used in the lab is Haas brand and has easy automatic conversion between G-Code and tooling, allowing precise and complex geometries to be machined that would take both a lot of time and skill if done by hand. The CNC mill used for this project is 3-axis, meaning it is able to move in all three cartesian directions.

3D Printing will additionally be used in manufacturing our wing design. Fused Deposition Modeling (FDM) is the most common and affordable type of 3d printing currently on the market. FDM uses layer-by-layer extrusion of hot plastic to build 3d geometries, often which are impossible to achieve with subtractive manufacturing.

## III. Design Theoretical Analysis

As there are multiple parts to design, design, optimization, and analysis was split up by wing elements: I-Beam, Bulkheads, Skin, and Rivets. A discussion of the process for each part is as follows below. After conducting an analysis of each component, a final design was formulated using an amalgamation of each component, after thorough discussion amongst the team. These findings are in the conclusion, under next steps.

## A. I-Beam

### Truss

Upon an initial overview of the stress distribution for the deformed beam, it was evident that the web of the beam has much lower stresses than the flange of the beam (see figure III.A.1). In general, the stress for an object undergoing bending increases linearly from the neutral axis. Therefore, the team of Wilson and Ella set out to investigate how to utilize this low stress in the web of the beam in order to reduce the total beam mass.

The method that we settled upon for removing beam material was cutting trusses into the beam. We focused primarily on the Pratt truss. See figure III.A.2 (source: teachengineering.org) for the differences in the truss type.

The Pratt truss is an appealing option because the diagonal beams in the truss are under tension, while the vertical beams are under compression. This configuration is effective because the vertical beams are shorter than the diagonal beams, and therefore are less likely to buckle due to compression.

We also investigated round holes. Round holes have the advantage of avoiding the stress concentration that trusses have at their corners, although round holes also can have stress concentrations at their tops and bottoms. Round holes also have the advantage of being easier to manufacture.

In order to design and build the trusses themselves, we parameterized characteristic dimensions of the trusses and ran sensitivity tests with these parameters in order to find truss geometries which balanced minimizing stress and mass. This process is covered in more detail in the procedure section.

### Geometry

The corners in the web of the I-beam were rounded instead of left sharp. This was decided based on the well-established principle that sharp internal corners produce stress concentrations, which can significantly increase the likelihood of cracks forming or failure due to fatigue. Rounded corners more gradually and evenly distribute stress, reducing localized stress peaks and improving the overall strength of the beam. Figures III.A.3 and III.A.4 show the stress distributions in a non-rounded and rounded beam, respectively, and despite one beam being trussed and one not, the rounded beam displays less stress where the flange and web meet. The round radius was parameterized, and sensitivity tests were run to narrow down a final radius.

The flanges of the beam experienced more stress than the web (see Figure III.A.1), so it was decided that they should be thickened.

**Material selection**

For the beam material, we selected Aluminum 7075. Aluminum 7075 has a relatively high yield stress of 60 ksi and a low density of 0.1 lbms/in$^3$. For selecting this material, we collaborated with Glenn Northey to learn what had worked in past wing projects. Furthermore, we did research on McMaster-Carr to determine which materials would be optimal for our use based on the criteria of yield strength and density.

## B. Bulkheads

When thinking about the design of the bulkheads in the wing, there were two main questions: how many to have and how strong to make them. These questions were answered based on analyses done to determine the importance of the bulkheads to the structural integrity of the wing as a whole. First, static analyses were conducted on the wing to assess the amount of stress placed on the bulkheads. Since the load that the wing will experience is quite simple (only a downwards force placed on the end of the wing), the static analyses were quite simple. The analyses were conducted with varying numbers of bulkheads as well as varying bulkhead strength. Then, buckling analyses were conducted to determine the effect that the bulkheads have on the buckling of the skin on the wing. As with the static analyses, they were conducted with varying numbers of bulkheads and bulkheads of varying strength.

After the analyses were completed and the results were analyzed, the number and strength of the bulkheads was decided. This included the material that would be used for the majority of the bulkheads. It is of note that the two end bulkheads were predetermined to be made of solid aluminum due to mounting and other test constraints.  It was determined that there should be nine equally spaced bulkheads with a tenth fit in between the second and third bulkheads. It was also determined that the middle eight bulkheads would be made of 3D printed PLA and have sizable holes in the section of the bulkheads near the trailing edge of the wing.

## C. Skin

The design of the skin of our wing involves 4 main components: the material, the thickness, and how these vary across the entire surface area of the wing, and creating a separate leading edge. An important aspect of this wing is that the skin, being as thin as it is, does very little to support the load (as compared to the central I-beam and first and last bulkheads). Moreover, the top piece of skin will contribute the most, as the bottom piece will buckle quickly under compression. Considering these variables, before doing any stress tests or CAD, we determined that the bottom piece of skin should be strong enough to not snap when buckling, with little care for load bearing capacity. So, in general, it should be much thinner and softer than the top piece.

After some research, we decided that 2024 aluminum, a common alloy used in aerospace applications, would be a wise choice for the top piece due to its high strength to weight ratio

(yield strength of 41 ksi, density of 0.100 lb/in^3). The bottom piece, given its lack of importance, would be a weaker, cheaper material. We chose 6061 because it is softer, weaker, and cheaper in comparison.

The next step was to perform stress tests. This revealed that tensile stress was concentrated in the center of the top piece of skin, and closer to the base of the wing. The idea of possibly using thicker skin for the first 6-8 inches of the wing was considered, but this plan was abandoned due to technical complexity and uncertain benefit. The available (and reasonable) thicknesses of 2024 sheet metal on McMaster Carr were 0.020, 0.025, 0.032, and 0.040 inches. To pick exactly which thickness, a number of discrete stress and buckle analyses were performed. In the end, we decided on 0.032 inches for the top piece, and 0.025 for the bottom.

Finally, we decided that the leading edge of the wing should be 3D-printed with PLA and riveted onto the bulkheads. This was because it would reduce weight in an area of the wing that experiences minimal stresses. It follows the original profile of the wing shape with a thickness of 0.13 to 0.08 inches (decreases linearly along the length of the wing). It is in 3 pieces so that the material can shift as the wing bends instead of snapping (as PLA is very brittle).

### D. Rivets

To simulate the conditions for rivet failure in the wing skin, we modeled the attachment point of the skin to the bulkhead as the overlap of two 5”x5” sheets 0.030” thick (Figure . To find a load approximating material failure in the skin, we treat the two plates as bonded and apply a load sufficient to induce failure beyond a safety margin. Keeping this load constant, we then apply the same stress while simulating plate attachment via rivets, allowing us to simulate the stress concentrations due to the rivets as well as the stresses within the rivets themselves.

To fully explore the design space, we considered two key parameters affecting stress concentrations within the plate. The distance between the rivet holes and the edge of the plate and the center-to-center distance between the rivets were the two most important parameters to consider. By varying both of these values independently, we could infer how these parameters altered stress in the skin.

## IV. Material Selection and Bill of Materials

### A. Bulkheads

For the bulkheads, we were choosing mainly between PLA and PETG materials, both from Bambu brand. Since the bulkheads experience very little stress compared to the rest of the wing,

the main focus for the bulkheads was reducing weight while not compromising the strength (which would be hard to do with so little strain). When choosing between PLA and PETG, we looked at the specs for both materials.

PLA:

| Physical Properties | | Mechanical Properties | |
|---|---|---|---|
| Density | 1.24 g/cm³ | Tensile Strength | 35 ± 4 MPa |
| Vicat Softening Temperature | 57 °C | Breaking Elongation Rate | 12.2 ± 1.8 % |
| Heat Deflection Temperature | 57 °C | Bending Modulus | 2750 ± 160 MPa |
| Melting Temperature | 160 °C | Bending Strength | 76 ± 5 MPa |
| Melt Index | 42.4 ± 3.5 g/10 min | Impact Strength | 26.6 ± 2.8 kJ/m² |

PETG:

| Physical Properties | | Mechanical Properties | |
|---|---|---|---|
| Density | 1.28 g/cm³ | Tensile Strength | 34 ± 4 MPa |
| Vicat Softening Temperature | 70 °C | Breaking Elongation Rate | 8.6 ± 1.2 % |
| Heat Deflection Temperature | 69 °C | Bending Modulus | 2050 ± 120 MPa |
| Melting Temperature | 214 °C | Bending Strength | 64 ± 3 MPa |
| Melt Index | 28.2 ± 2.7 g/10 min | Impact Strength | 31.5 ± 2.2 kJ/m² |

As seen here, the density is slightly higher in the PETG than the PLA, which means it would be slightly heavier for our model (although not by much). However, the PLA also has a slightly higher tensile strength, which could help with the small strains that the bulkheads do experience, especially where the rivets might be pulled. Finally, the PLA has a much higher bending modulus, which is not as great because our wing could bend more, but in this case may actually be preferred, since the wing will also potentially carry more weight with more deflection before it fails.

Also, for the first and last bulkheads, we needed to order 6061 aluminum in order to fasten the wing to the support and to hold the weight bearing beam at the end. For this, we used the size of our first and last bulkhead. Our first bulkhead is 6” long, 1.08” tall, and ¾” thick. Our second bulkhead is 2.9” long, and smaller in both height and thickness. For this, we will be able to get the smallest piece of 6061 aluminum that is at least large enough for both pieces. We needed it to be ¾” thick and at least 1.08” tall, so we chose the 0.75”x 1.25”x 6” bar. For this, we can cut both bulkheads from the same piece.

## B. Skin

Due to the skin being thin sheet metal, maximum load-bearing capacity was not as important as optimizing the design for minimum weight, while still meeting some bare standards. We focused on reinforcing the places where the most stress exists, while cutting weight everywhere else. We chose 0.032 inch 2024 aluminum for the top piece. It has a yield strength of 41 ksi, a hardness of Brinell 120, and a density of 0.100 lb/in^3. This alloy is commonly used in aerospace applications because of its strength and lightweight nature. Next, we chose 0.025 inch 6061 aluminum for the bottom piece. It has a yield strength of 35 ksi, a hardness of Brinell 90, and a density of 0.0975 lb/in^3. This alloy is used generally in many applications. It is about 13% weaker than 2024 aluminum, but only about 3% lighter. This shows how efficient 2024 aluminum is in terms of strength to weight ratio. Going back to 6061, it is also a bit softer, which will allow it to bend easier under compressive load without snapping. There are weaker options, such as 3003, which bend even more without breaking (yield strength 16.5 ksi, hardness Brinell 25). However, while most of the force is felt by the top skin, some is felt by the bottom, and we do not want it to fail completely, or rip the rivets out. 16.5 ksi would be cutting it too close for the sake of malleability and reduced weight. Our precise reasoning for 0.032 and 0.025 inch thickness will be explained in more depth in later sections, involving multiple stress analyses.

## C. Beam

We knew that the beam was going to be supporting a majority of the weight, so it had to be made out of a strong material. Our options were 2024 aluminum, 6061 aluminum, and 7075 aluminum. We chose 7075 aluminum because it is easier to machine than the other alloys and has higher tensile and yield strengths.

## D. Bill of Materials

| Details | Subteam | Retailer | Qt. | Price |
|---|---|---|---|---|

| | | | | |
|---|---|---|---|---|
| Blind Pop Rivets | Rivets | Shop Spares | x20 | $0 |
| 0.032 2024 AL Sheet (12”x24”) | Skin | McMaster | x1 | $35.72 |
| 0.032 6061 AL Sheet (6”x24”) | Skin | McMaster | x2 | $12.95 |
| 0.75 6061 AL Rod (1.25”x 6”) | Bulkheads | McMaster | x1 | $8.64 |
| 1” 7075 AL Rod (1”x24”) | | Shop Spares | x1 | $83.50 |

# V. Procedure

## A. I-Beam

### Truss/Holes

The design of the truss was conducted with the goal of maximizing the ability to modify and conduct sensitivity studies upon different geometry configurations. In order to accomplish this, a single truss was first sketched in the plane that ran through the center point of both I-beam end cross-sections. After this sketch was completed and an extruded cut removed the material from the web, we applied a dimension pattern to the truss. The benefits of the dimension pattern is that other dimensions within the truss sketch can be set to be relative to the modified dimension in the pattern. This permitted, for example, the distance from the edge of the truss cut to the edge of the web to vary across the length of the I-beam. The greatest bending moment is on the fixed end of the truss. This typically corresponds with the greatest stress magnitude as well, however tapering the beam distributes this stress magnitude throughout the beam. Nonetheless, our group evaluated the fixed end of the beam to be a potential failure point, so we designed our dimensions such that the distance between the edge of the web and the truss cut to start large at the fixed end of the I-beam and decrease along the beam. We repeated the above steps with the hole configuration as well, and compared the results of the optimized beams in order to determine which would be ideal for final use.

Overall, we conducted sensitivity analyses on the number of truss/hole cuts, the minimum distance from the truss/hole to the edge of the flange, the truss angles (truss only), and the rate at which the distance between the edge of the web and the truss/hole cut varies along the length of the beam. We ran these tests sequentially, and applied the ideal result from each test to the subsequent tests. Our ideal is that the beam trusses are not the point of failure, so in general, we selected numbers for the parameters for which the change in number resulted in a small change

in stress. We ran these tests on the beam after first thickening the flanges and adding the rounds. The results for these analyses are discussed in the next section.

### Geometry

To decide on an appropriate radius for the rounds where the flanges meet the web, a copy was made of the most recent trussed beam, and a round of arbitrary radius was added to each edge where the web met a flange. A multi-pass adaptive sensitivity test was performed on the radius of the rounds, the results of which are discussed in the next section.

The flanges were thickened by editing the dimensions of Section 1 and Section 2 of the swept blend that created the beam.

For manufacturing the beam, we began with a 24” long piece of 1” by 1” square 7075 aluminum rod. With the finished I-beam (steps for finished parameters outlined in the next section), we generated a toolpath for the CNC machine to run. Because the beam is tapered, we needed to use a fixture of fasteners supporting the I-beam to the CNC base rather than clamping it. We drilled and counterbore holes in the aluminum rod to place the fasteners. In order to prevent the CNC machine from destroying an end mill by hitting a fastener, we added a volume in the toolpath for the CNC machine to miss. We also added a volume on the end of the I-beam for the CNC machine not to cut out for the fixture of the wing to the testing mount. This volume is not reflected in the engineering drawing *figure VI.A.22* but was necessary to properly test the wing. After completing the toolpath and running the CNC operation, we did some post-processing on the beam, including drilling holes for rivets to connect the bulkheads to the I-beam and deburring the edges of the beam.

## B. Bulkheads

The two end bulkheads were made of solid aluminum and cut out using a water jet machine. The first bulkhead was also drilled and tapped according to the specifications. This involved three holes that were on a line and separated by 1” each. They were all 10-32 threaded holes. The eight middle bulkheads were 3D printed using PLA filament. At first, when printing there was not enough clearance in the center square hole of the bulkhead for the I-beam to fit through, so the bulkheads had to be re-printed with a slight bit of clearance in the holes for them to be able to fit onto the beam. The clearance was 0.075 inches on all sides of the square hole.

## C. Skin

### Analysis/Design

To determine the material and thickness for the skin, we first researched common aluminum alloys used in aerospace. We settled on 2024 for its strength, and 6061 for its slightly weaker, but also cheaper and lighter nature. Next, we considered how the top and bottom skin would react to the load at the tip of the wing. Through a bending analysis, shown in VI.C.2.5, we confirmed our suspicions that the top skin would not bend, while the bottom would. Knowing this, we knew that the top skin would need to carry much more load than the bottom, so it would make sense to place a stronger, thicker piece of sheet metal on the top. Next, we first performed some preliminary stress tests in Creo to see where and at what magnitude the stresses would be in the wing skin. VI.C.1 and VI.C.2 demonstrate how the stresses reduce as skin thickness increases. We saw that even with 0.025 skin thickness, the skin was not even close to its yield strength. Wanting a reasonable margin of safety, we settled on 0.032 inches 2024 for the top (ensuring the skin would never break), and 0.025 inches 6061 for the bottom (weaker and thinner because it would only need to resist bending, not any real stress).

To design the leading edge, the process was simple. We wanted the outer profile of the wing to maintain constant, so we simply replaced the leading edge portion of the wing with a separate part with a rough thickness of 0.13 inches, that scaled down linearly until 0.08 at the tip of the wing. This part would produce some rigidity in the wing design, but most importantly, it would prevent us from needing to bend the skin around the front edge, simplifying the manufacturing and assembly process.

### Manufacturing

To manufacture the metallic portions of the skin, a planform sketch of the wing was produced and then copied onto the sheet metal. The metal was then cut on these lines with a bandsaw, and the edges were smoothed using a belt sander. Finally, the cut-out wings were slightly bent using a roller to fit the shape of the airfoil. This manufacturing method led to a mildly distorted shape, as the skin was a bit smaller than it was supposed to be along the chord length of the wing. However, this difference was insignificant, so for the sake of simplicity, it was neglected.

Next, the leading edge was 3D-printed in three separate parts. They were printed with 80% infill, so that when holes were drilled for rivets, the plastic did not rip apart. The inside of the leading edge was offset slightly (on the order of 10-thousandths of an inch) to allow for it to fit snugly against the bulkheads.

## D. Rivets

To establish a base condition for skin failure, a single part model representing an upper and lower plate bonded together perfectly was created and simulated on its own. By constraining one end of the bonded plates and applying a downwards load to the other end, we were able to find a load that we consistently used through the rest of the tests (see figures III.D.1 and III.D.2 in the Appendix).

Within the design space, we made three individual templates that we then tested and compared. All are constructed of two 5”x5” plates, 0.030” thick riveted together. One has a 0.375” margin between the rivet centers and plate edges with 1” rivet spacing, one has a 0.5” margin with 1” rivet spacing, and one has 0.5” margin with 0.5” rivet spacing (see figure III.D.3). For all three models, the plates were attached via simulated fasteners and constrained at one end with an identical load applied at the other. The stress concentrations and calculated fastener stresses were then compared.

## E. Assembly

Once all the individual parts were manufactured, the entire wing was assembled. First, the bulkheads were fitted onto the I-beam in the correct order and orientation. Next, holes were drilled manually in the metal bulkheads for attaching them to both the beam and the skin. One hole was drilled per bulkhead. Holes were also drilled manually into the I-beam for rivets for all the bulkheads as well as for the weighting jig. Once these holes were drilled, the bulkheads were securely fastened onto the I-beam at their measured positions via rivet. The skin was then bent into shape, and lined up with the bulkheads. Hole position was marked on the skin and rivet holes were drilled manually. Two rivets were used to connect each bulkhead to the skin. The skin was then lined back up with the bulkheads and beam, and match holes were drilled in the bulkheads. The skin was then securely attached to the beam assembly with rivets. The same process was completed with the leading edge, where holes were marked, drilled and then match drilled before placing rivets everywhere. Finally, duct tape was added to the leading edge and the back (where the two skin pieces meet) to clean up the design.

## F. Testing

Testing was completed using a weighting jig set up by Al and Glenn. The wing was attached to the wing at the wider end of the beam, with several bolts into the beam itself and the end bulkhead. The jig allowed a variable amount of weight to be added to the end of the beam, which was attached via a bolt. A pulley system pulled up the weight once it was added, to allow more weight to be added each trial. Deflection was measured after each weight was added and lifted to observe the wing’s behavior.

# VI. Results and Discussion

## A. I-Beam

### Trusses

*Sensitivity study 1: Truss count.* The first analysis that we ran for the I-beam was the amount of truss patterns cut into the web of the beam. For max stress, increasing the trusses from 20 to 32 trusses has almost no effect on maximum stress (figure VI.A.1), and only a small impact on maximum displacement (figure VI.A. 2). We designed equations to have it such that a larger number of truss patterns would mean that the material for each pattern would be thinner. Thus, it is unsurprising that upon running the study, an increase in truss number corresponded to a decrease in the total mass of the beam (figure VI.A.3). Therefore, we selected 32 trusses as the optimal truss number.

*Sensitivity study 2: Minimum truss clearance.* The second analysis was focused on the clearance between the truss holes and the flange of the beam. When looking at max stress, increasing minimum clearance had a major impact on decreasing maximum stress up until about 0.045" (figure VI.A.4). Increasing clearance also resulted in a decreasing maximum displacement, but with returns that diminished as the minimum clearance increased (figure VI.A.5). A larger clearance results in smaller truss holes, and therefore more mass (figure VI.A.6). As a result, we select 0.045" as the minimum truss clearance.

*Sensitivity study 3: Asymptote Rate.* The third analysis was focused on how the asymptote rate of the truss clearance impacts the truss stress. Upon noticing that the fixed end of the beam had a high stress relative to the free end of the beam, we decided to make the truss clearance variable dependent on the position along the beam. The clearance starts off high and decreases further down the beam. The asymptote rate captures this decrease. This parameter was designed such that a change in Asymptote Rate would have a small impact on the total mass: it changes how the mass is distributed along the web. We observed that the mass change was very small, with a range of about 0.0005 lbm over the whole range that we tested (figure VI.A.9). However, the parameter had a non-negligible impact on stress. Around 1.3, the stress spikes and for higher numbers, the stress is lower but erratic (figure VI.A.7). Furthermore, the maximum displacement increases slightly with an increasing asymptote rate (figure VI.A.8). As a result, we chose 0.8 as the number for this parameter. This number has no units or physical significance besides denoting the rate at which the clearance from the truss to the flange changes along the wing.

*Sensitivity study 4: Truss angle.* The fourth analysis was based on the angle of the trusswork. Changes in truss angle caused unpredictable changes in stress, so it was important that we did it last out of the analyses. Upon running the analysis, the maximum stress was relatively stable as

the angle changed, but at higher angles the geometry began to change more dramatically, resulting in more erratic stress behavior (figure VI.A.10), and in general, higher angles tended to correspond with greater displacements (figure VI.A.11). A larger angle resulted in thinner truss beams, and therefore smaller mass (figure VI.A.12). With all of this in consideration, we chose 45° as our truss angle.

**Holes**

*Sensitivity study 1: Hole count.* This simulation is visible in figures VI.A.13-15. This simulation was very similar to the simulation for trusses. However, each truss has two holes (one on either side of the truss), while this parameter corresponds one-to-one with the number of holes for this configuration. Therefore, it makes sense that the optimal number of holes (based on stress, displacement, and mass) was about twice that of the optimal number of trusses. We selected 60 holes as optimal.
*Sensitivity study 2: Minimum hole clearance.* This simulation is visible in figures VI.A.16-18. Once again, this simulation was similar to that for the trusses although slightly less erratic, and the final parameter that we selected was 0.046".
*Sensitivity study 3: Asymptote rate.* The results for this sensitivity study are shown in figures VI.A.19-21. This was similar to the simulation for trusses, although again was less erratic. The number that we selected was 0.8.

**Deciding between Holes and Trusses**

*Final properties for trusses:*
Max Stress: 46.7 ksi
Max Displacement: 3.572 in
Mass: 0.392 lbm

*Final Properties:*
Max Stress: 45.50 ksi
Max Displacement: 3.562 in
Mass: 0.393 lbm

As can be seen from the properties above, both the beam with trusses and holes have very similar properties. While deciding between them, we considered the fact that the simulations with the trusses tended to be more erratic, and we also considered that the beam with holes had both a lower maximum stress and maximum displacement, while it was only heavier by 0.001 lbs. Therefore, we chose to continue with the beam with holes. *Figure VI.A.22* depicts the final drawing of the beam with the holes, and *figure VI.A.23* shows the stress and displacement of this final beam design.

*Fatigue and Modal Analysis*

*Figure VI.A.24* shows the results of a fatigue analysis to determine how the beam will respond to being loaded and unloaded. *Figure VI.A.25* shows the results of a modal analysis, showing which frequencies are resonant in the beam. These numbers are interesting, but are mainly concerning for the design process, since the beam will not be undergoing appreciable oscillations while being tested.

### Geometry

*Sensitivity study 1: Round Radius.* The first analysis was based on the radius of the rounds. It showed a sharp decrease in maximum stress between a 0.10-inch and 0.125-inch radius (Figure VI.A.9). The study showed the lowest maximum stress with a 0.175-inch round radius, but the tapering of the beam prevented us from using any round radius larger that 0.14-inch if we wanted to maintain uniform rounds, which we decided to use as they provided the largest reduction in maximum stress throughout the beam.

### Combined

Combining the truss cuts, rounded edges, and larger flanges resulted in a beam with acceptably low stresses. The drawing for this final beam is located in the appendix (figure VI.A.10). The stresses were below 50 ksi, which was low enough to be acceptable due to the yield stress being closer to 60 ksi for our choice of material (figure VI.A.11). In addition, fatigue analysis revealed that the beam could be loaded at least twice before any components would yield (figure VI.A.12). The position of first yield on the fatigue analysis was in the corner of the fixed end of the I-beam, which is geometry that will not exist in the final model, as the fixed end of the I-beam will be connected to a square cross-section, so the fatigue analysis result was very promising. In addition, we conducted a modal analysis. The first mode that the modal analysis showed was 4.6 Hz (figure VI.A.13).

## B. Bulkheads

### Geometry

The first question when designing the bulkheads was the geometry of them. While the wing profile was predetermined, the question of bulkhead geometry was related to how solid they would be. A completely solid bulkhead would be one where the space inbetween the top and bottom of the airfoil is completely filled with material (besides the space for the I-Beam). On the opposite side of the spectrum would be a bulkhead which has a large hole and only has material where it contacts the skin of the wing. This would necessarily affect the strength since generally less material leads to a lower part strength. Therefore, static analyses were conducted to determine the role that the bulkheads play in withstanding the stress from the applied load.

Two static tests were performed, one with nine solid bulkheads, and one with only the end bulkheads. Looking at the static test with nine solid bulkheads in figure VI.B.1 it can be seen that while the stress concentration is not entirely on the beam, the stress drops off significantly as distance from the beam increases. Moving to the static test with only the end bulkheads in figure VI.B.2, it can be seen that the stress is still primarily concentrated close to the beam. There is more overall stress in the test with fewer bulkheads, but in both tests the stress drops off dramatically as distance from the beam increases. Therefore, by looking at these two tests, it can be seen that more bulkheads do reduce the overall stress in the wing, but only close to the beam. Therefore, it was hypothesized that material could be removed from the bulkheads in the parts that were farther away from the beam.

### Number

The second question when designing the bulkheads was the number of them. While the two end bulkheads were necessary, in between them there could be any number. Since the static analyses in figures VI.B.1 and VI.B.2 showed a slight decrease in overall stress when there were more bulkheads present, it was hypothesized that in general, more bulkheads would lead to slightly less overall stress in the wing. The other question about wing integrity was related to the buckling of the wing skin. Since buckling is related to the length scale over which the buckling happens, it was hypothesized that more bulkheads would lead to less buckling. In order to determine this, buckling analyses were performed on the wing.

Two buckling tests were performed, one with nine solid bulkheads, and one with ten solid bulkheads (the tenth was added in between the second and third bulkheads from the large end of the wing). Looking at the buckling test with nine solid bulkheads in figure VI.B.3, it can be seen that there is a large buckling location close to the large end of the wing, with a buckling factor for the first mode of -0.92. Therefore, the skin will most likely buckle there. In order to combat this buckling as well as reduce the overall stress on the wing, a tenth bulkhead was added in between the second and third bulkheads. The buckling test with this additional bulkhead can be seen in figure VI.B.4. While the buckling factors for this test were essentially the same as the previous test, the buckling location was smaller and moved closer to the large end of the wing. Therefore, it was determined that while this tenth bulkhead didn't completely change the buckling outcome, due to the light weight of the bulkheads, and the minor stress and buckling improvements, it was worth adding the tenth bulkhead to the final design.

### Final Design

The two findings related to geometry and number were combined to create a wing with ten bulkheads. In addition, the eight middle bulkheads had holes in the parts close to the trailing edge of the wing. The final designs can be seen in figures V.B.1 through V.B.10. In order to confirm this final design, static and buckling analyses were performed on the ten bulkhead wing with and without the holes in the middle eight bulkheads. Looking at figure VI.B.5 which was a

static analysis of the wing with bulkheads with holes versus figure VI.B.6 which was a static analysis of the wing with all solid bulkheads, it can be seen that there is very little difference in the stress magnitude or concentration in the wing. This similarity is in spite of the middle bulkheads in figure VI.B.5 having far less material in them. Additionally, looking at figure VI.B.7 which was a buckling analysis of the wing with bulkheads with holes versus figure VI.B.4 which was a buckling analysis of the wing with all solid bulkheads, it can be seen that there is very little difference in the buckling magnitude or concentration between the two tests. Therefore, it was determined that the bulkheads could afford to have the holes, and that the tenth bulkhead was a good idea.

A note is that none of the buckling tests with a skin thickness of 0.032 inches or thinner had a first buckling mode factor over 1. This theoretically means that with the current bulkhead setup, the wing skin would buckle in all of the tests performed with that skin thickness. A buckling test was also performed with ten bulkheads and a skin thickness of 0.040 inches as seen in figure VI.B.8 and that test did have a first buckling mode factor of 1.34, implying that for that test the skin would not have buckled. So, it seems that the buckling factor relationship is more related to the skin thickness than the number of bulkheads.

## C. Skin

In order to make a fully informed decision on the thickness and material of sheet metal used in our design, we performed a series of stress analyses. All tests were performed with 100 lbs of load placed on the wing tip, and the material for all non-skin components was set to 6061 aluminum for simplicity. We opted to do individual experiments, as opposed to optimizations, as there are realistically only 4 reasonable choices for skin thickness on McMaster Carr (0.020, 0.025, 0.032, 0.040). In our first test (figure VI.C.1), the skin is 0.025 inch 6061 aluminum. The maximum stress is concentrated along the outline of the central beam, and is strongest around the second bulkhead (outdated in this model). This will be a common theme among all of the tests. We can see that the maximum stress sits in between 18.75 - 20 ksi, which is well below the maximum yield strength of 6061 aluminum (35 ksi). Already there is quite a bit of headroom in this design, but we decided to go further in optimizing it. Having some more headroom, especially if our wing is capable of carrying far more than 97 lbs, is optimal. After this test, we knew that our most likely skin thicknesses would be 0.025 or 0.032.

Next, we experimented with 0.032 on both sides and achieved the results in figure VI.C.2. In this test, we can see that the internal stresses are reduced by about 2 ksi. This was expected, however the magnitude is pretty small considering a 28% mass increase. An important factor that these tests do not account for is buckling of the bottom skin. Thin sheets of metal do not do well under compressive force, and will bend before they yield to the internal stress. As a result, the effective strength of the bottom piece is not what this test indicates. Figure VI.C.2.5 demonstrates that the

bottom side will buckle, but not the top. Because of this, we decided that 0.032 inches would be good for the top piece, while 0.025 would be fine for the bottom.

In figure VI.C.3, 0.032 top thickness and 0.025 bottom thickness was tested. With these thicknesses, we reach a maximum stress of about 16-17 ksi on the top, and 18-20 ksi on the bottom. These values are still well within our safe range, and since the bottom will be buckling, it will not actually experience this high of a stress. On the flipside, the top side will be experiencing more, so we want to ensure it is strong enough to possibly handle all of the stress on its own.

In the final test outlined in figure VI.C.4, we used 2024 T3 (a standard, strong aerospace sheetmetal) at 0.032 thickness on the top, and no skin on the bottom. Not surprisingly, the new highest stress peaks at just about 26.75 ksi. But, this is still well below the yield stress of 2024 T3 aluminum (41 ksi), and is also unrealistic since there will be skin present on the bottom of the wing.

Finally, the leading edge design is very simple, and follows the profile of the original wing. It is 0.13 to 0.08 inches thick, decreasing linearly along the length of the wing, and will be made of PLA. It will also be divided into 3 separate pieces, and attached to the wing bulkheads with rivets. A plastic leading edge will serve to reduce weight and simplify the assembly process, as the sheet metal will not need to be bended as much. Dividing it into 3 pieces will allow it to warp and shift without snapping, as PLA is brittle. Drawings of each component, as well as the top skin, are in figure VI.C.5.

## D. Rivets

### Number

From the design analysis, we saw that a spacing of 1 rivet per inch was sufficient to avoid overly stressing any individual rivet. In the 0.5” margin case (which we use as standard for reasons discussed below), the individual load on any one rivet was very low, only about 15 lbf maximum on the edge rivets. However, there were still some stress concentrations from the rivets, which were absent in the test with 0.5” margins and 2 rivets per inch (see figure VI.D.1-3). To err on the side of caution, we will opt for around 1.25 rivets per inch or more on average on the starting and ending bulkheads.

### Location

The most important factor in the rivet simulation was the size of the margin between the rivet holes and the edge of the plate. At a 0.375” margin with 1 rivet per inch, we began to see high stress concentrations near the rivet holes when the plate was stressed (see figure VI.D.4).

Increasing the margin to 0.5” caused the stress concentration to mostly disappear, with it nearly entirely dissipating when rivet density was increased to 2 rivets per inch. Since the starting and ending bulkheads are 0.75” wide, we will ensure that our margin is as large as possible by biasing our rivet holes towards the inside of the wing, allowing us to avoid a stress concentration in the thin sheet.

## E. Assembly

Several minor adjustments were made during the assembly of the wing. Firstly, the first time the bulkheads were printed, they did not align with the locations expected, being too small to make it further up the taper to their positions. Thus, to prevent an excess amount of filing, the bulkheads were reprinted with more clearance. Upon trying the new bulkheads out, they fit much better and were able to align properly.

Additionally, the hole for attaching the wing to the rigid end of the testing rig was supposed to be match drilled while the testing rig was attached. Unfortunately, the team proceeded with drilling this hole in the I-beam during the main assembly step, resulting in a misalignment with the testing rig. A match hole was promptly redrilled and testing commenced.

## F. Testing

The final wing design is shown in figure VI.F.1. When tested, the wing weighed 1 pound 11.3 oz, on the heavier side. Then, the wing was pulled down with subsequently increasing weights. The first weight placed on the wing was 65 lbs, which the wing comfortably held with a deflection of 2.75”. Then, a chuck was added to increase the weight to 97.5 lbs, the required holding weight. The wing additionally comfortably held this weight, with a 3” deflection. After each of these times there was very minimal permanent deflection. Since the wing held the required weight, the team made the decision to keep adding places to the rig until the wing failed.

The next weight tested was 130 lbs roughly, and the wing deflected 4.5 inches. After this, the team did not expect much more weight to be held. 195 lbs was tested next, and the rivets holding the skin onto the large end bulkhead all snapped off. However, the wing did sustain this much weight, deflecting 7.25 inches. 260 lbs was then added, and the wing deflected 9.25 inches. At this point the wing was deflected enough that the I-beam was effectively in tension, a loading method in which the beam is very strong. Thus, at both 325 lbs and 390 lbs, the beam still did not shear or snap, deflecting 12” and 14.75” respectively. After 390 lbs (and the huge amount of deflection), the beam was permanently deflected, and the team made the decision to stop adding weight, as the beam did not officially “pass” this weight. However, despite the beam’s permanent deformation, the beam did not break (much to the team’s surprise!).

A relatively large amount of torsion was observed during the testing process, with the beam twisting more and more as higher weights were placed on it. Additionally, early into the process,

the bottom skin buckled significantly in one spot, popping off the rivets that held it in that location. The final deformed wing (with the skin removed to show the bent beam) is shown in Figure VI.F.2.

# VII. Conclusion

## A. Overview of Purpose (see above comment)

The purpose of this project was to build a lightweight wing that was able to support 97.5 lbs and meet the guidelines set forth to our team, including minimizing deflection and wing weight and constructing a wing with effective workmanship. We considered multiple designs, ran many analyses, and carefully assembled the final wing.

## B. Preliminary design summary

**Design specifications**

*I-Beam:* The I-beam originally was designed as a beam with Pratt Truss patterns in the preliminary design report and a thickened flange with rounded edges. From the preliminary design report to the final design report, we changed the beam to have holes instead of trusses, but retained the thickened flanges and rounded edges.

*Skin:* The skin is created through three parts: two pieces of sheet metal for the top and bottom surface of the wing, and 3 3D printed pieces for the leading edge. The top piece is 0.032 inches thick, while the bottom is 0.025 inches thick. This difference is simply because the top piece will be under tensile stresses, while the bottom will be under compressive stress, meaning it will buckle almost immediately. Next, the leading edge is designed to conform to the shape of the airfoil, while extending slightly into a groove in the bulkheads to allow for stability and easy assembly. It will be in 3 pieces to allow it to shift as the wing bends instead of snapping. Due to a typo in the order, the final thickness of the bottom skin was 0.032 inches. This had no significant impact on the design of the wing other than increasing the weight by approximately 0.05 lbs.

*Rivets:* Through analysis, it was determined that the rivets should be placed as far away from the edges of the wing's skin as possible. Moreover, a higher rivet density reduced the chances of the rivets pulling out under stress. In construction, we erred on the side of a higher rivet density than theoretically necessary and moved the rivet locations as close to the inside of the wing skin as possible on the first and last bulkheads.

*Bulkheads:* Through many analyses, it was determined that the bulkhead's main structural role was to prevent buckling in the skin. Therefore, it was decided that there should be a large number of bulkheads, including an extra bulkhead near the large end of the wing where the most buckling was expected to occur. However, since the bulkheads didn't receive much of the stress from the beam, a large section of each of the 3D printed bulkheads near the trailing edge of the

wing was removed in order to reduce weight. Additionally, the bulkheads were printed with 100% infill in order to reduce the chance of splitting.

**Material choices**

*I-Beam:* It was decided to make the I-beam out of aluminum 7075 because it was the strongest option we had available to us.

*Skin:* The top piece of skin is made of 2024 T3 aluminum, a common alloy used in aerospace. The bottom piece is made of 6061, a generally weaker and cheaper alloy used in many different applications. The leading edge is made of 3D-printed PLA with 80% infill.

*Rivets:* The rivets were constrained to be fully made of 5052 aluminum by project constraints.

*Bulkheads:* The two end bulkheads were made out of 6061 aluminum due to design constraints. The middle eight were made out of PLA and 3D printed due to high strength, low weight, and manufacturability. Since it was determined that the bulkheads undergo very little of the stress applied to the wing, it would be best to reduce weight and increase the ease of manufacturing with the bulkheads. Therefore, 3D printing was chosen as the best route to make them, giving two possible material options: PLA and PETG. Since they have very similar structural properties, but PLA is slightly less dense, PLA was chosen in order to reduce weight.

## C. Manufacturing summary

Once the design was finalized, the wing components were manufactured using a number of shop tools and machines. The I-beam, with its internal trusswork and rounds, was machined using the Haas CNC milling machine, which allowed for accuracy and precision during machining. The end bulkheads, which had to be made to specifications provided to us in the assignment, were cut out of metal using a water jet cutter. The intermediate bulkheads and leading edge were 3D-printed out of PLA plastic on a Bambu Labs X1C 3D-printer. The wing skin was cut to its rough size using a band saw and brought to its final dimensions using a combination of sheet metal snips, files, and a bending roller.

## D. Assembly summary

Once all the parts were manufactured, they were assembled to become the final wing.Holes in the I-beam were drilled at bulkhead attachment points, and bulkheads were then riveted to the I-beam. Next, the skin and bulkheads were mutually manually drilled to connect them, which was also done with rivets. Finally, the leading edge was similarly attached with rivets, and final holes were drilled in the I-beam to allow connection to the testing jig. To prevent cuts and clean up the design, lastly, blocking tape was placed around the leading and trailing edges.

## E. Final wing details and testing summary

The final wing assembly weighed in at 1 lb 11.3 oz, which is on the heavier side. Upon testing, it held the required 97.5 pounds at a deflection of 3”. It ended up vastly surpassing this weight, ultimately supporting, but permanently deforming, at 390 lbs with a deflection of 14.75 inches. During testing, all the rivets on the larger end bulkhead snapped off, but the beam continued to perform. Additionally, the skin on the bottom of the wing deformed early into testing, popping off a set of rivets.

## F. Things we learned

With this project, we learned how to make decisions based on empirical evidence and then be willing to pivot when challenges arose. Because it was very open-ended, there were so many variables we could have maximized or minimized in the design process, and we had to choose where to draw the line and where to make educated guesses. For the bulkhead cutout geometry as well as the truss geometry, we did analyses and then made educated choices for the geometry based on those analyses, doing a rough minimization of stress and weight while maximizing strength. Compared to other groups, our wing was slightly heavier than others and somewhat stronger, as other groups chose to do things differently and prioritize weight rather than strength. Part of that could have been due to our extra bulkhead, or our thick web in our I-beam.

Also, we learned that it is important to add slight clearances for parts that need to fit together, such as our bulkheads sliding onto the I-beam. This was helpful for us to understand tolerancing and how to design tight fitting pieces.

## G. What we would have done with more time/differently

The results of testing indicate that the wing ended up bearing far more weight than the specifications required before failing. While it is important to build in a safety factor to designs to ensure that they do not fail, building the design to be over specification by a factor of four likely resulted in the wing being heavier than it needed to be. If repeating this process, it would be beneficial to tailor the design to more closely fit the specifications in order to more efficiently reflect the design criteria. Nonetheless, the deflection of our beam was also low, indicating that our trade-off of a heavier wing also lended to a stronger performance in that area.

Another thing that we would have done differently if we had more time would have been to do more real-world testing to validate our simulations. For example, we would have enjoyed setting up a testing rig to see exactly when the rivets would fail when different loads were applied. Furthermore, the closeness of the design results between the trusses and holes was interesting, and we considered resin 3D printing and testing our I-beam designs to validate whether there

was such a little difference in the performance of hole cuts vs truss cuts. We also considered trying different truss types.

## H. Future improvements

To improve on our design, the first thing to consider is how heavy our wing was, and how much headroom we had in terms of raw strength. It was 1lb, 11.3 oz, and held 390 pounds without any core components of the wing yielding. Our wing easily supported 97 lbs with no noticeable permanent damage to the wing structure. After that, the bending began to be permanent, and the 5 rivets holding the top skin to the first bulkhead popped out. In the end, our wing was much stronger than it needed to be, and it cost us a decent amount in weight. The first part of the wing to break was the rivets, not the incredibly strong I-beam, very thick skin, or numerous bulkheads. If we consider the 5 rivets popping as the moment our wing "broke," we most definitely did not need an I-beam that could hold 390 pounds, nor skin that was 0.032 inches thick, as the rivets were the weakest link.

If we were to do this project a second time, we would focus on making sure the components in our wing are similar in relative strength, so that there is no unrealized strength within any of the parts. As long as a weakest link exists, any extra strength in the wing will simply be dead weight. Whether it is strengthening the bond between the skin and first bulkhead, or downsizing other parts of the wing to match the strength of the 5 rivets, we would end up having a much better strength to weight ratio. To be more specific, our next moves would likely be: to reduce the thickness of the skin, hollow out the intermediate bulkheads, cut more material from the I-beam; or, to find a way to attach the top skin to the first and last bulkheads in a more secure manner, perhaps with more rivets, slightly different drilled holes, etc.

# VIII. Appendix

*All engineering drawings, graphs, charts and any other items related to the project cited in the report.*

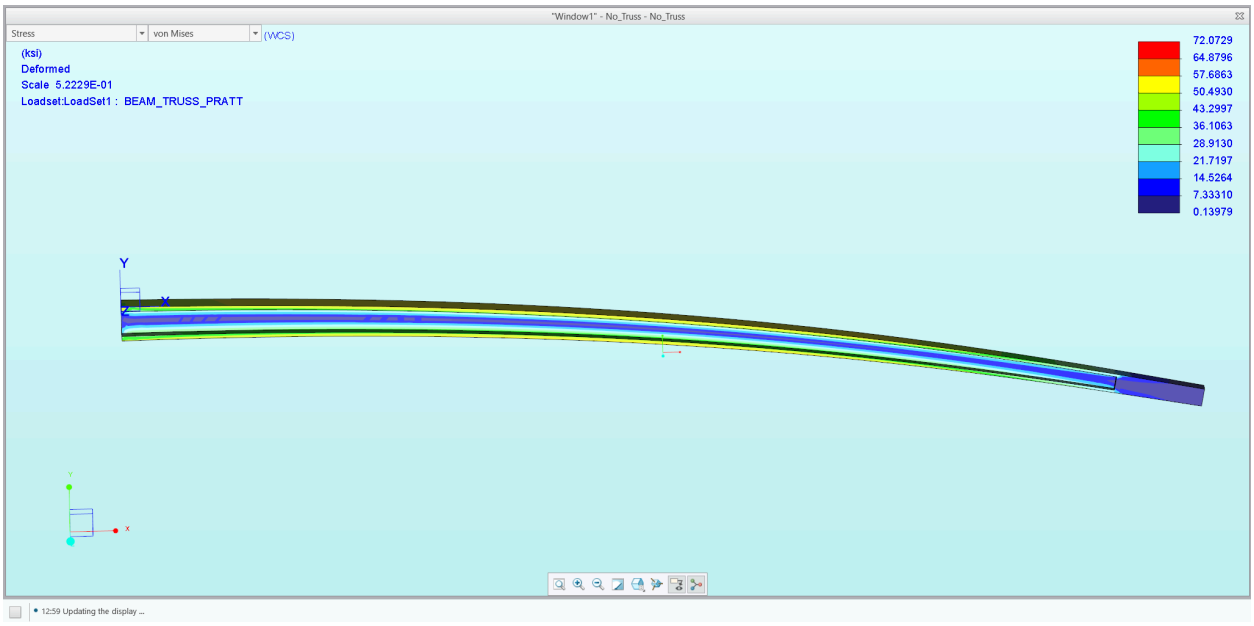


*Figure III.A.1 Beam with no trusses*

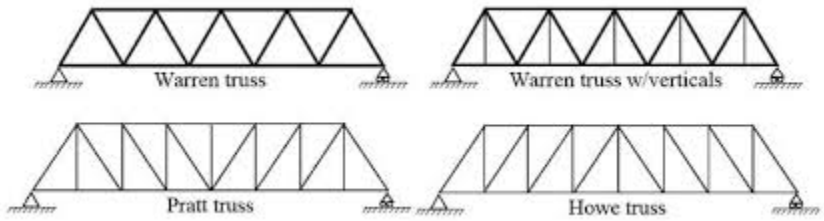


*Figure III.A.2 Truss Types*

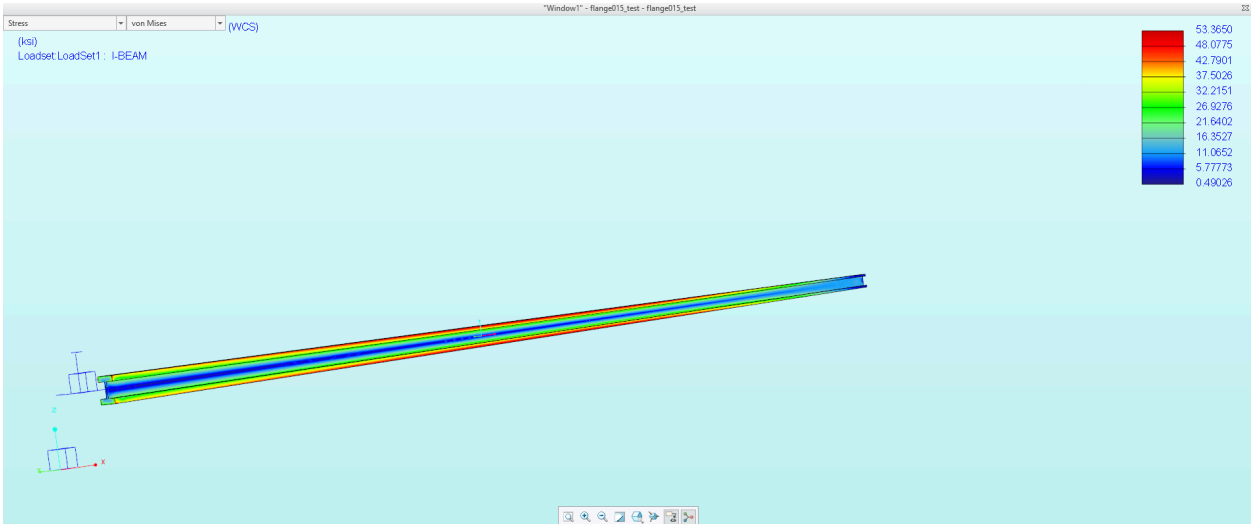

*Figure III.A.3 Non-Rounded, Non-Trussed Beam*

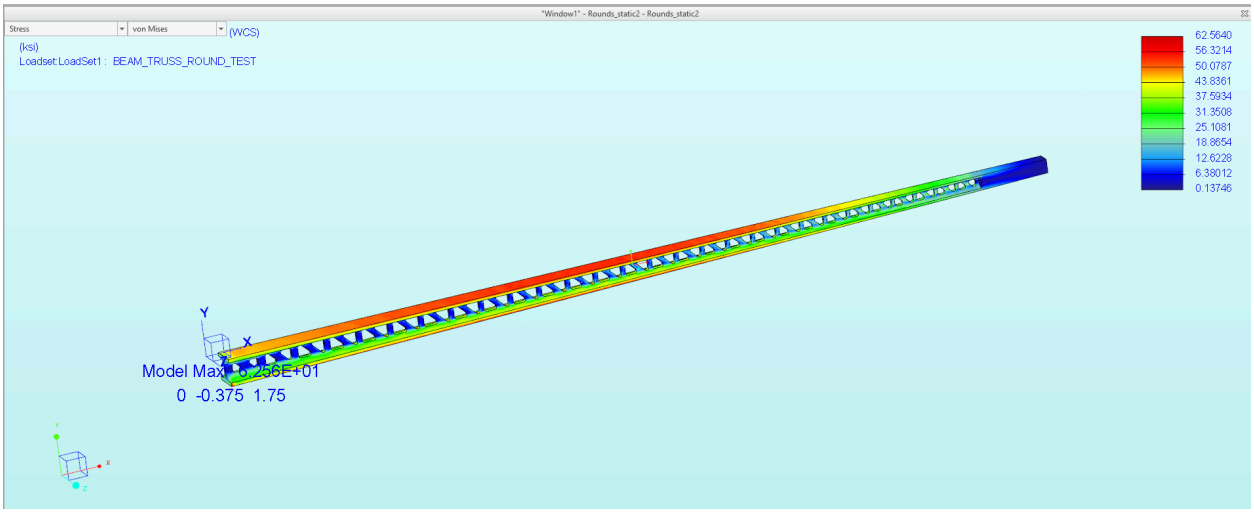


*Figure III.A.4 Rounded, Trussed Beam*

Following Figures: Bulkhead Geometry. These are the dimensions before the inner clearance on the rectangular square hole for the I-beam was enlarged for 3D printing.

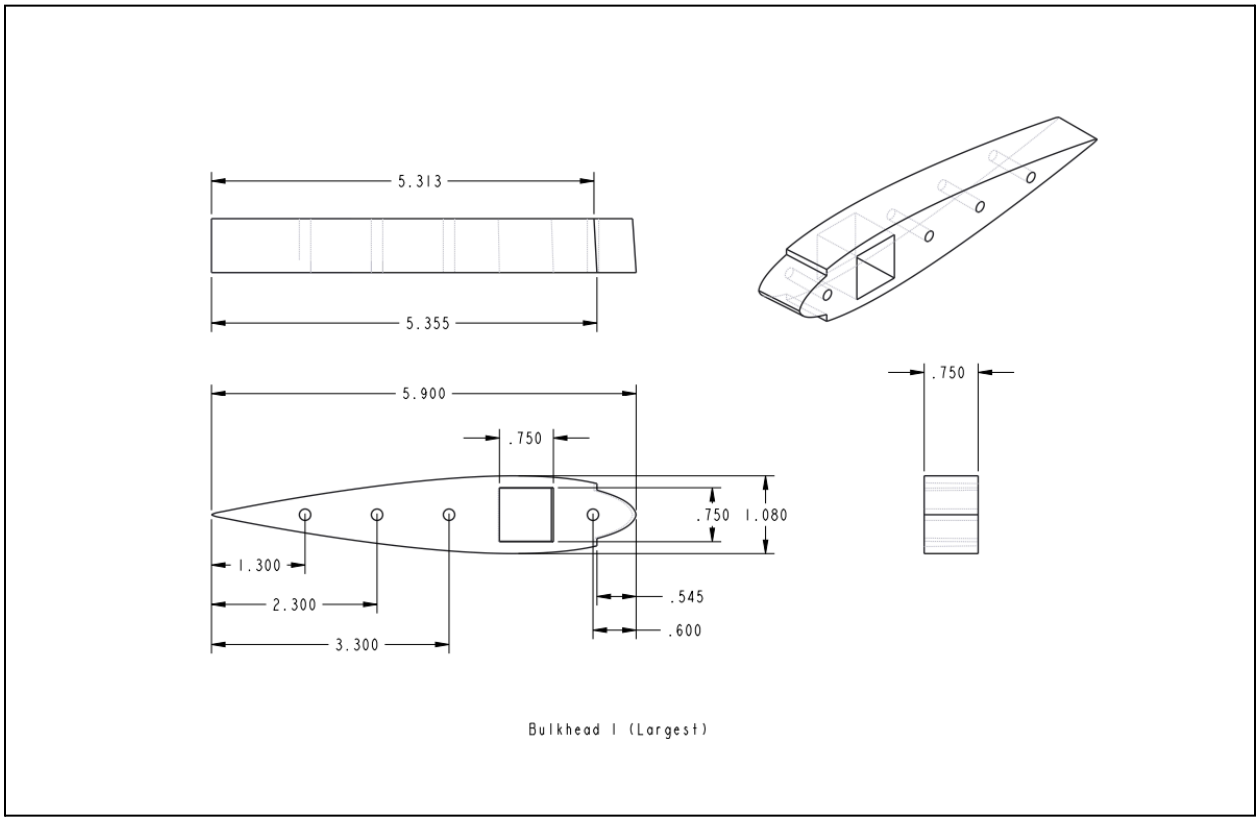


*Figure V.B.1: Engineering drawing of bulkhead 1.*

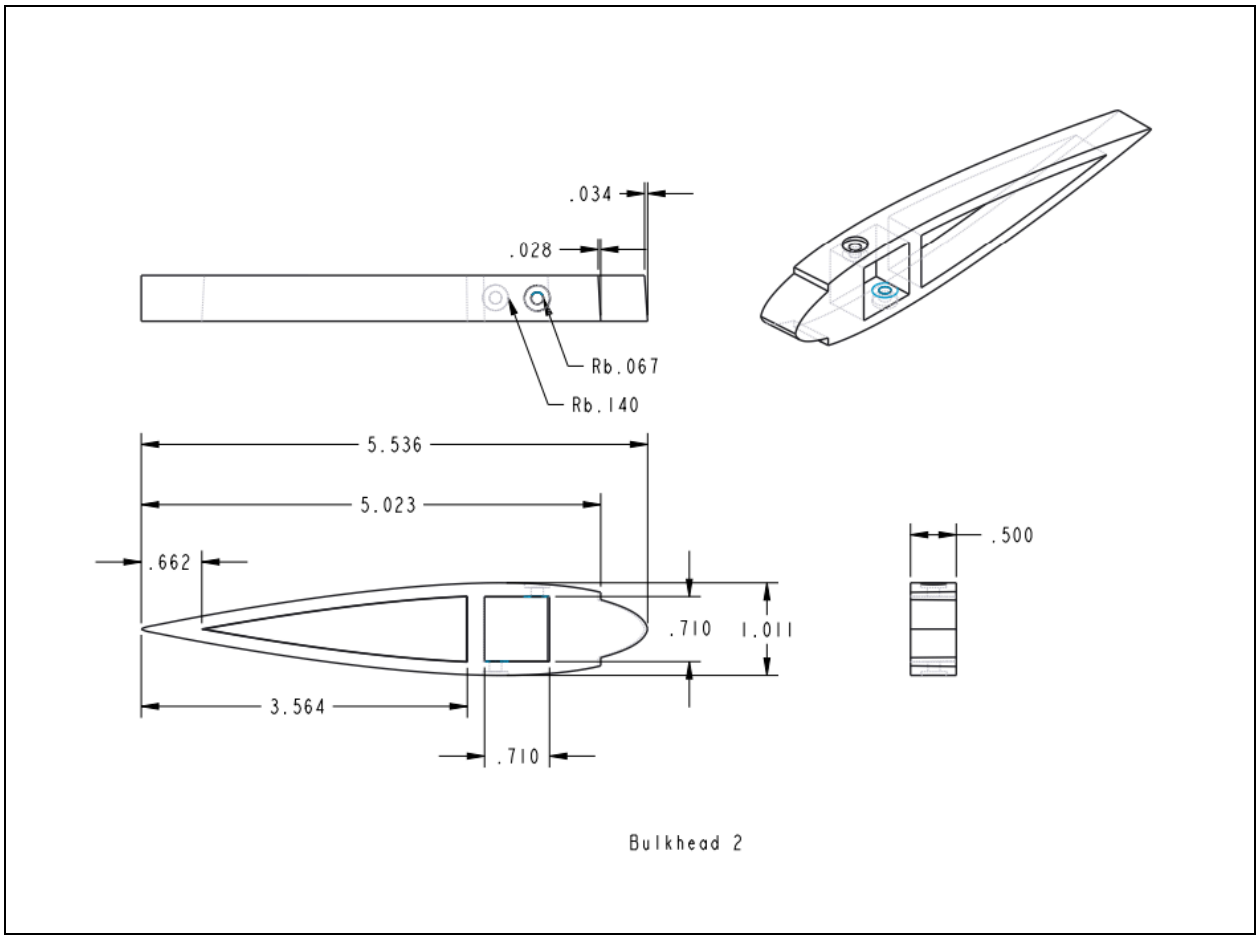


*Figure V.B.2: Engineering drawing of bulkhead 2.*

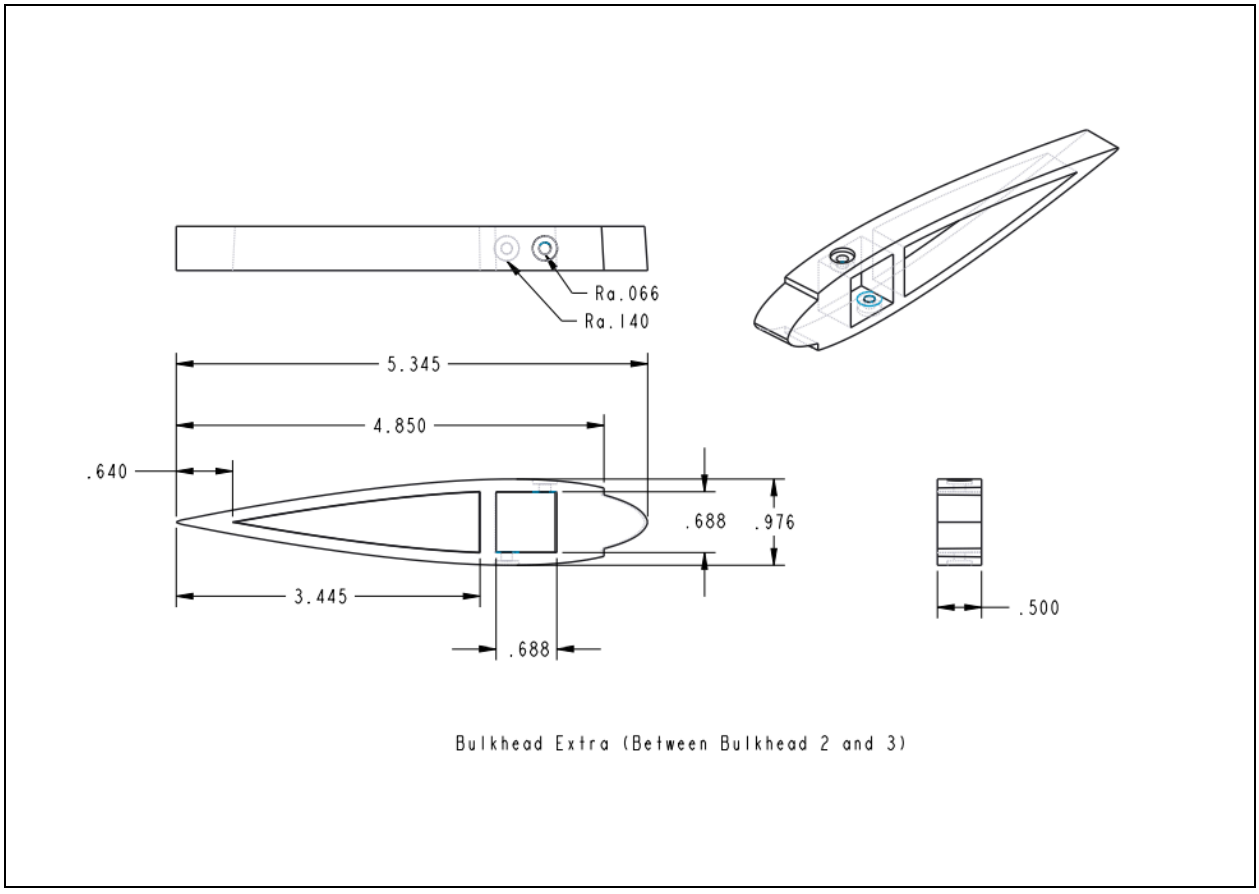


*Figure V.B.3: Engineering drawing of the extra bulkhead between bulkheads 2 and 3.*

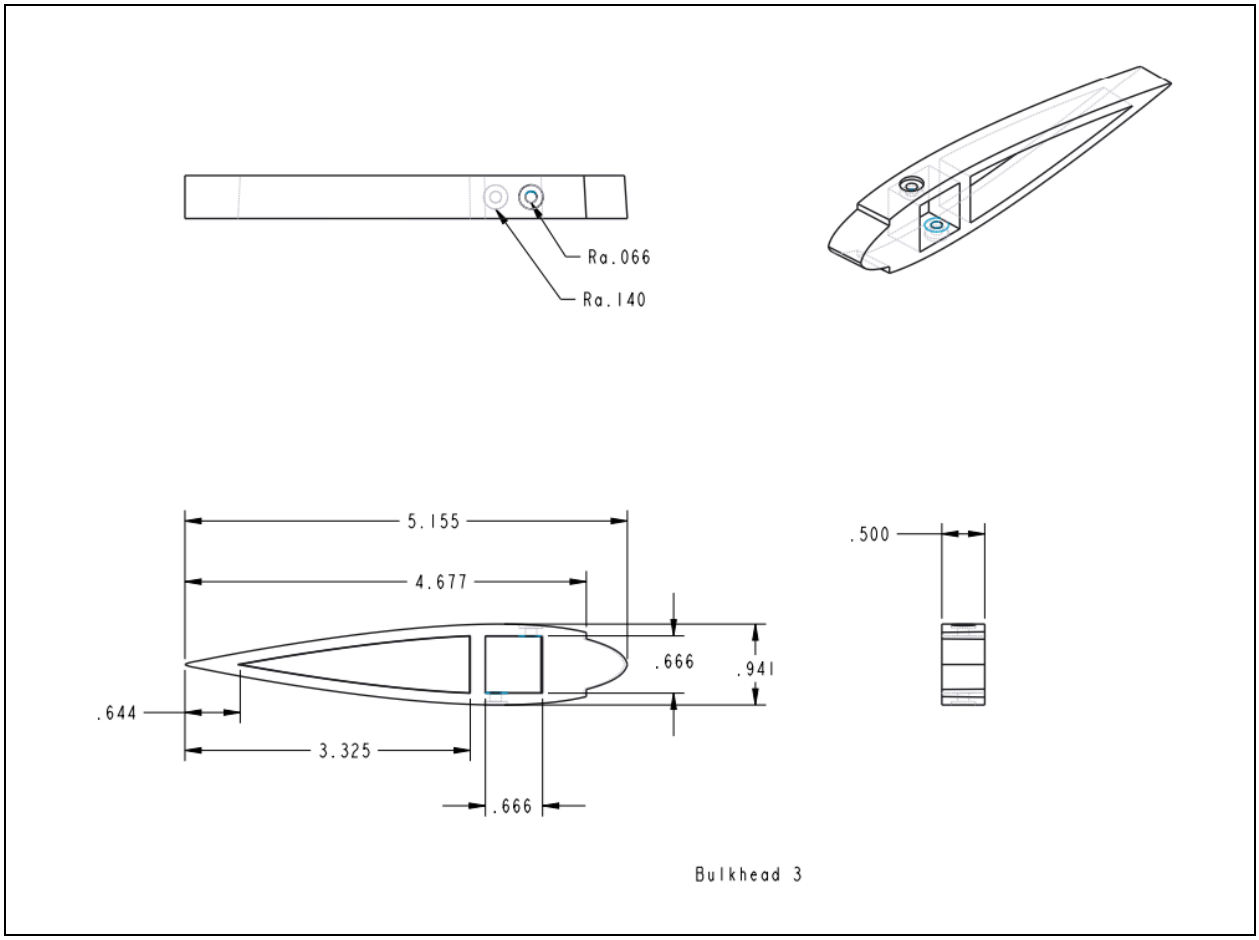


*Figure V.B.4: Engineering drawing of bulkhead 3.*

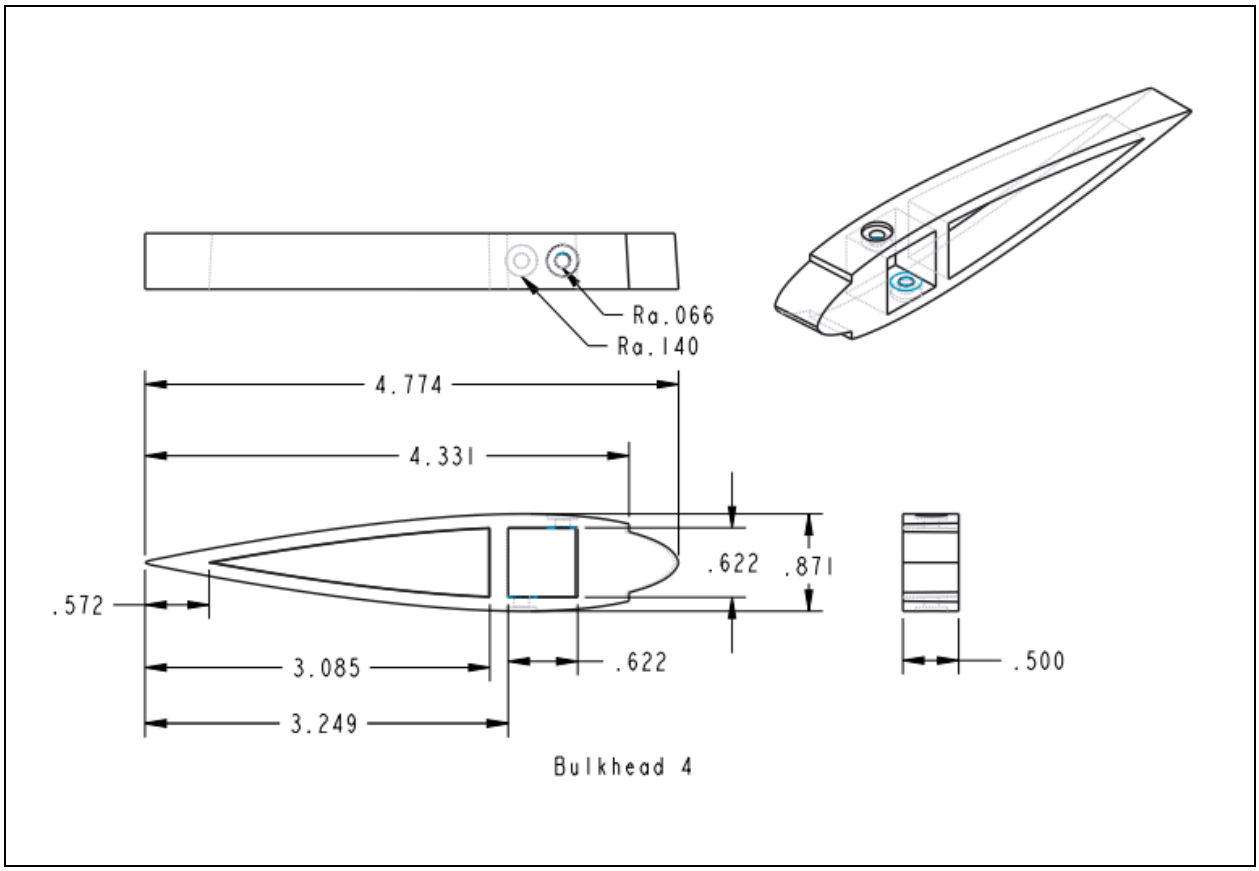


*Figure V.B.5: Engineering drawing of bulkhead 4.*

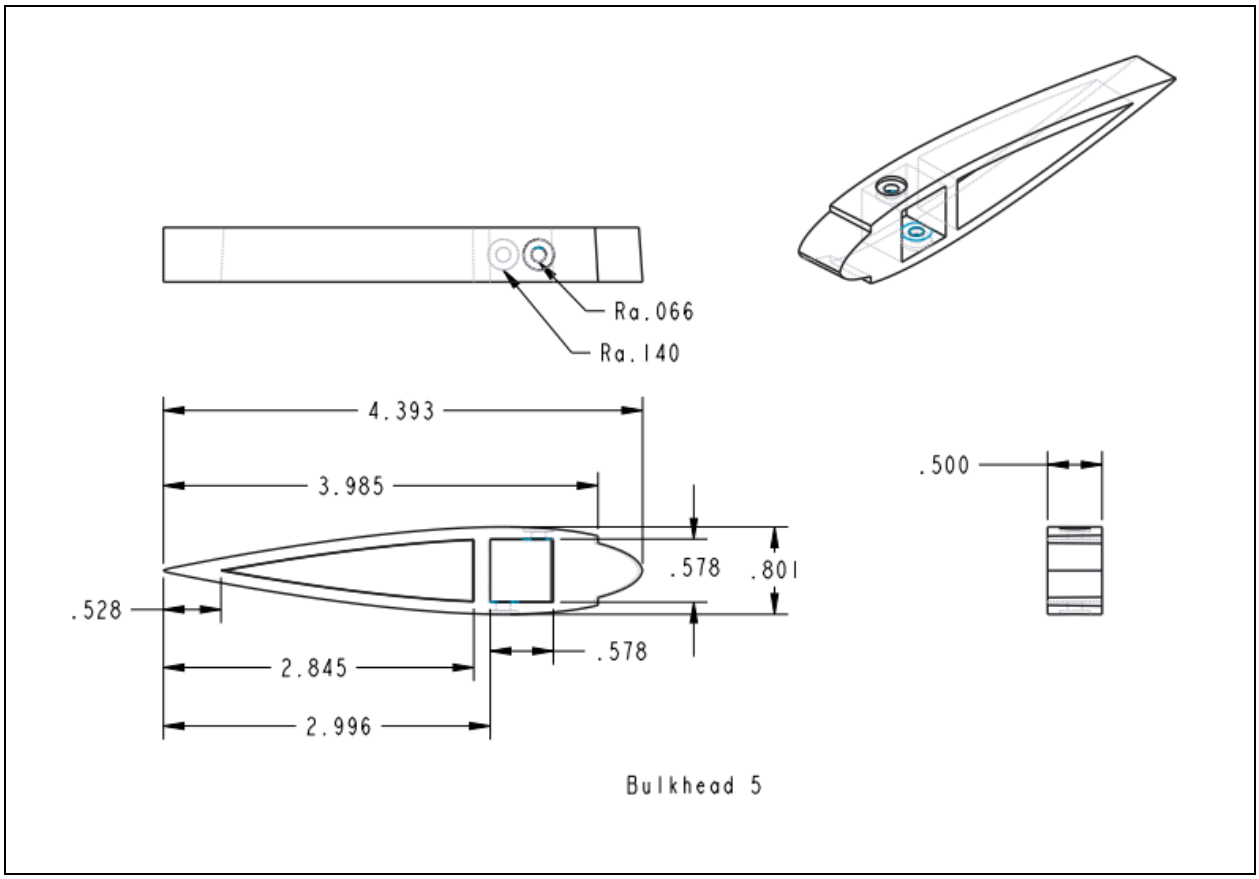


*Figure V.B.6: Engineering drawing of bulkhead 5.*

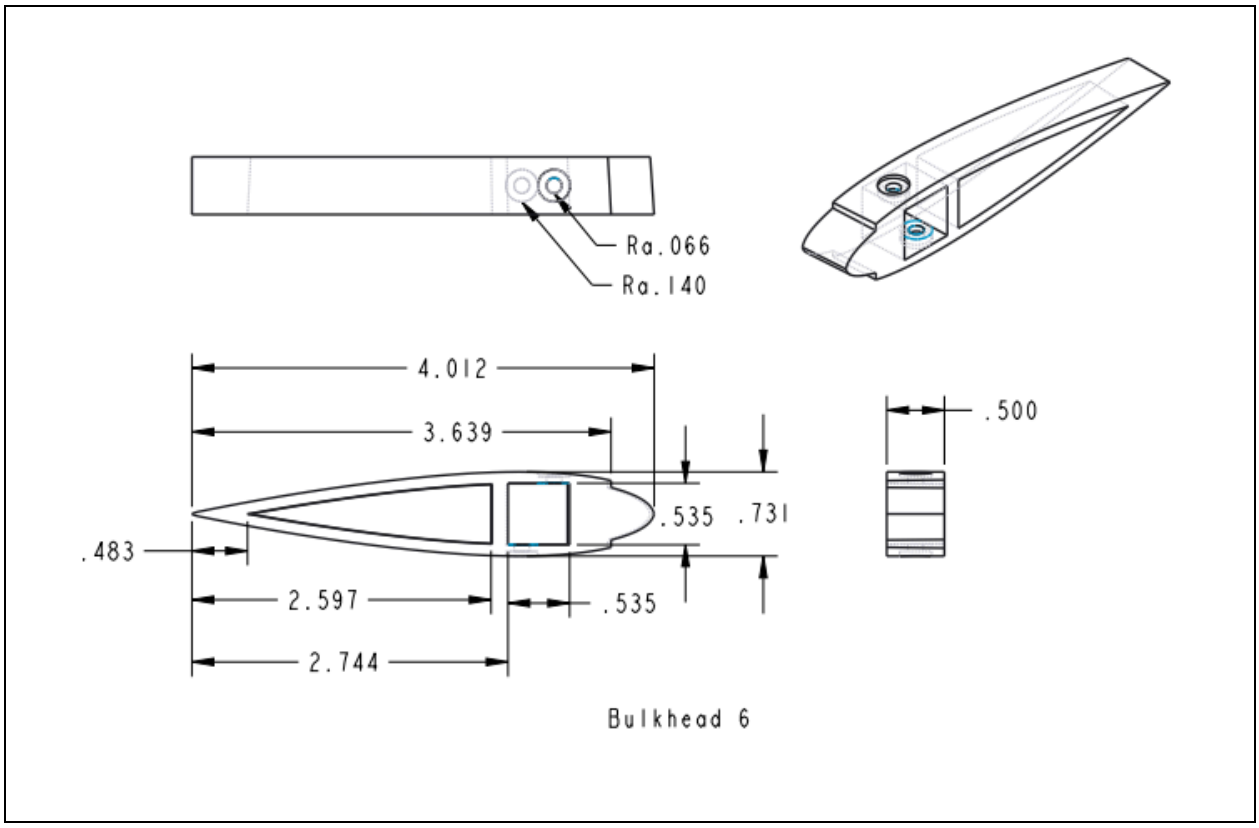


*Figure V.B.7: Engineering drawing of bulkhead 6.*

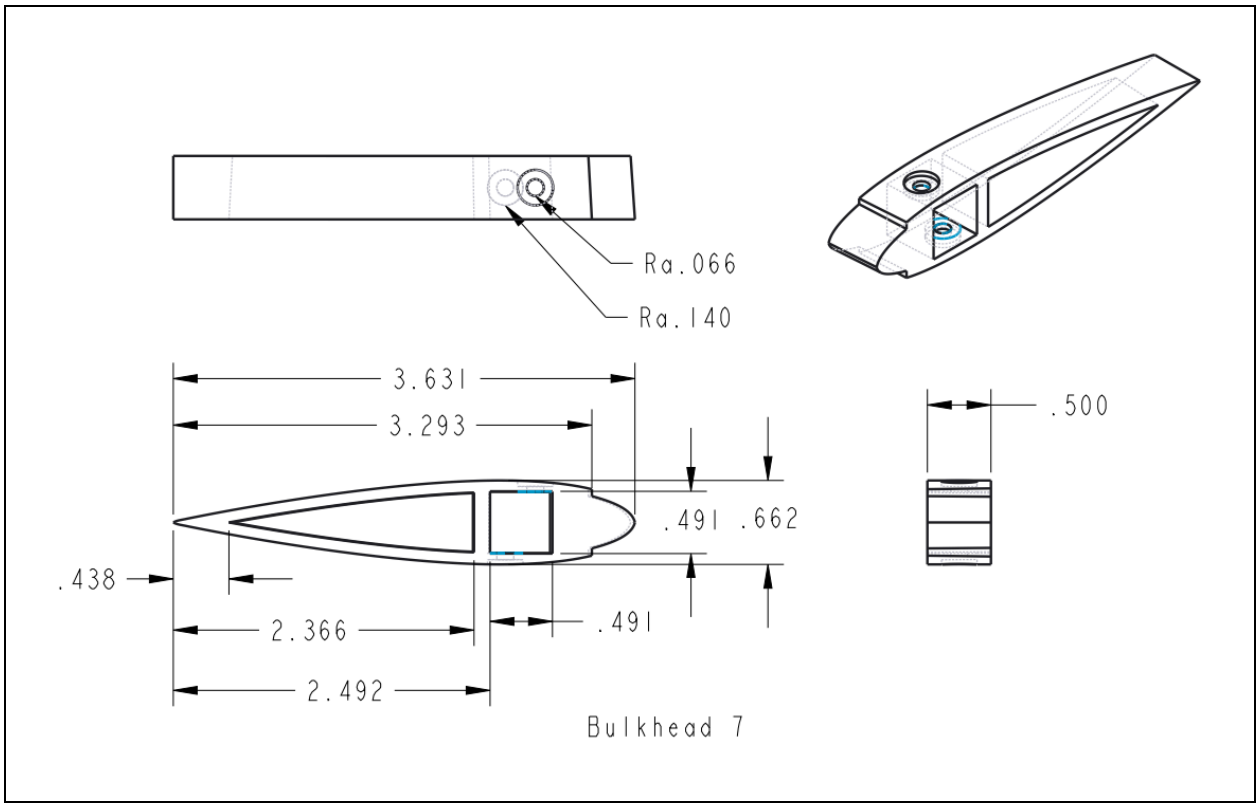


*Figure V.B.8: Engineering drawing of bulkhead 7.*

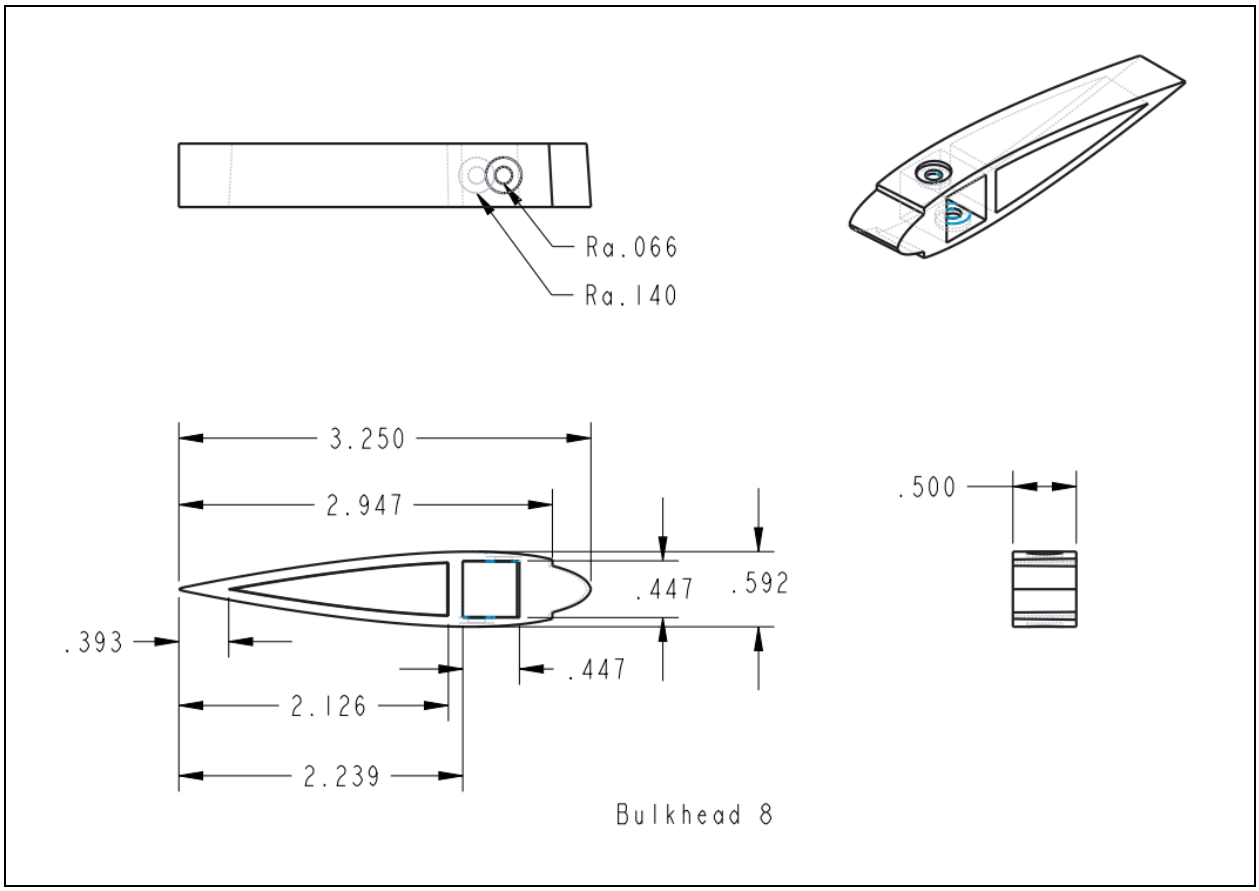


*Figure V.B.9: Engineering drawing of bulkhead 8.*

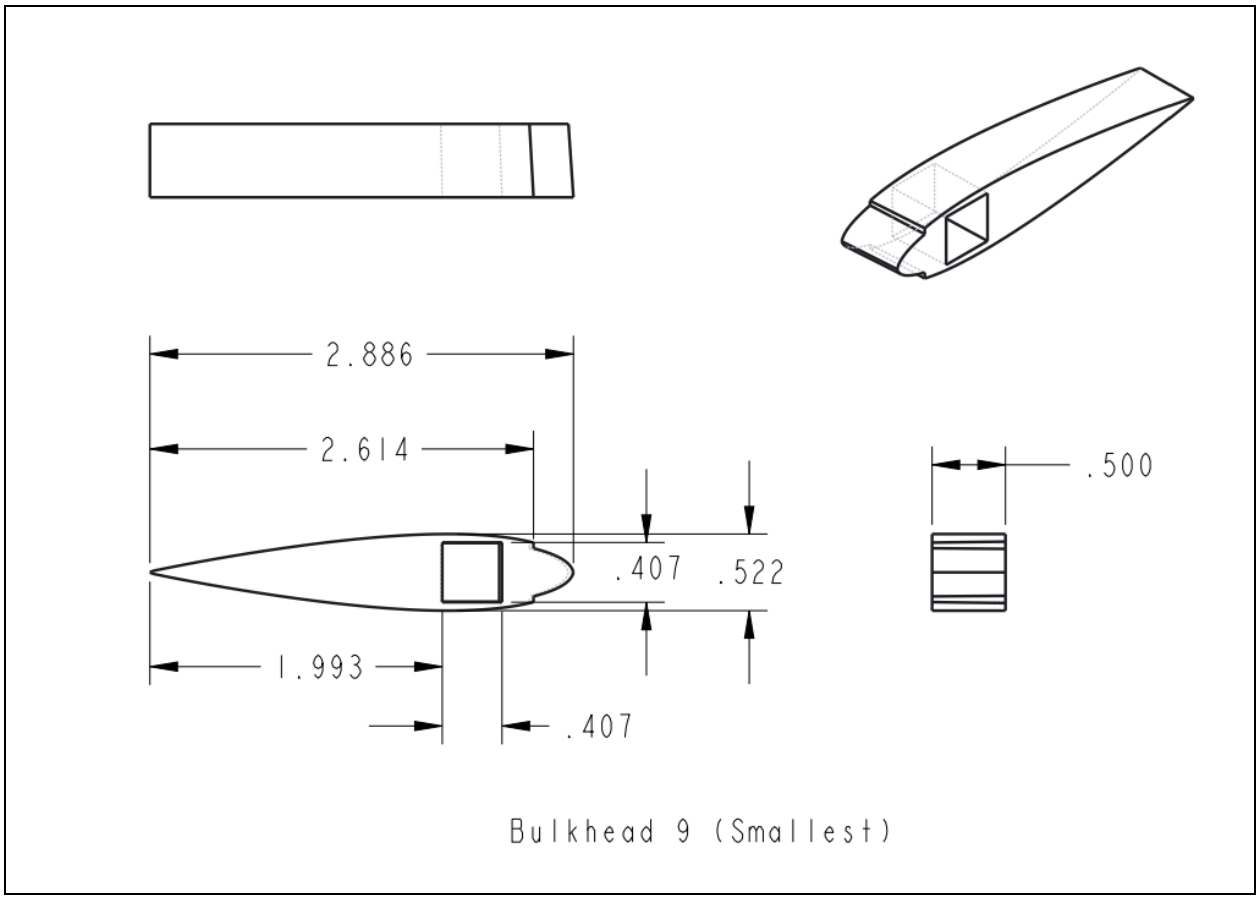


*Figure V.B.10: Engineering drawing of bulkhead 9.*

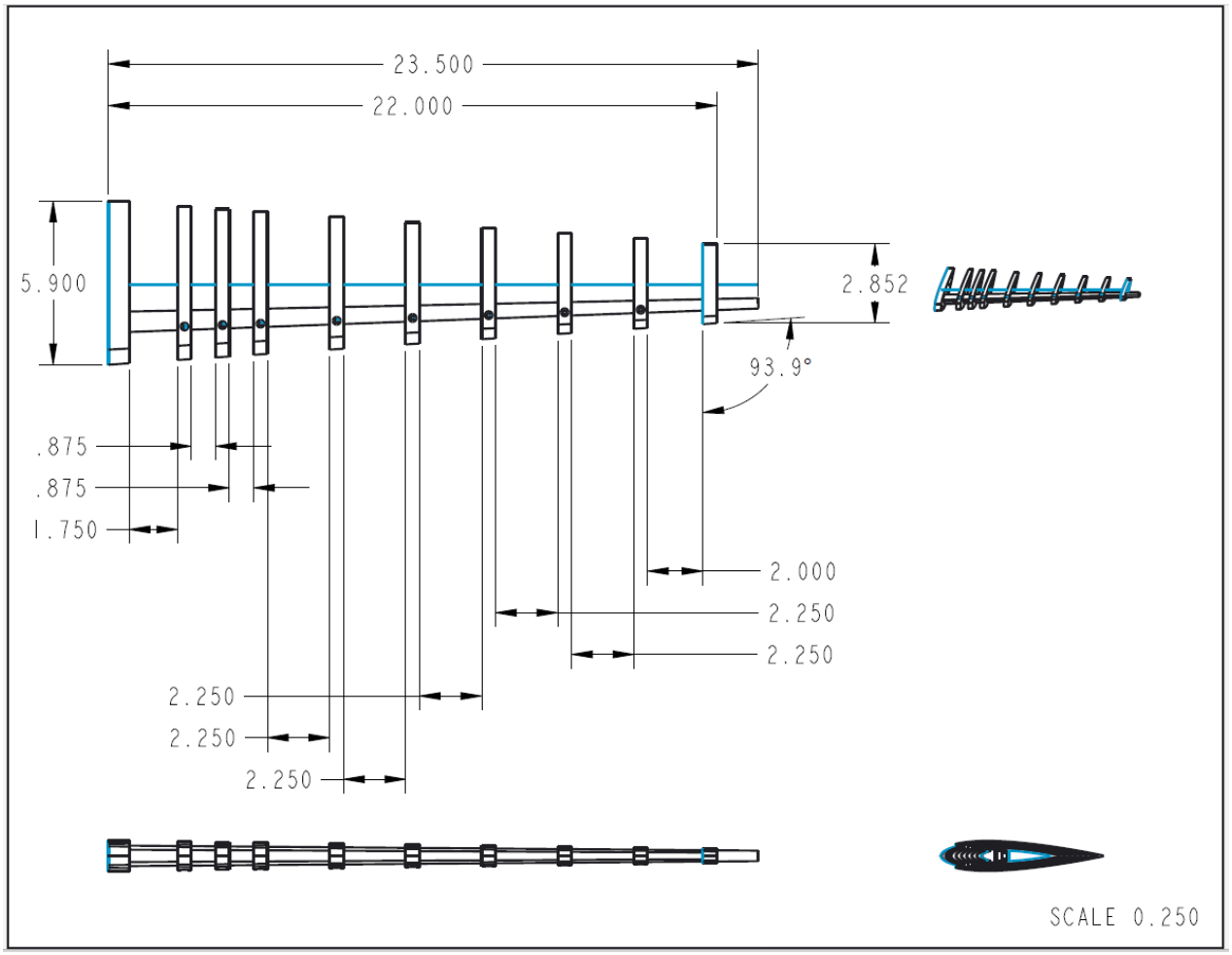


*Figure V.B.11: Engineering drawing of bulkhead spacing.*

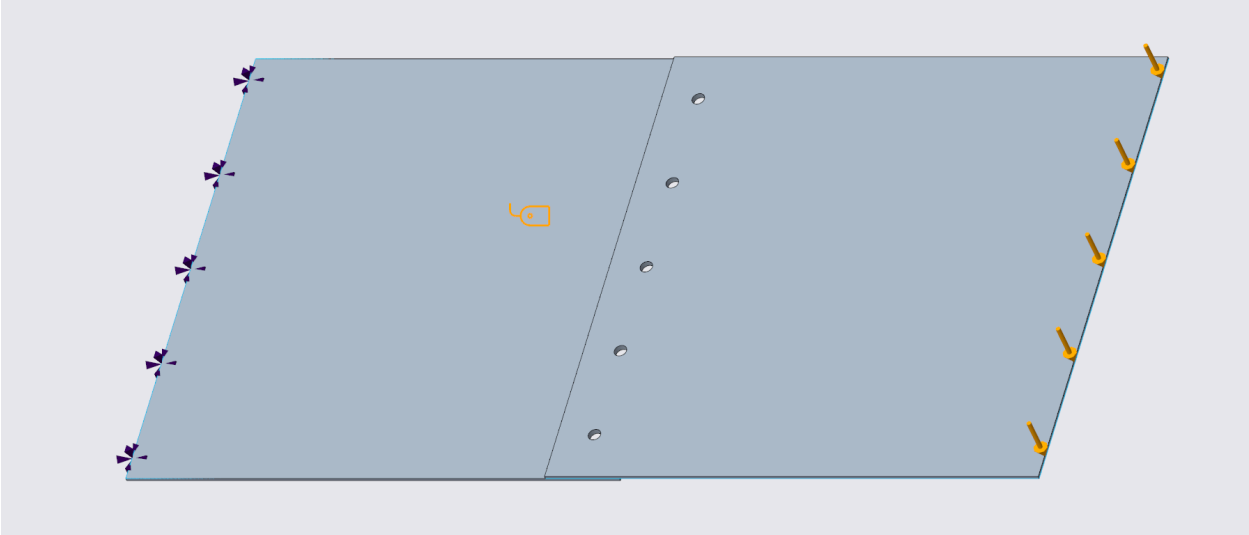

*Figure III.D.1: Bonded plate setup, constraints and loads pictured.*

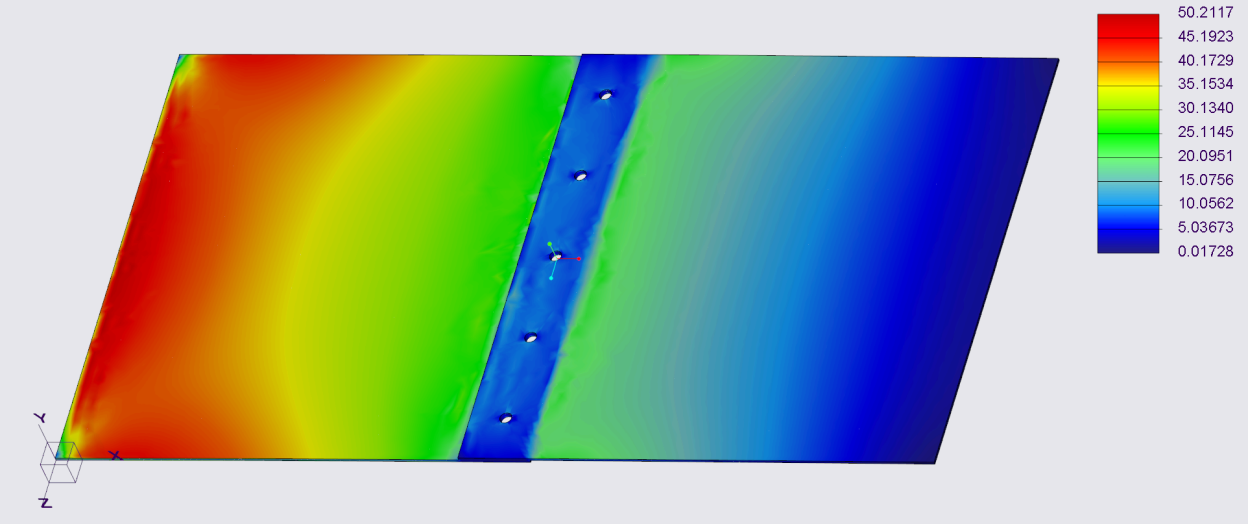


*Figure III.D.2: Under 4 lbf load, the plate model is brought well beyond yield.*

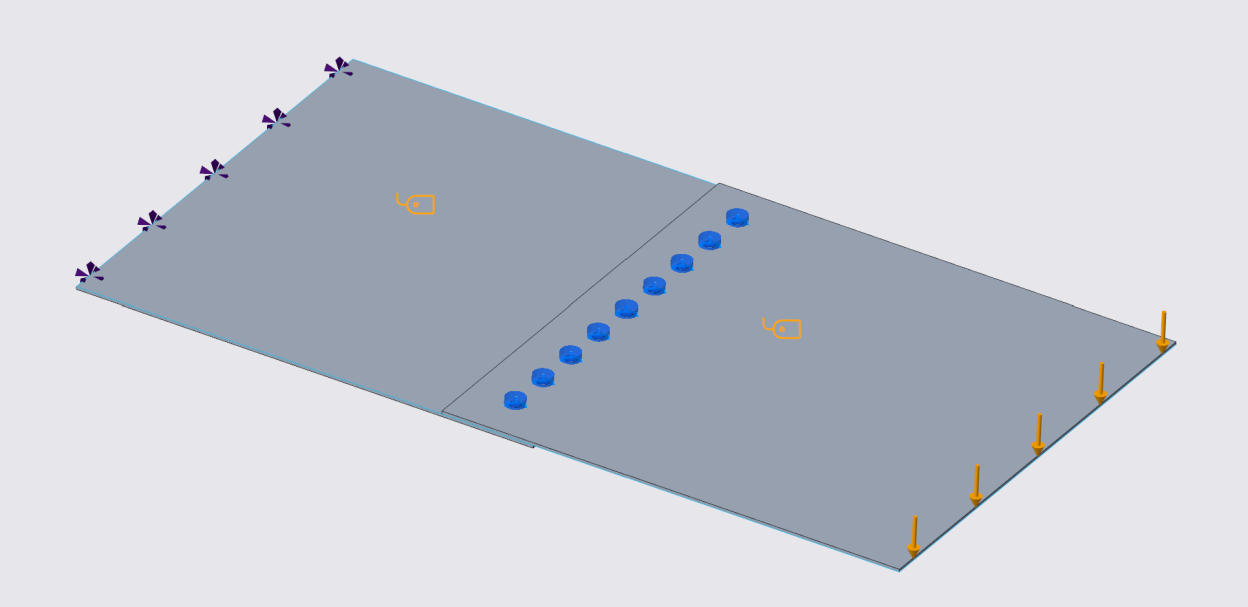

*Figure III.D.3: Sample plate prepared for simulation. Note the two separate parts and the fasteners. This sample is at 0.500" margin with 0.500" center-to-center distance.*

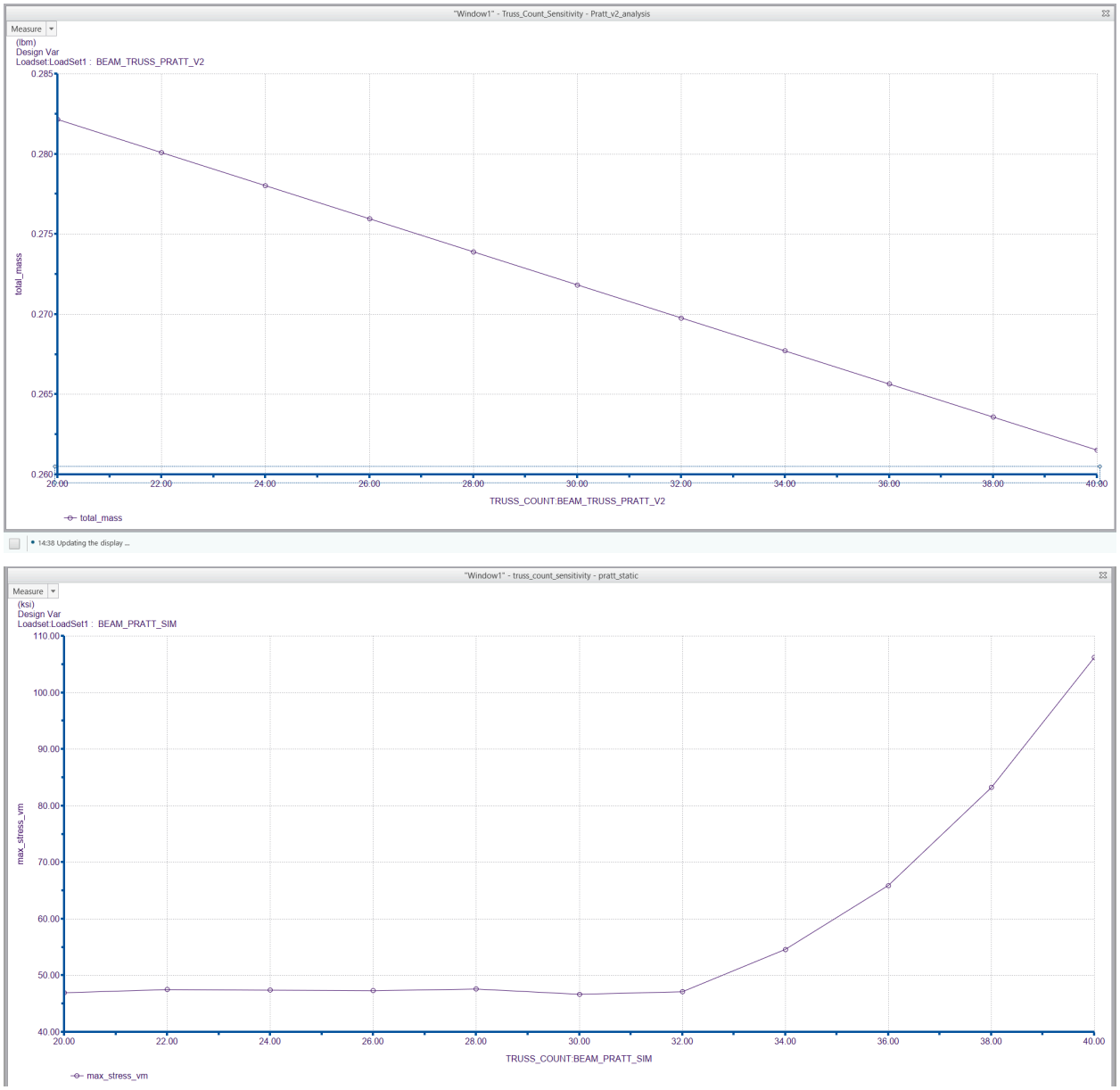


*Figure VI.A.1 Maximum stress in beam vs truss count*

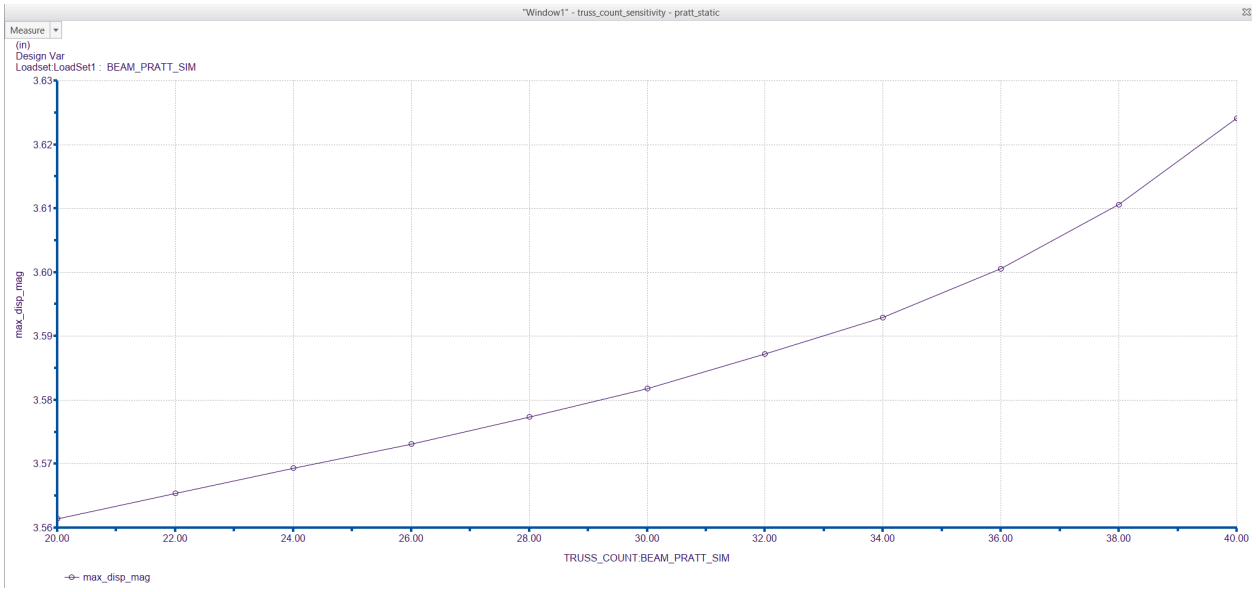


*Figure VI.A.2 Maximum displacement in beam vs truss count*

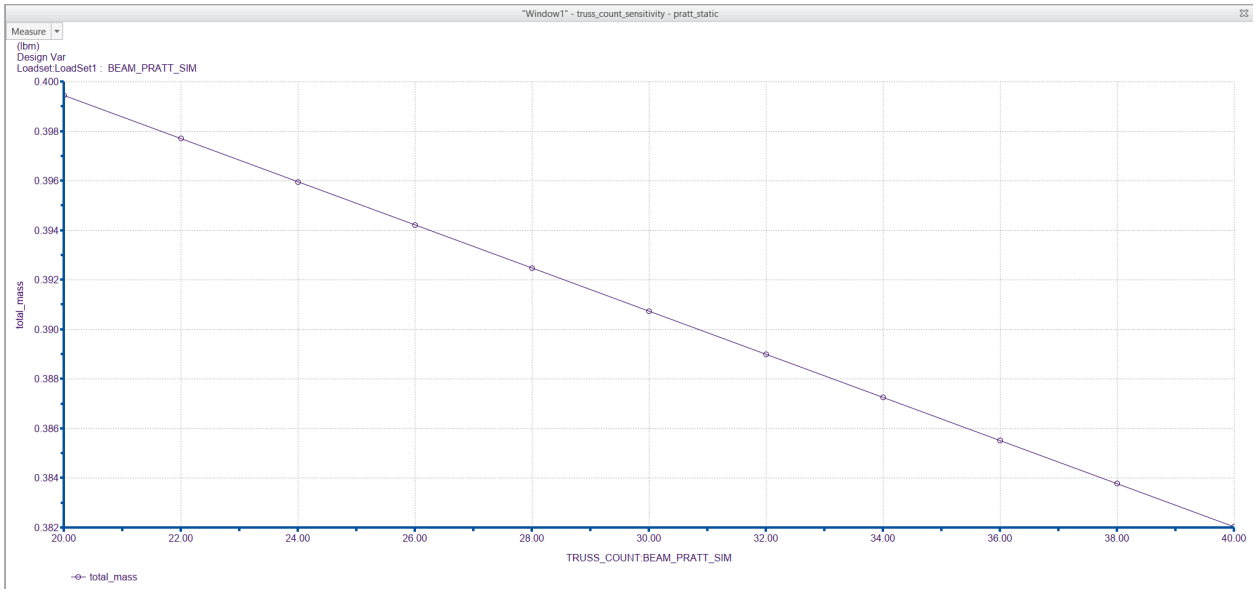


*Figure VI.A.3 Beam mass vs truss count*

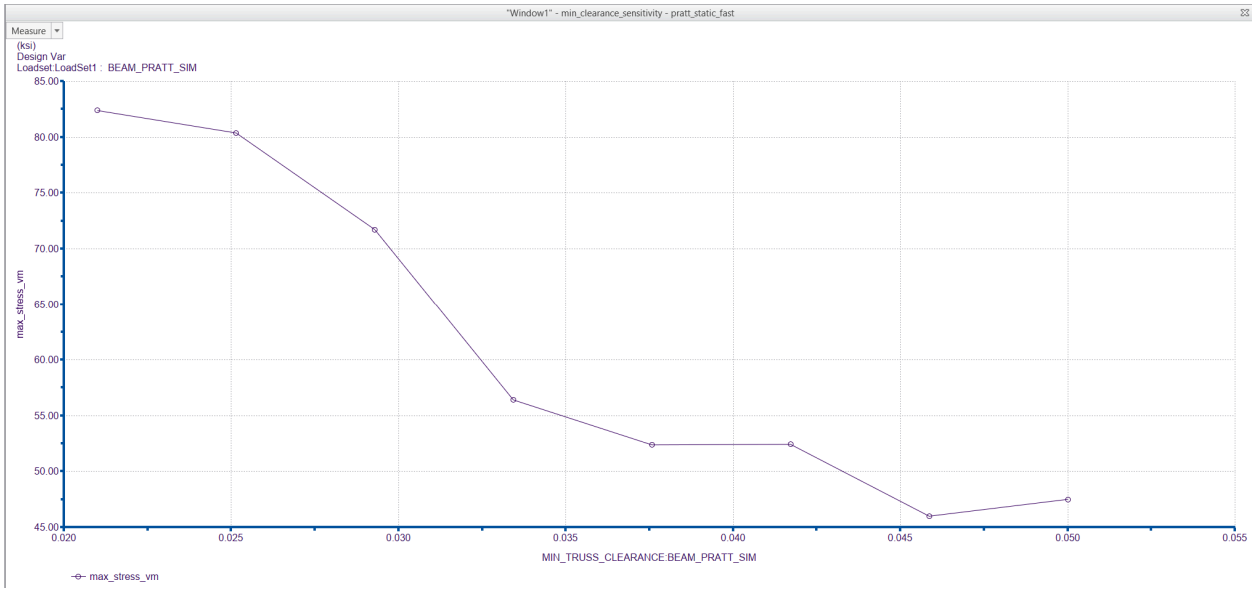


*Figure VI.A.4 Maximum stress in beam vs minimum distance from truss to edge of beam*

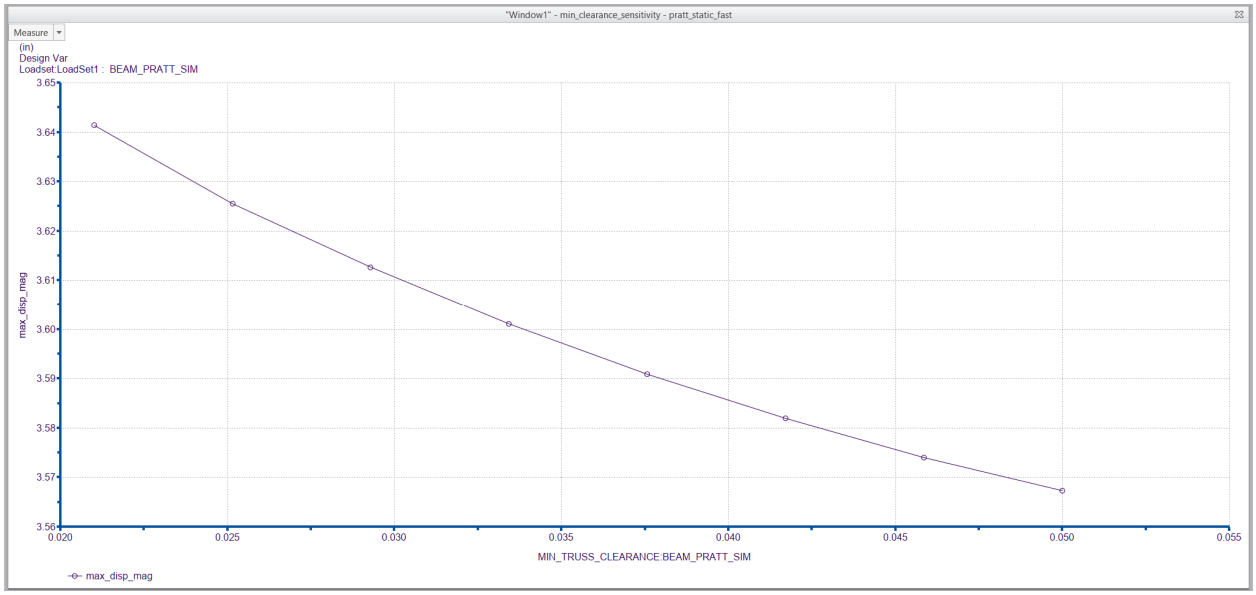


*Figure VI.A.5 Maximum displacement in beam vs minimum distance from truss to edge of beam*

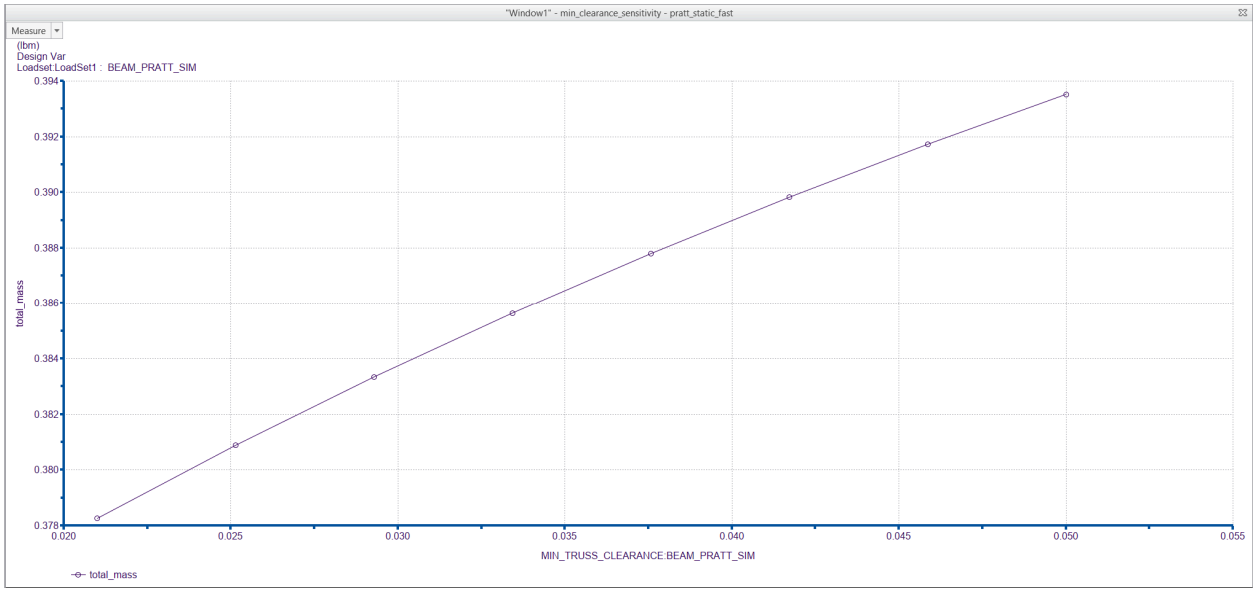


*Figure VI.A.6 Mass of beam vs minimum distance from truss to edge of beam*

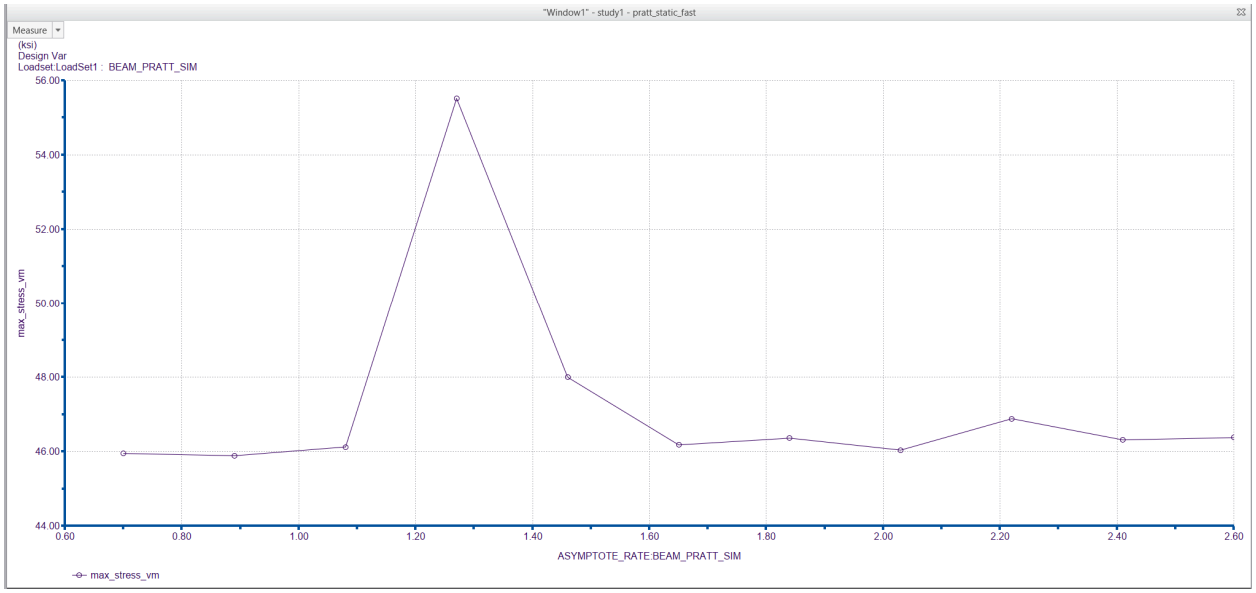


*Figure VI.A.7 Maximum stress in beam vs asymptote rate*

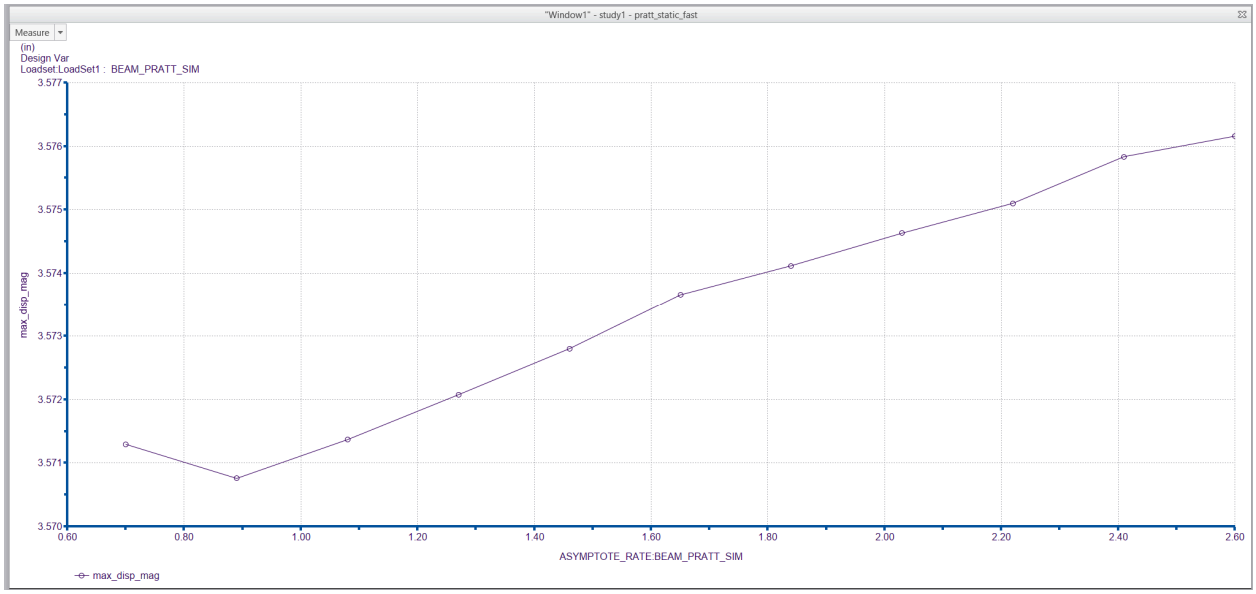


*Figure VI.A.8 Maximum displacement in beam vs asymptote rate*

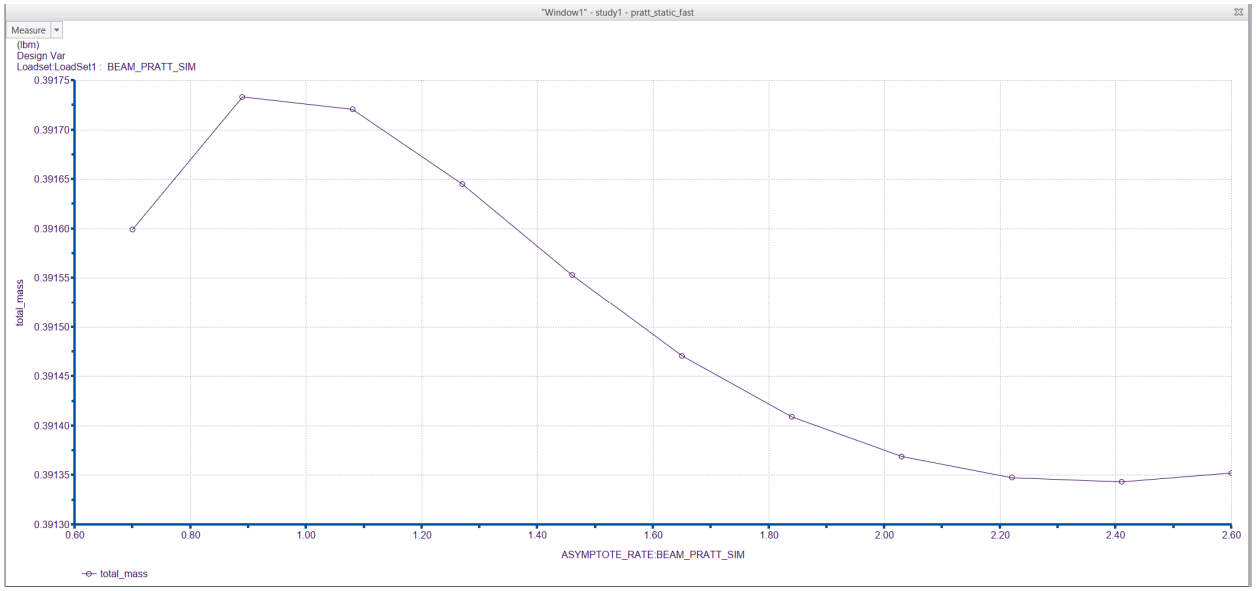


*Figure VI.A.9 Mass of beam vs asymptote rate*

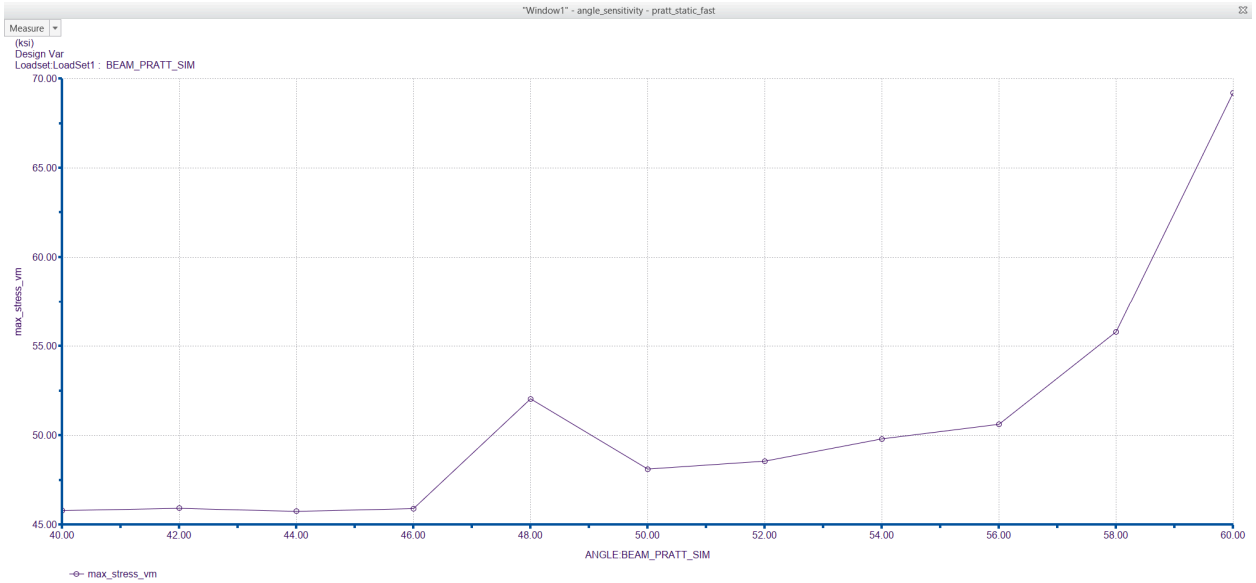


*Figure VI.A.10 Maximum stress in beam vs truss angle*

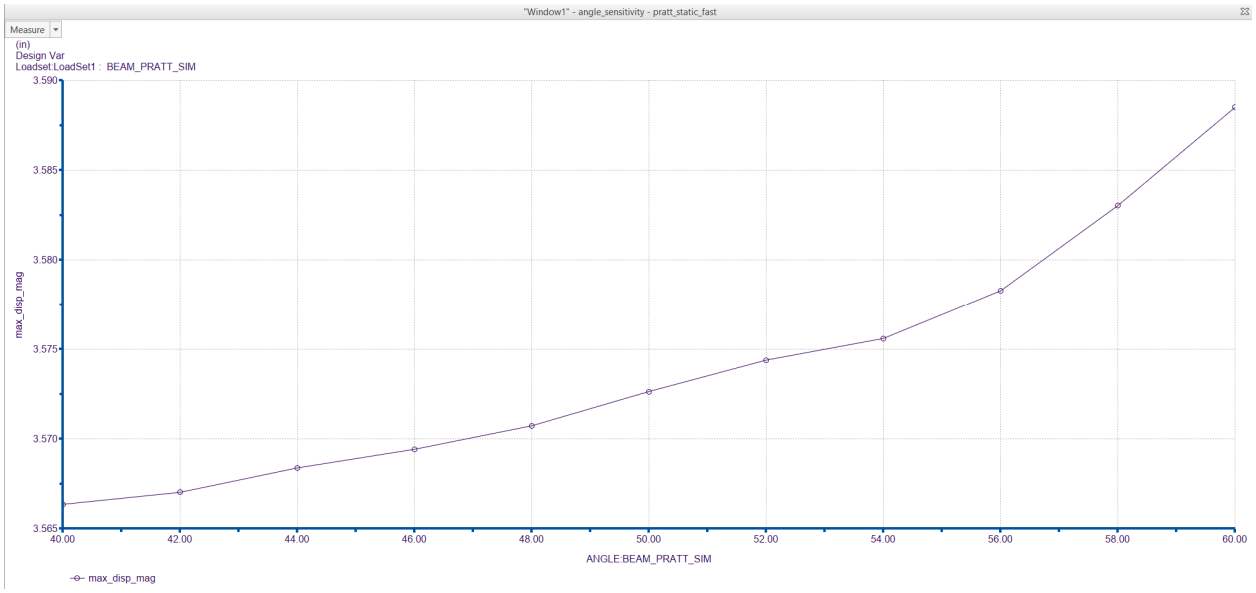


*Figure VI.A.11 Maximum displacement in beam vs truss angle*

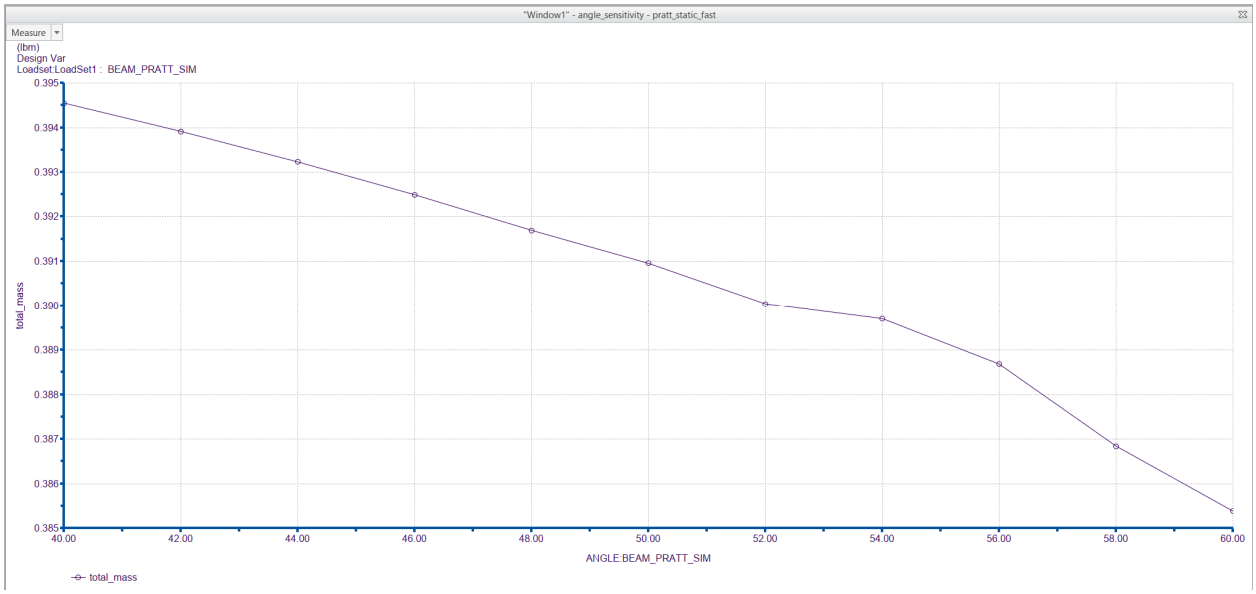


*Figure VI.A.12 Mass of beam vs truss angle*

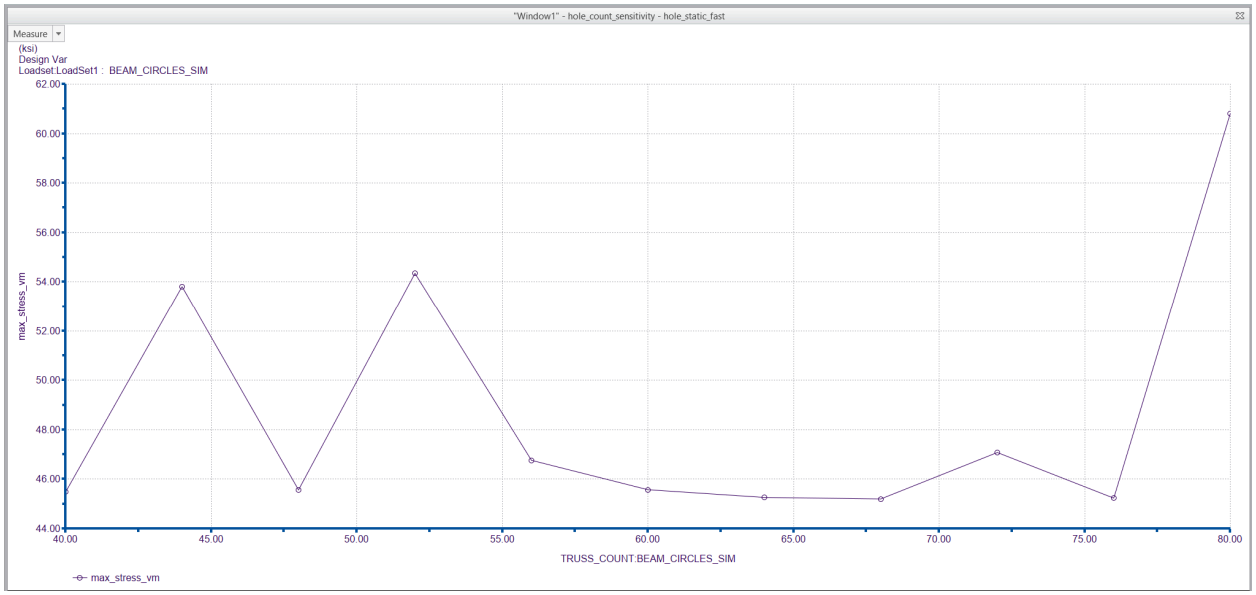


*Figure VI.A.13 Maximum stress in beam vs hole count*

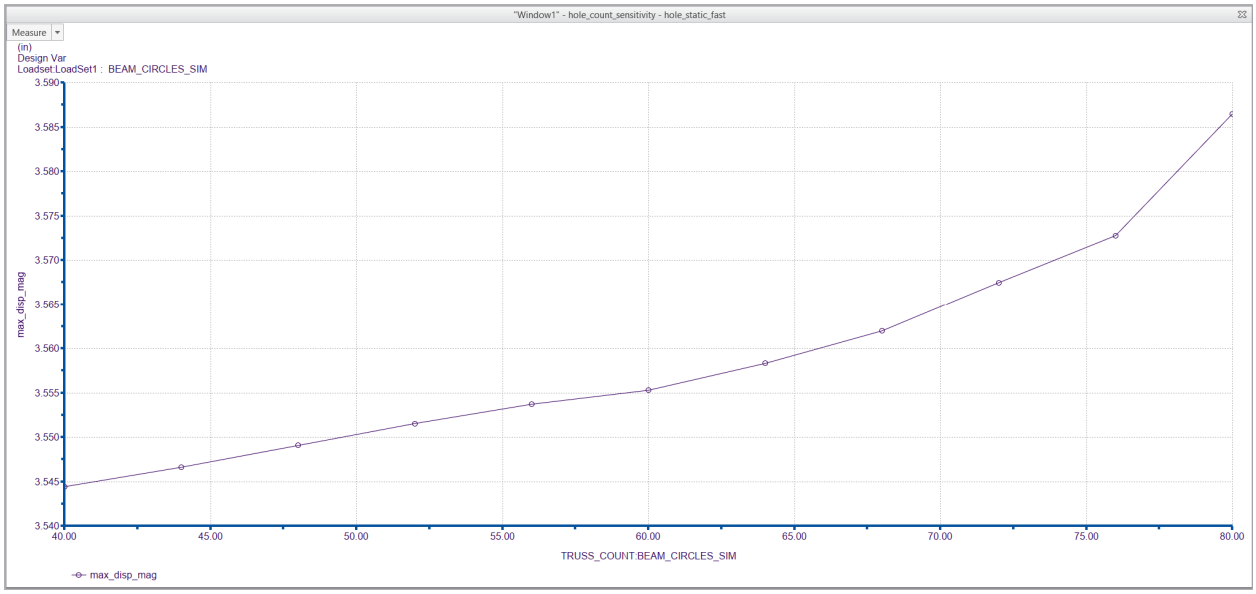


*Figure VI.A.14 Maximum displacement in beam vs hole count*

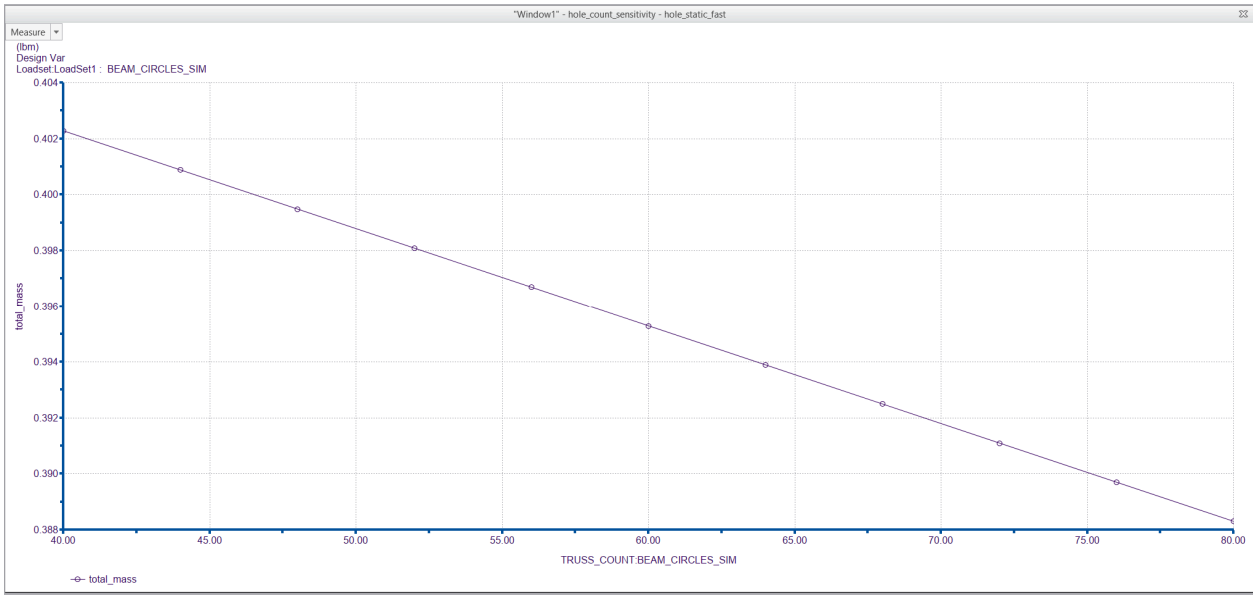


*Figure VI.A.15 Mass of beam vs hole count*

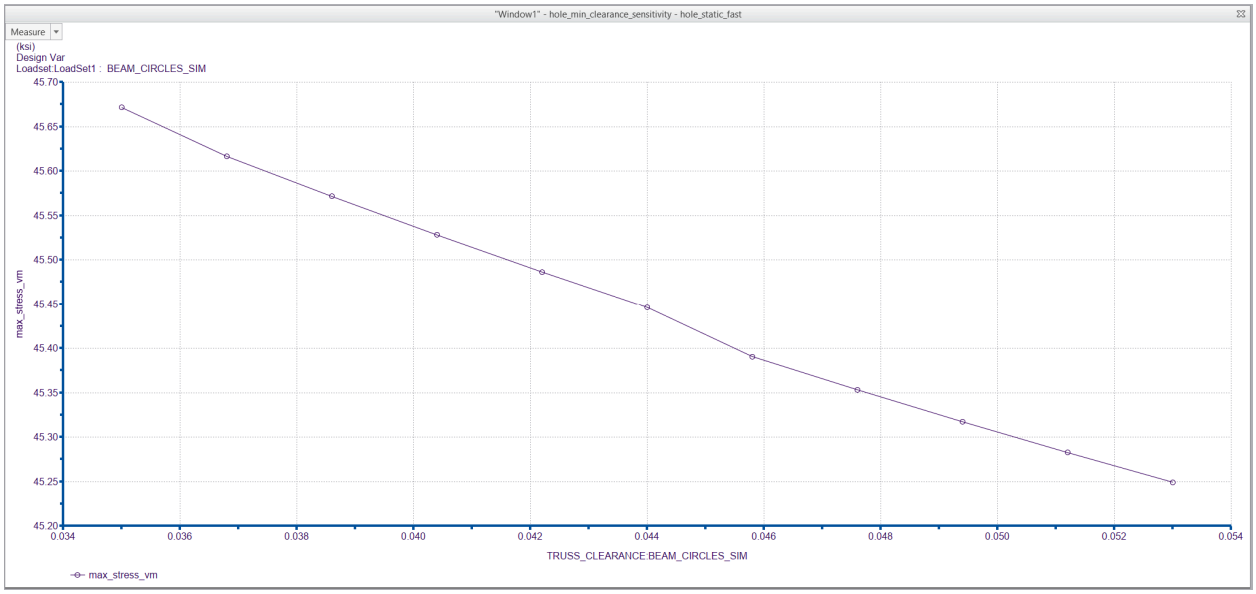


*Figure VI.A.16 Maximum stress in beam vs minimum clearance of holes*

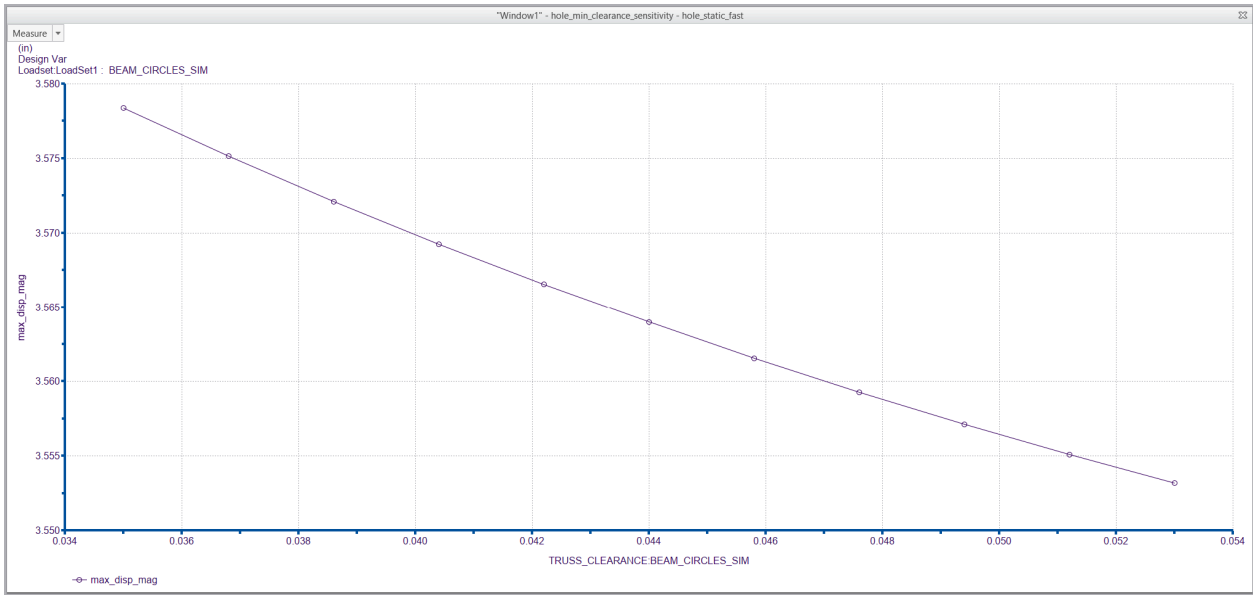


*Figure VI.A.17 Maximum displacement in beam vs minimum clearance of holes*

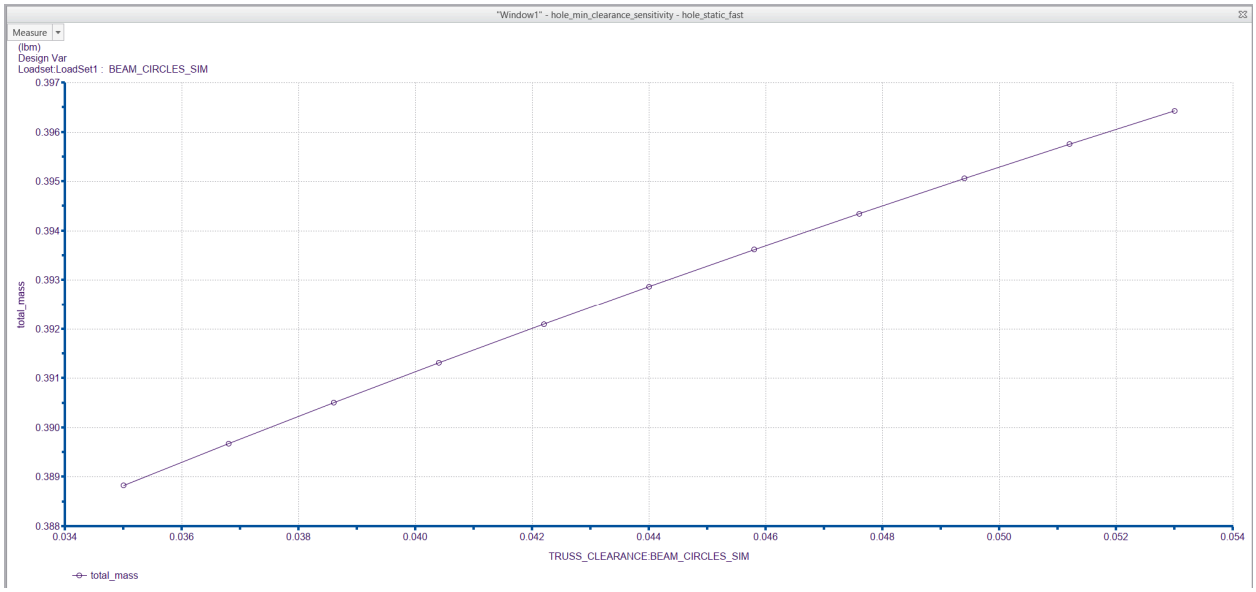


*Figure VI.A.18 Mass of beam vs minimum clearance of holes*

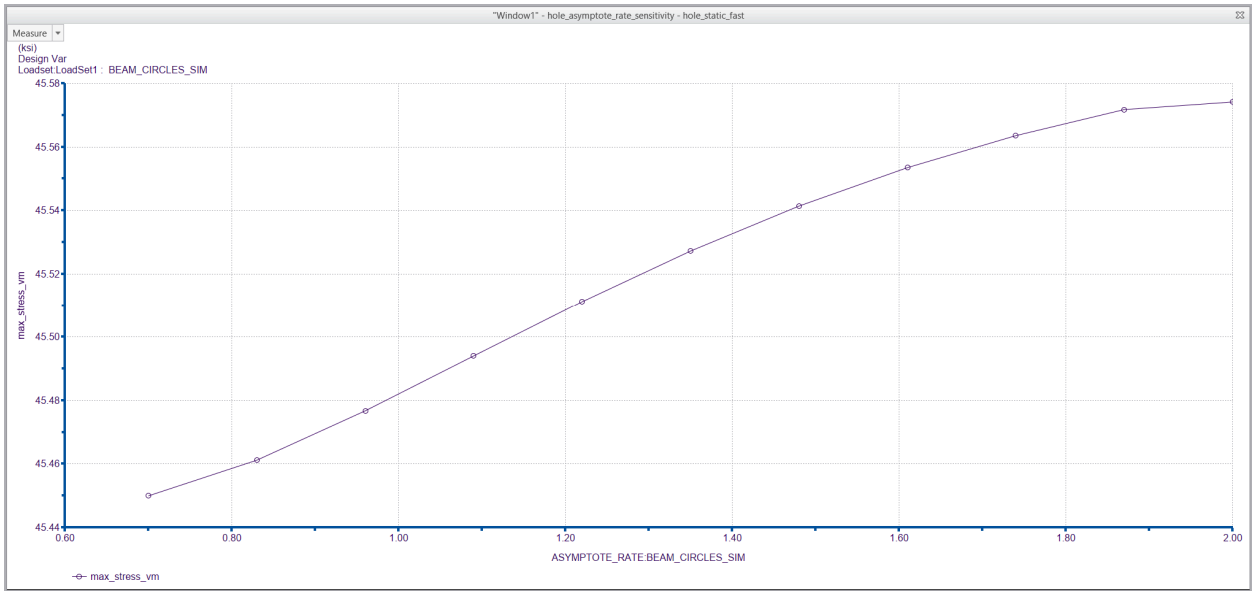


*Figure VI.A.19 Maximum stress in beam vs asymptote rate*

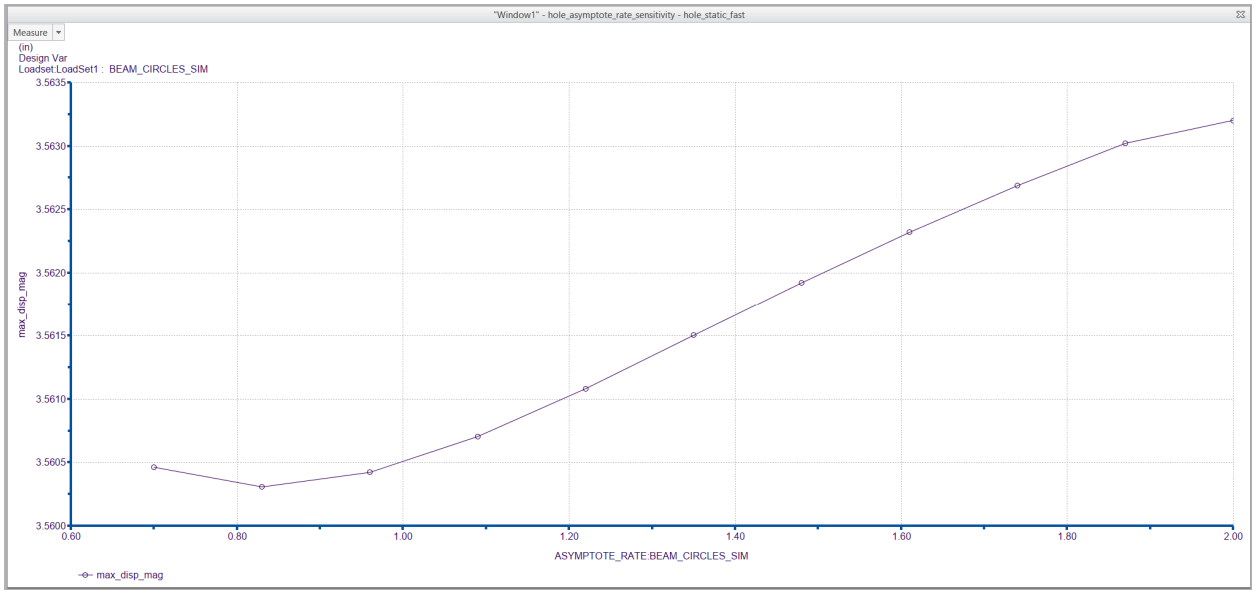


*Figure VI.A.20 Maximum displacement in beam vs asymptote rate*

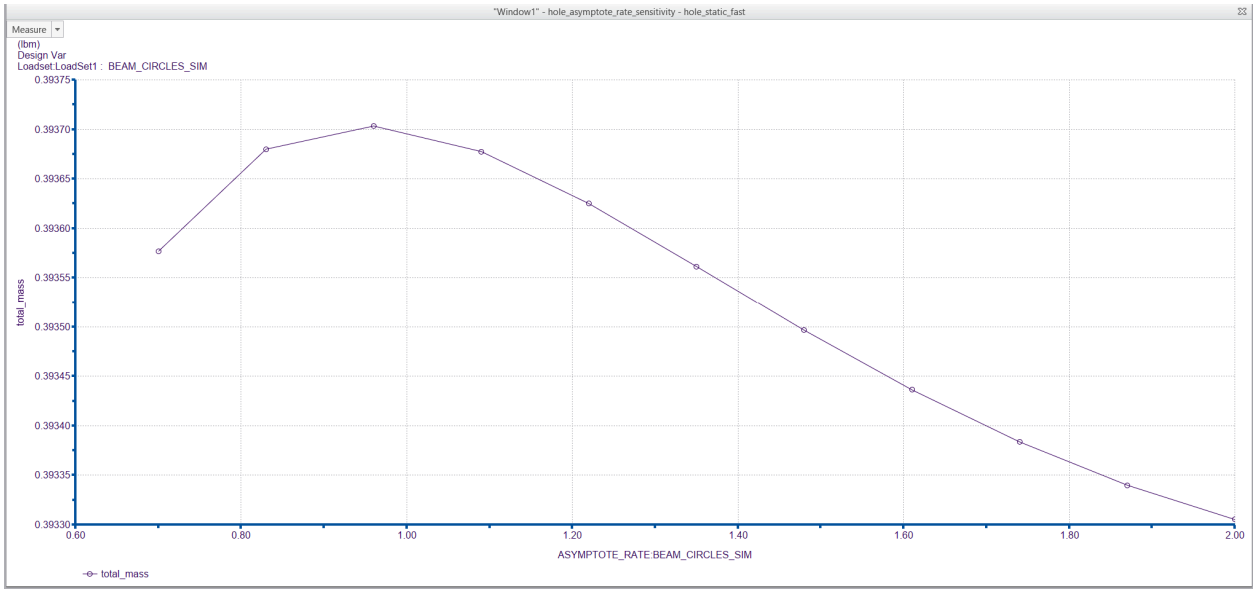


*Figure VI.A.21 Mass of beam vs minimum asymptote rate*

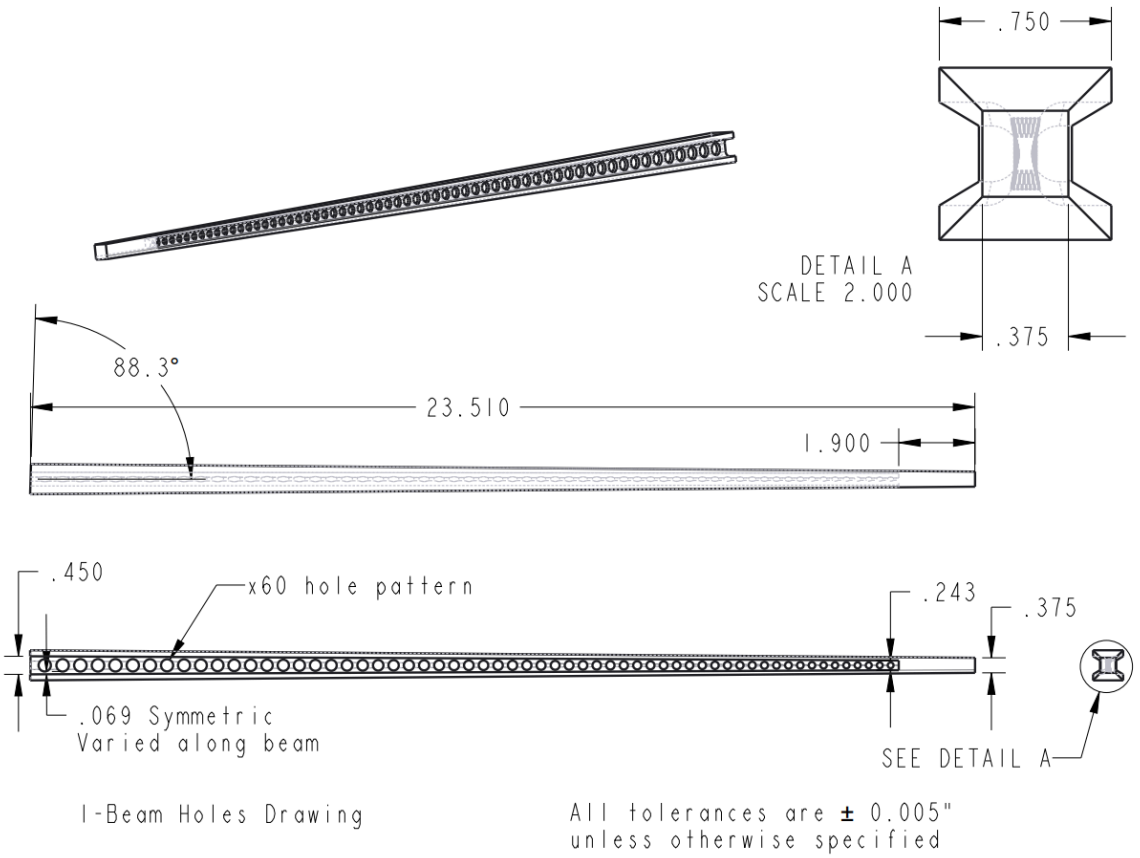


*Figure VI.A.22 Final beam drawing*

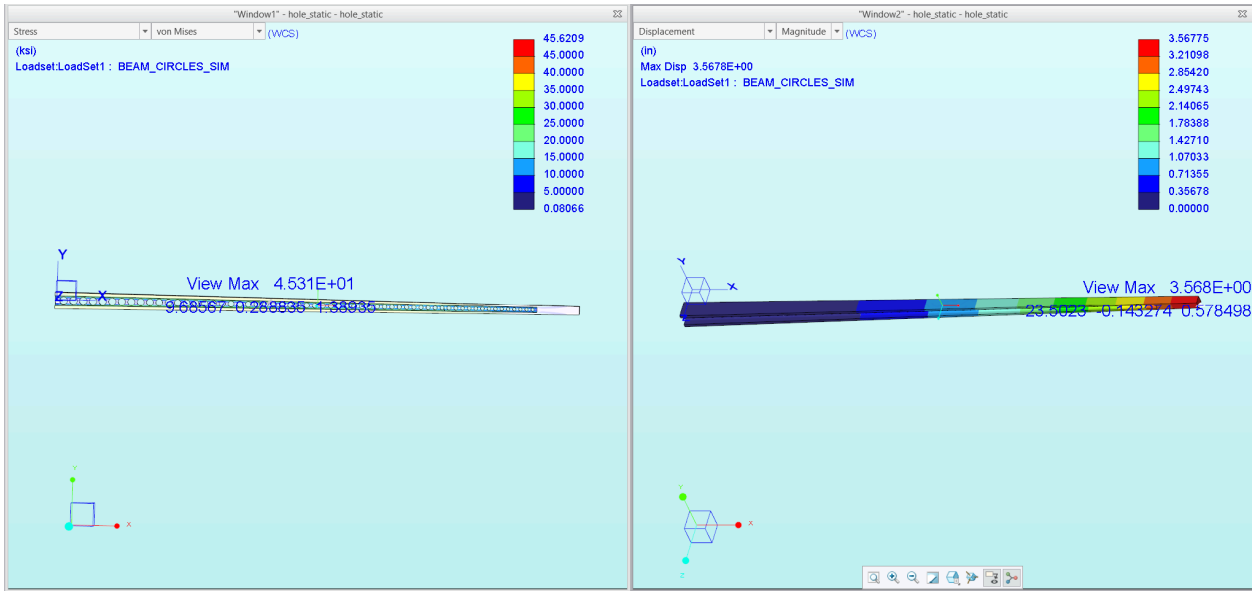


*Figure VI.A.23 Beam with holes final stress and displacement analysis*

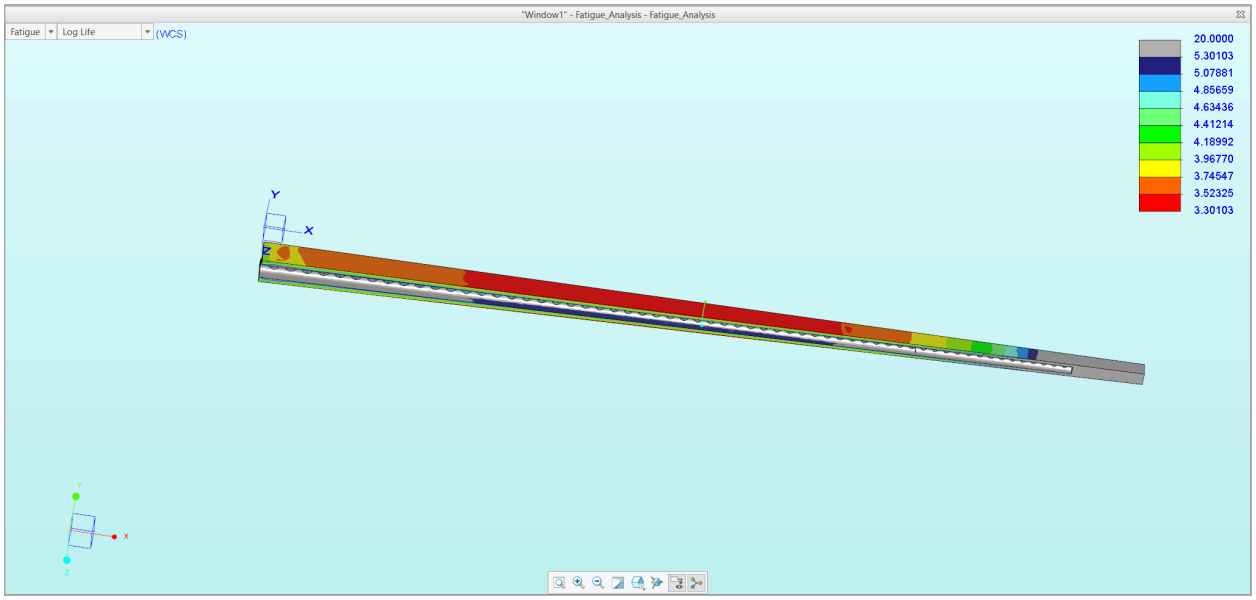


*Figure VI.A.24 Beam fatigue analysis*

```
Number of Modes: 4

    Mode   Frequency (Hz)
    ----   --------------
       1    4.629541e+01
       2    6.599888e+01
       3    2.029831e+02
       4    2.814420e+02
```

*Figure VI.A.25 Beam modal analysis*

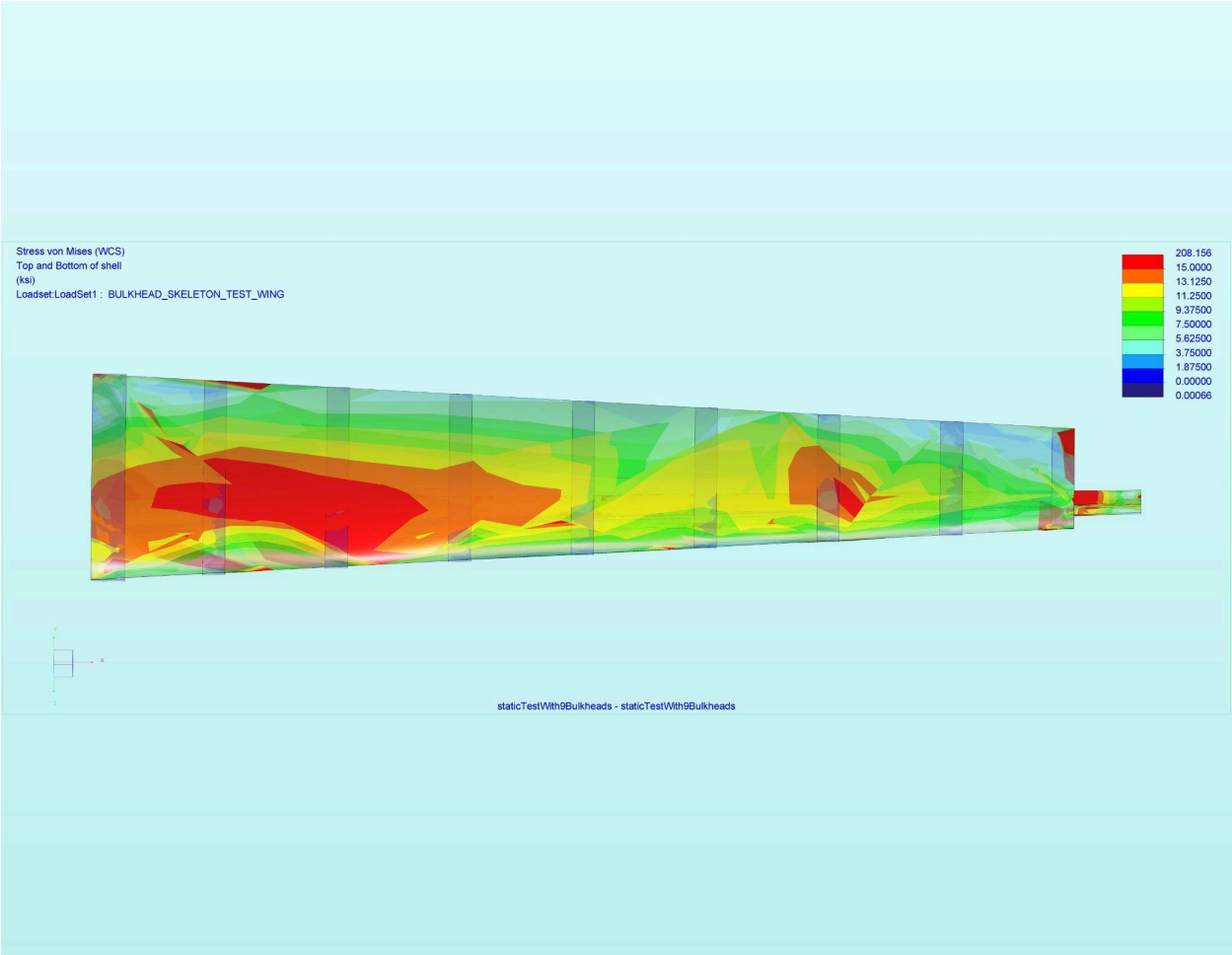


*Figure VI.B.1: Static test with nine solid bulkheads, load of 100 lbf. Skin thickness was 0.030 inches.*

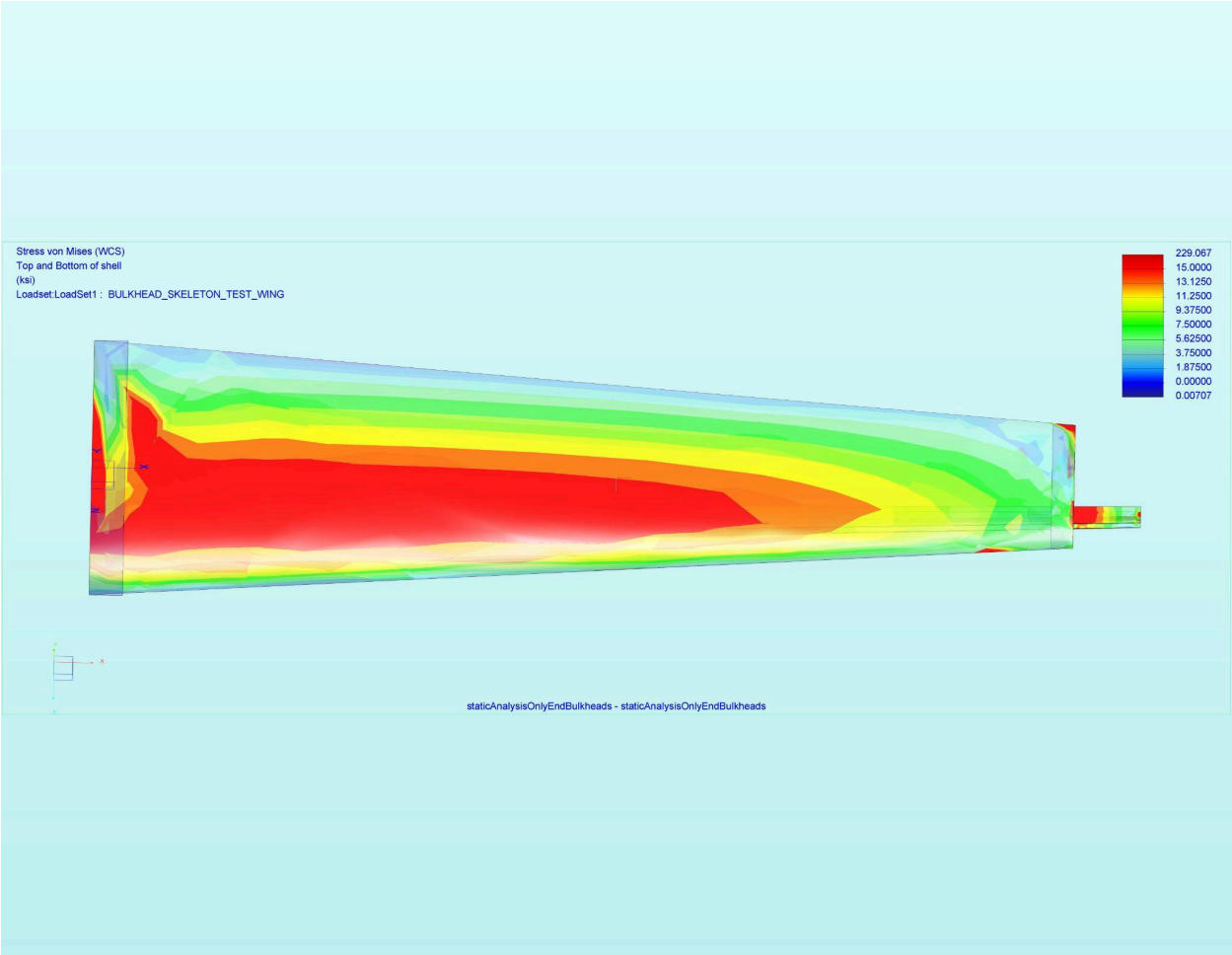


*Figure VI.B.2: Static test with only end bulkheads, load of 100 lbf. Skin thickness was 0.030 inches.*

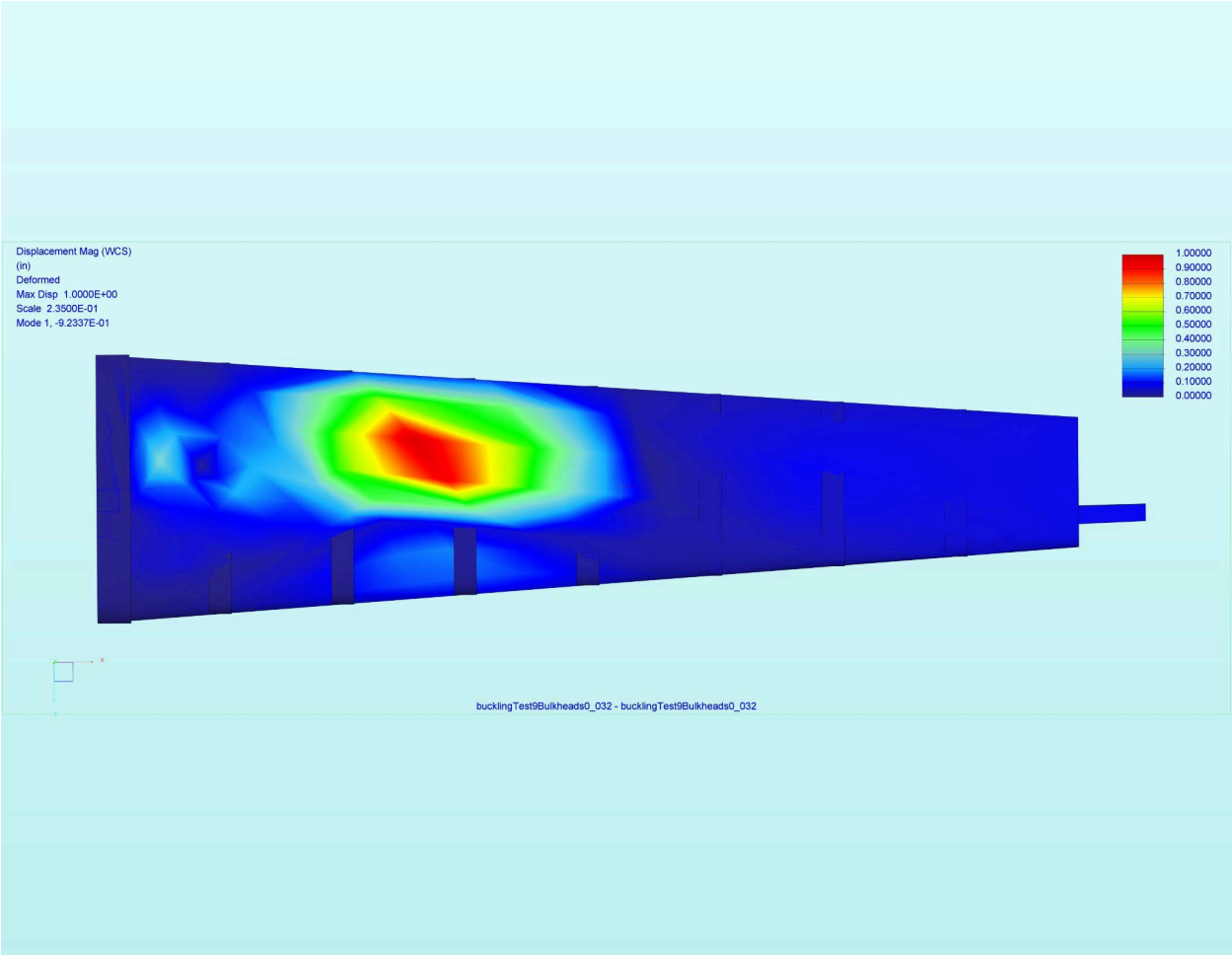


*Figure VI.B.3: Buckling test with nine solid bulkheads, load of 100 lbf. Skin thickness was 0.032 inches. Buckling factors were -0.92, -0.94, 0.95, -0.98, and 1.03 for modes 1, 2, 3, 4, and 5 respectively.*

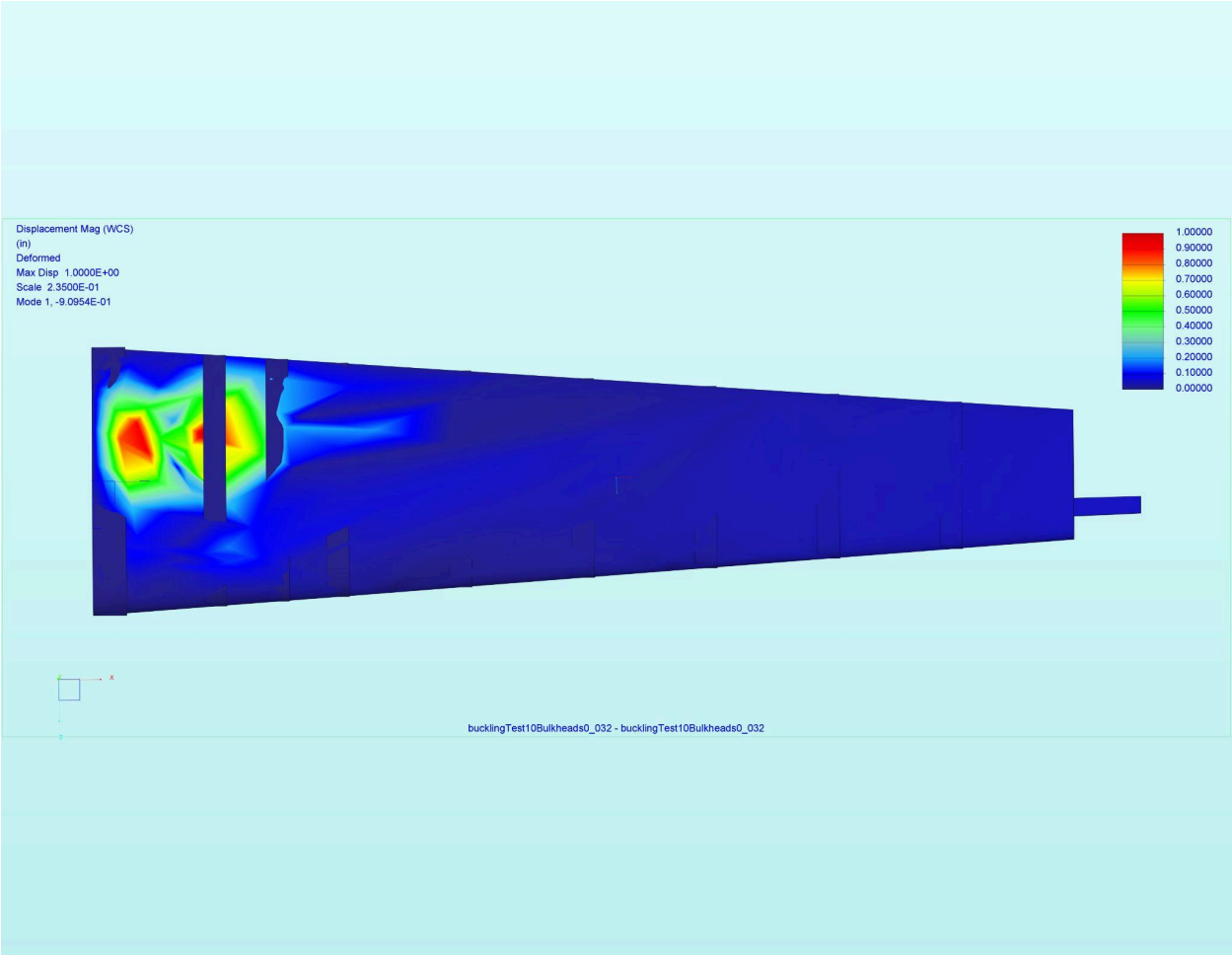


*Figure VI.B.4: Buckling test with ten solid bulkheads, load of 100 lbf. Skin thickness was 0.032 inches. Buckling factors were -0.91, 0.91, -0.98, 1.00, -1.13 for modes 1, 2, 3, 4 and 5 respectively.*

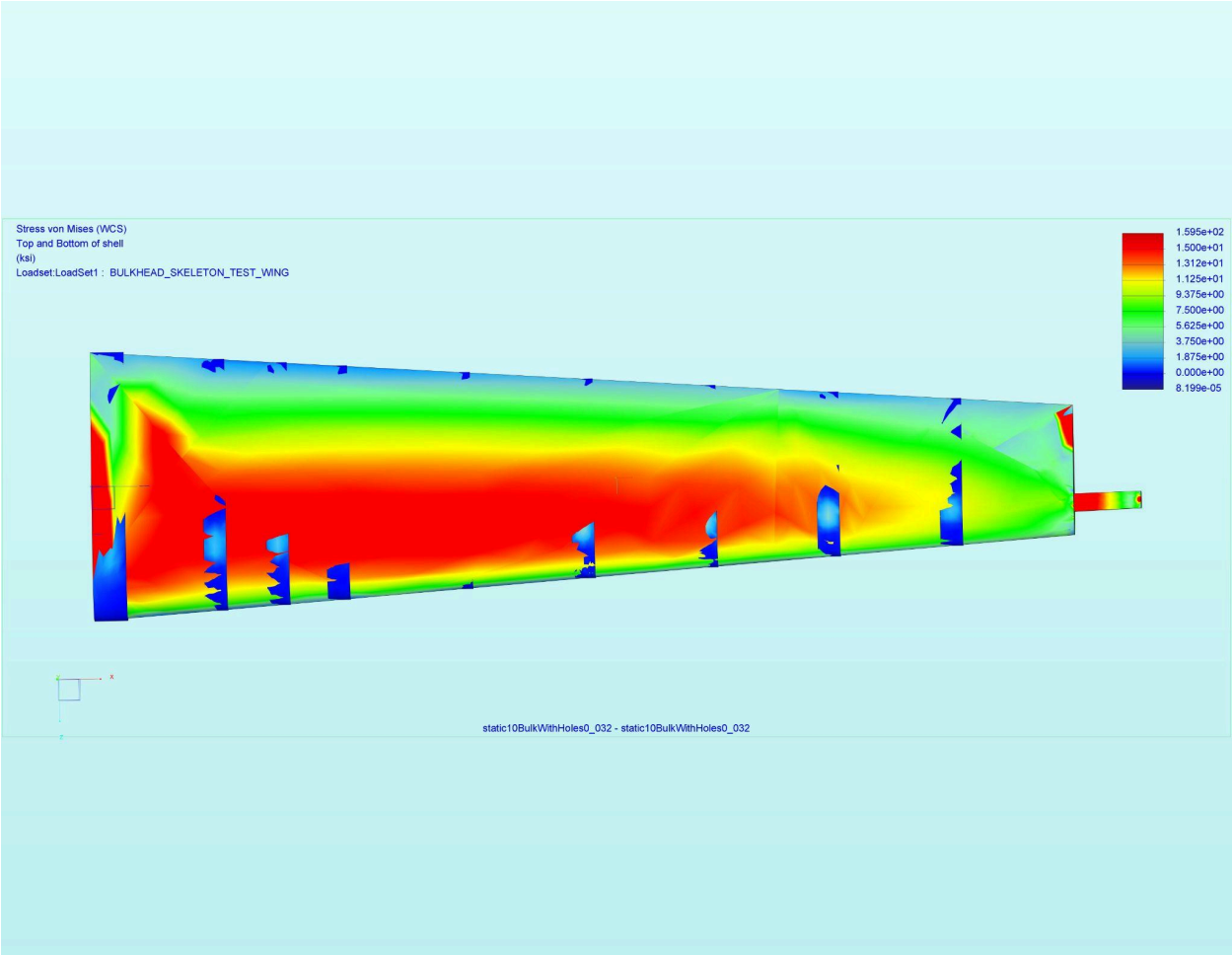


*Figure VI.B.5: Static test with 10 bulkheads with holes, load of 100 lbf. Skin thickness was 0.032 inches.*

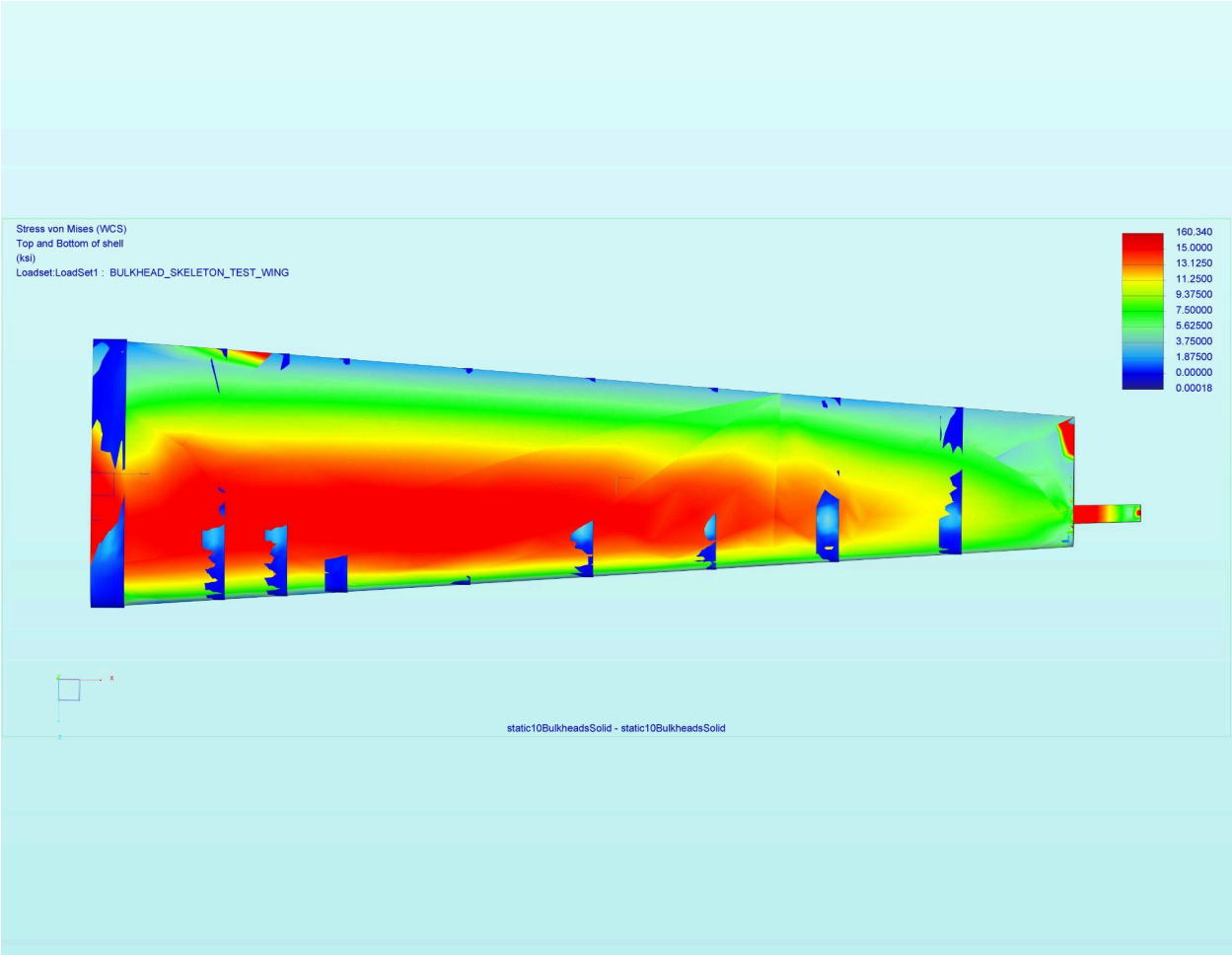


*Figure VI.B.6: Static test with 10 solid bulkheads, load of 100 lbf. Skin thickness was 0.032 inches.*

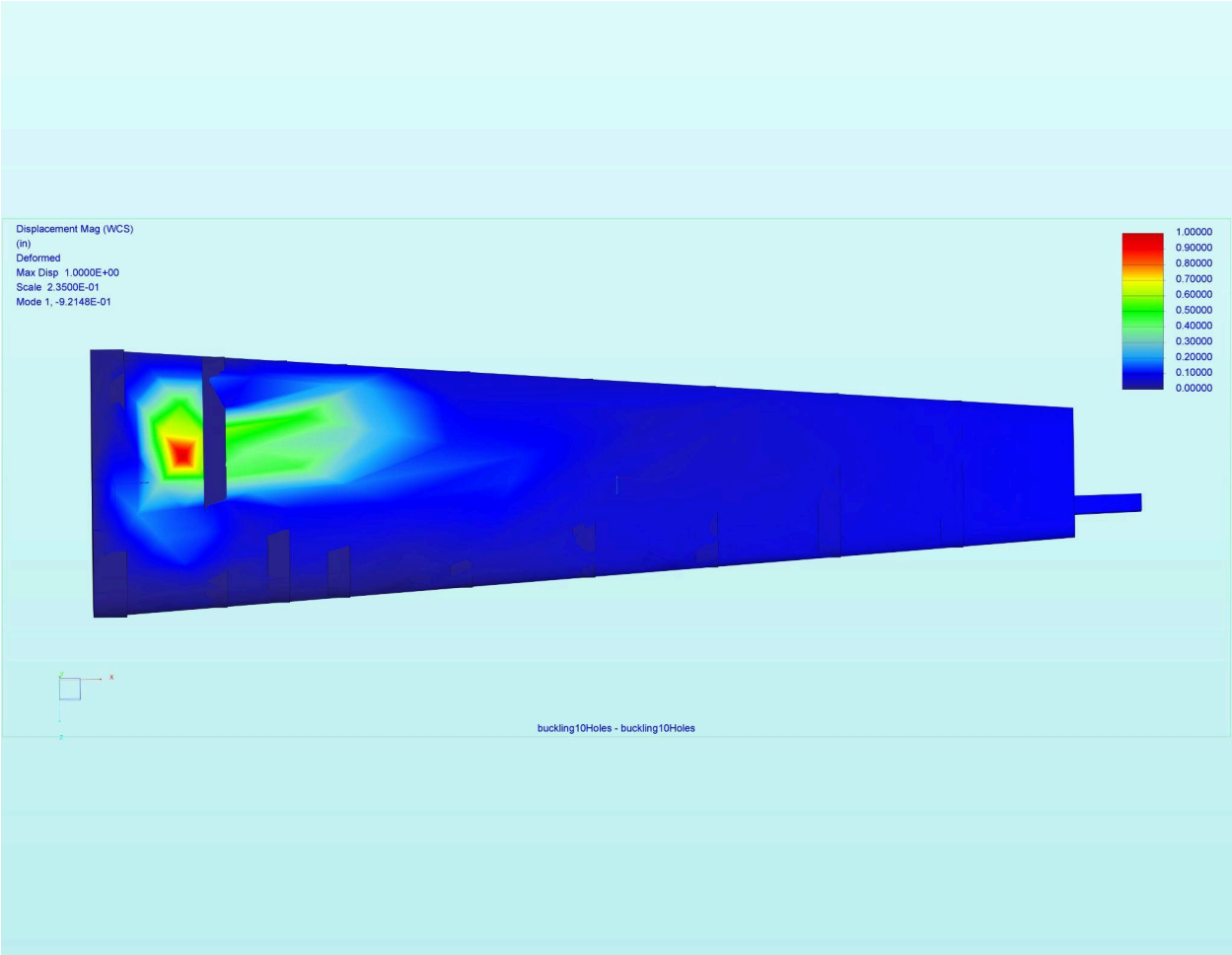


*Figure VI.B.7: Buckling test with 10 bulkheads with holes, load of 100 lbf. Skin thickness was 0.032 inches. Buckling factors were -0.92, -0.97, 0.98, 1.00, 1.04 for modes 1, 2, 3, 4, and 5 respectively.*

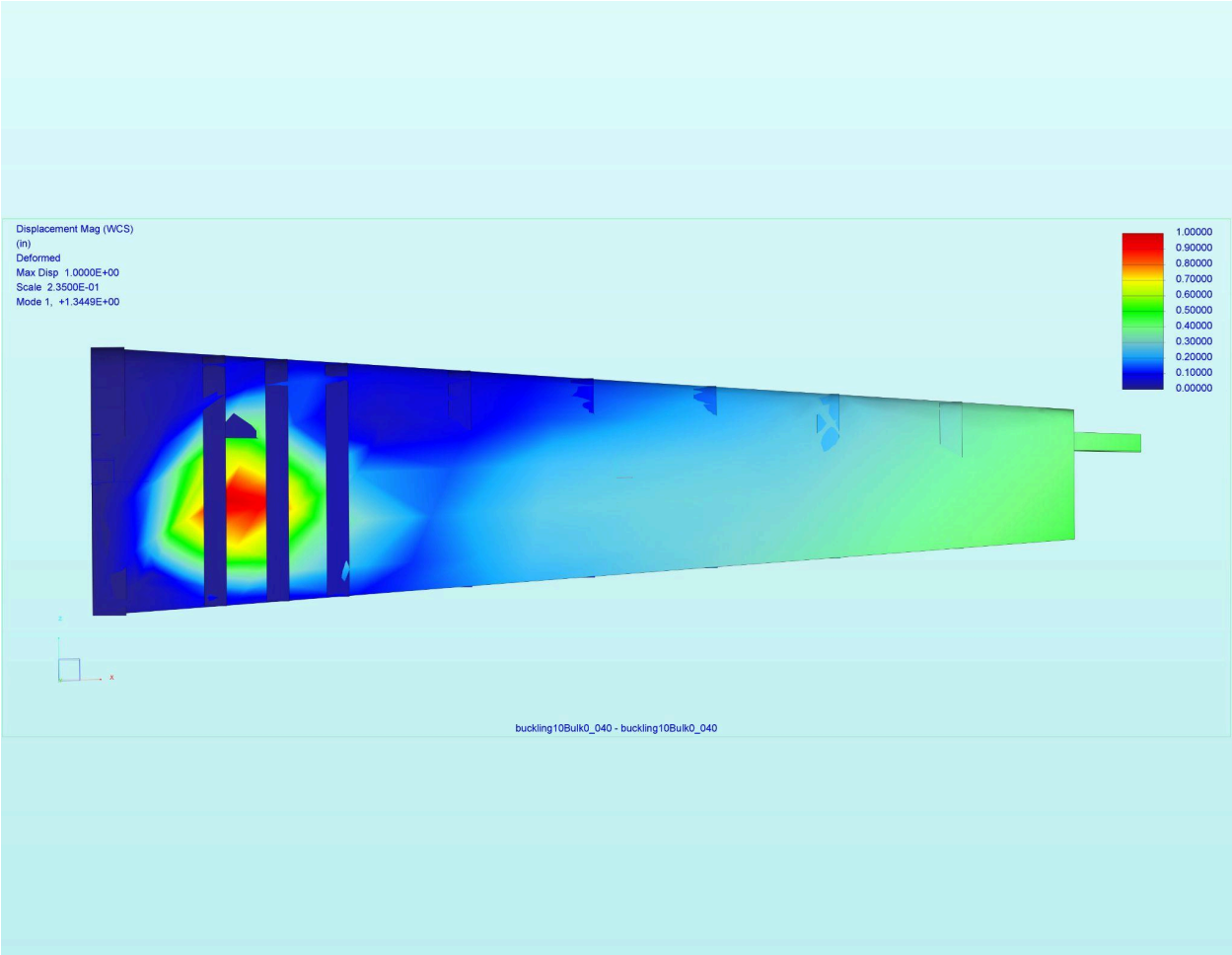


*Figure VI.B.8: Buckling test with 10 solid bulkheads, load of 100 lbf. Skin thickness was 0.040 inches. Buckling factors were 1.34, -1.38, -1.46, 1.51, 1.72 for modes 1, 2, 3, 4, and 5 respectively.*

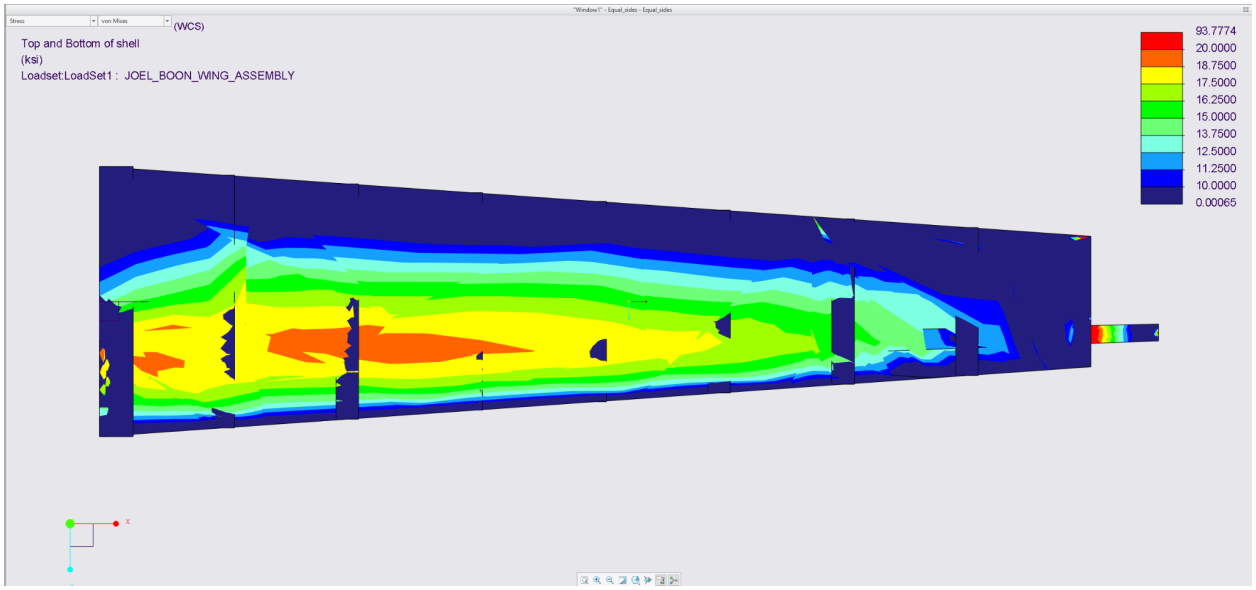


*Figure VI.C.1: stress analysis of skin for 0.025 thickness, 6061 both sides*

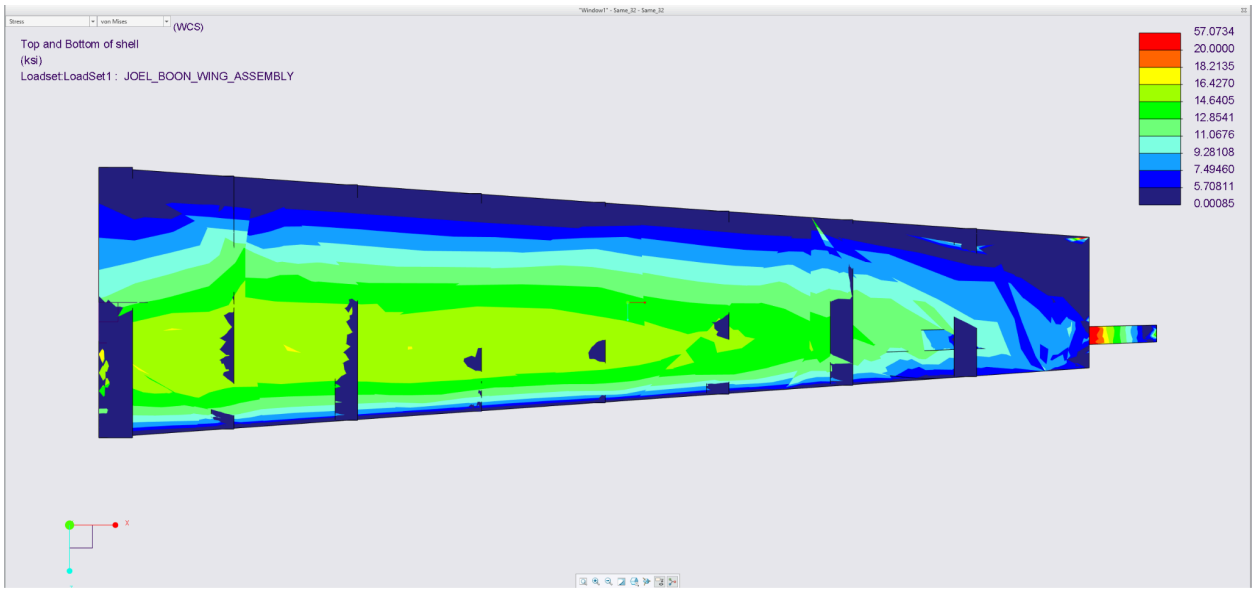


*Figure VI.C.2: stress analysis of skin for 0.032 thickness, 6061 both sides*

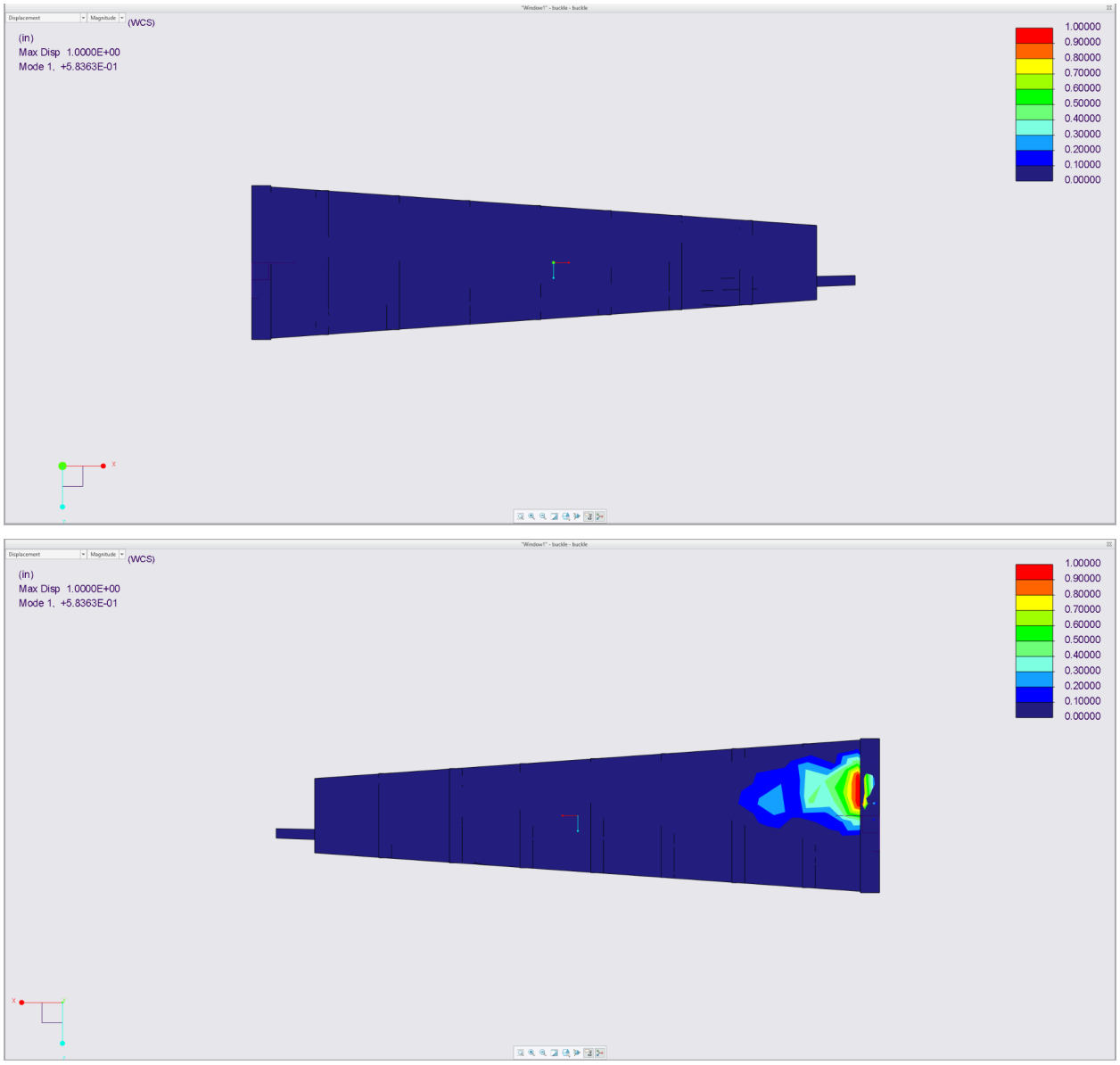


*Figure VI.C.2.5: buckling analysis demonstrating general trend of the bottom skin to buckle under load, while the top side does not. Buckling factor of 0.5836, showing strong tendency.*

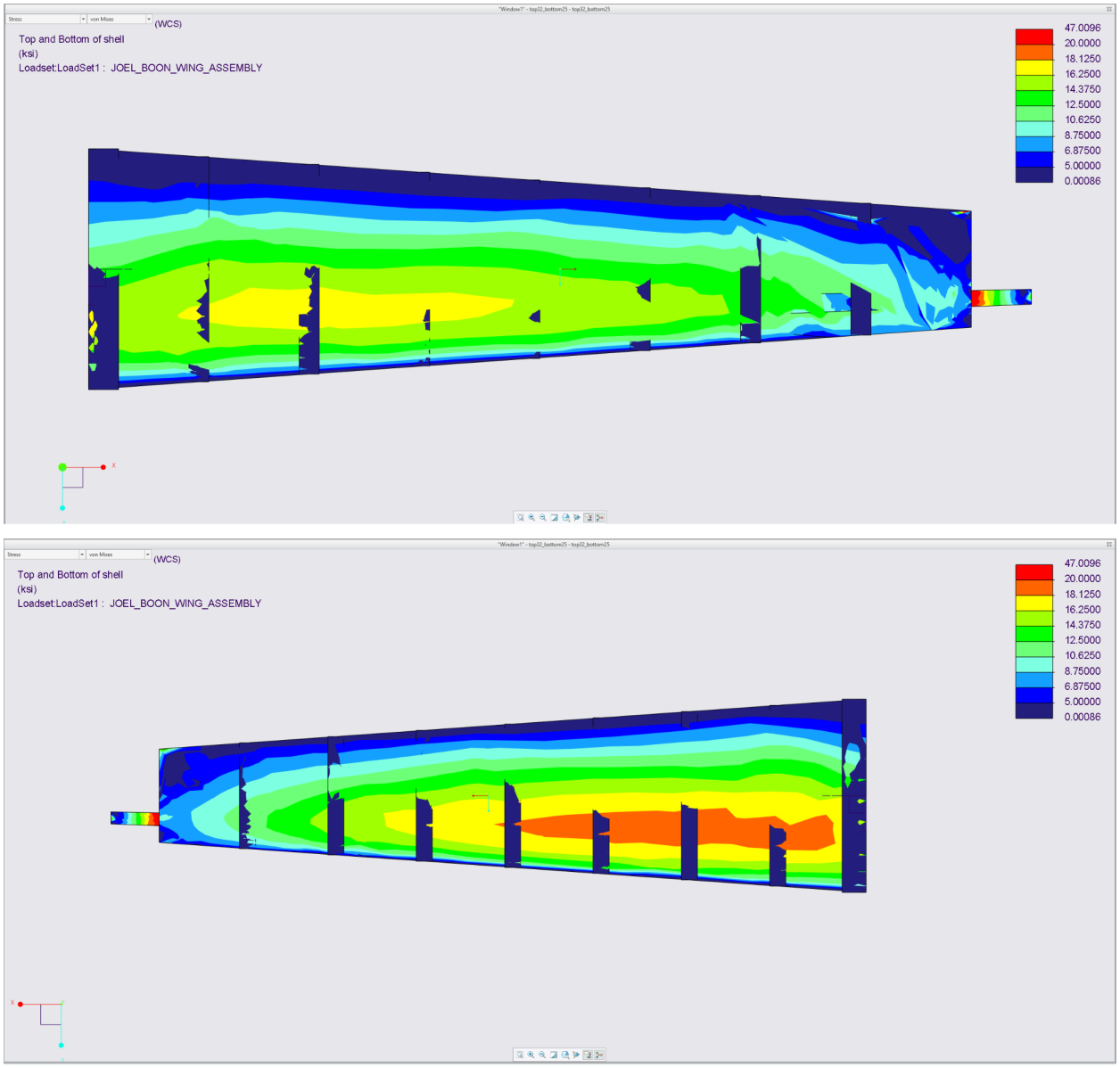


*Figure VI.C.3: stress analysis of skin for 0.032 thickness on top, 0.025 on bottom, 6061*

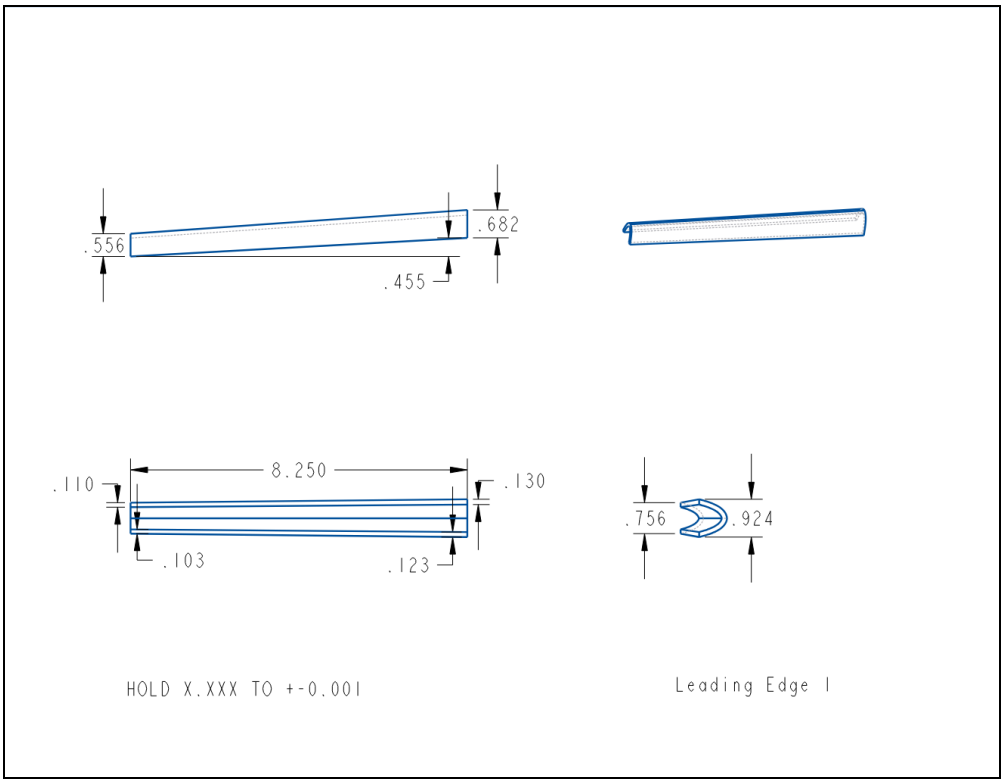


*Figure VI.C.5.1*

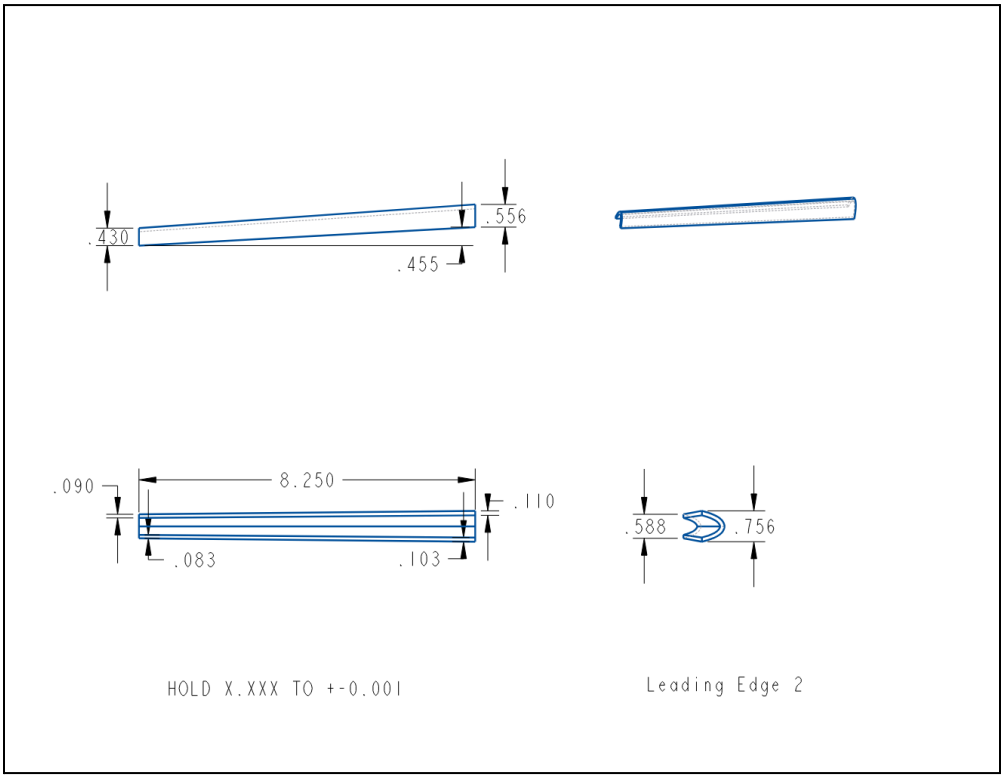


*Figure VI.C.5.2*

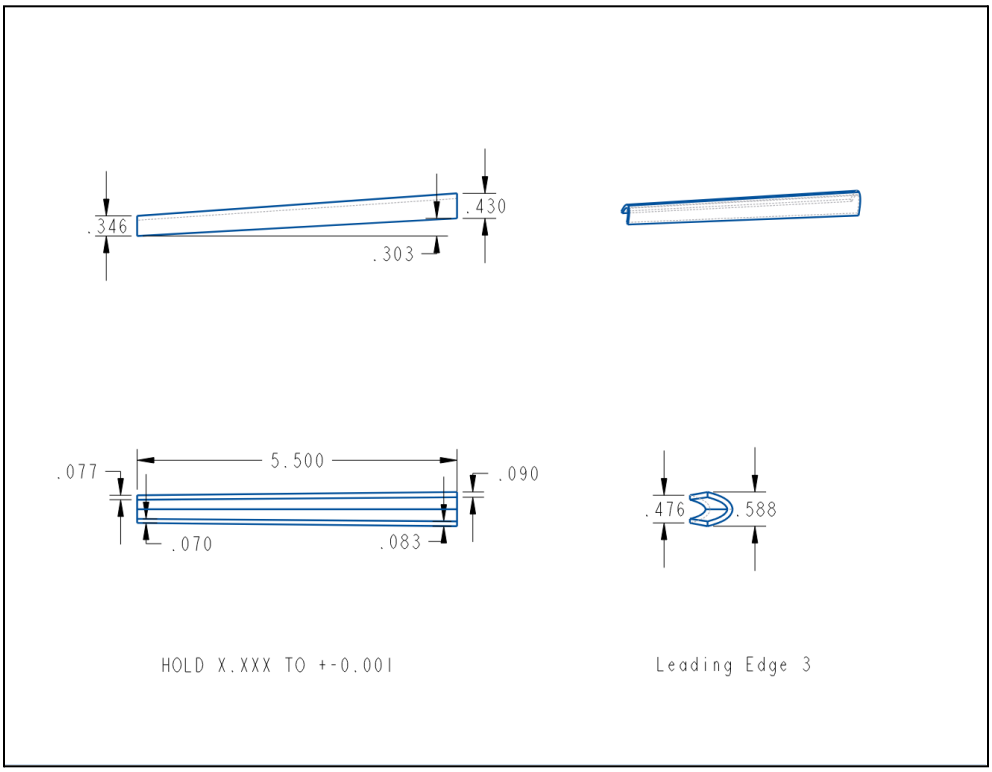


*Figure VI.C.5.3*

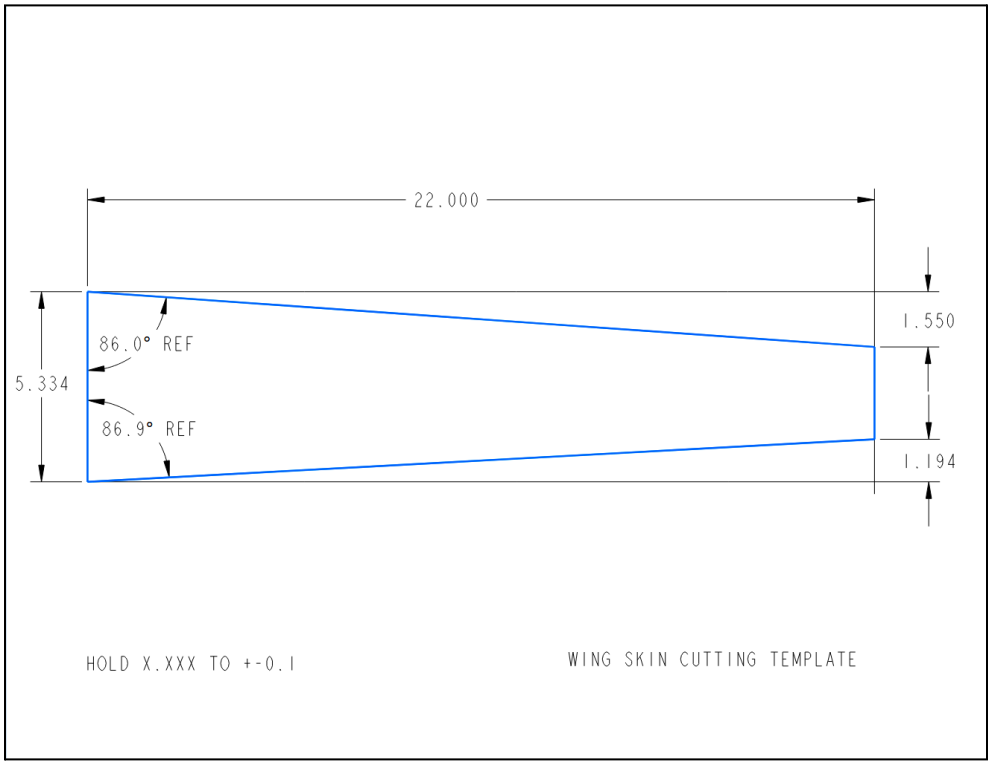


*Figure VI.C.5.4*

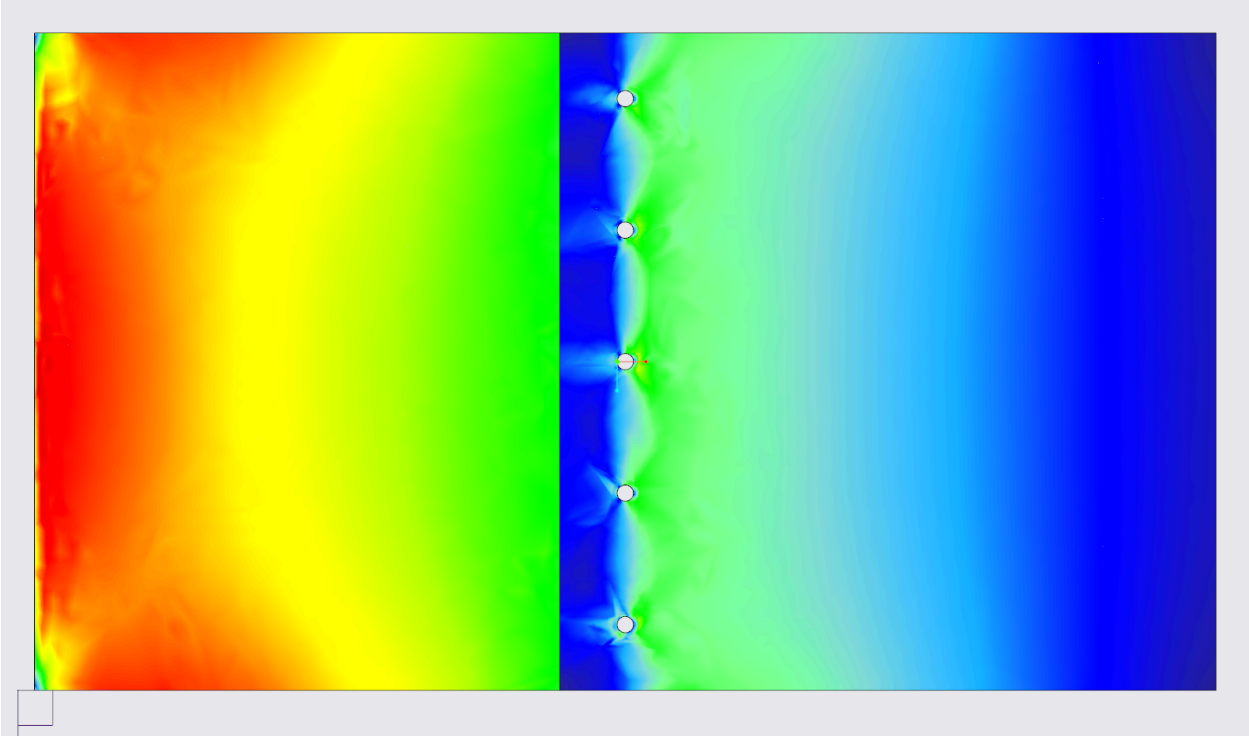

*Figure VI.D.1: 0.5” margin, 1” spacing test results. No major stress concentrations, although some minor ones near the middle.*

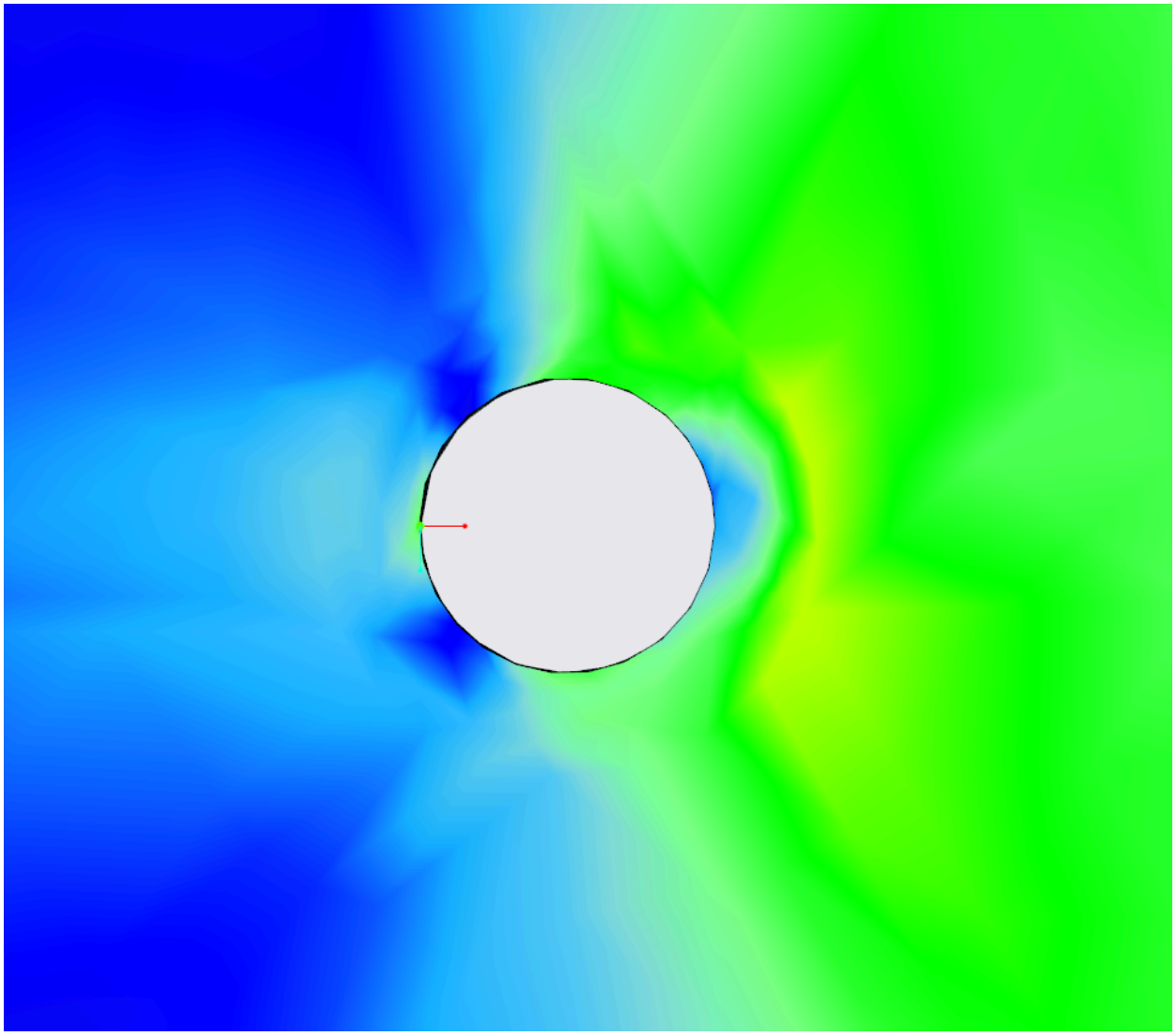

*Figure VI.D.2: Highlighting minor stress concentration (~35 ksi) near the middle fastener.*

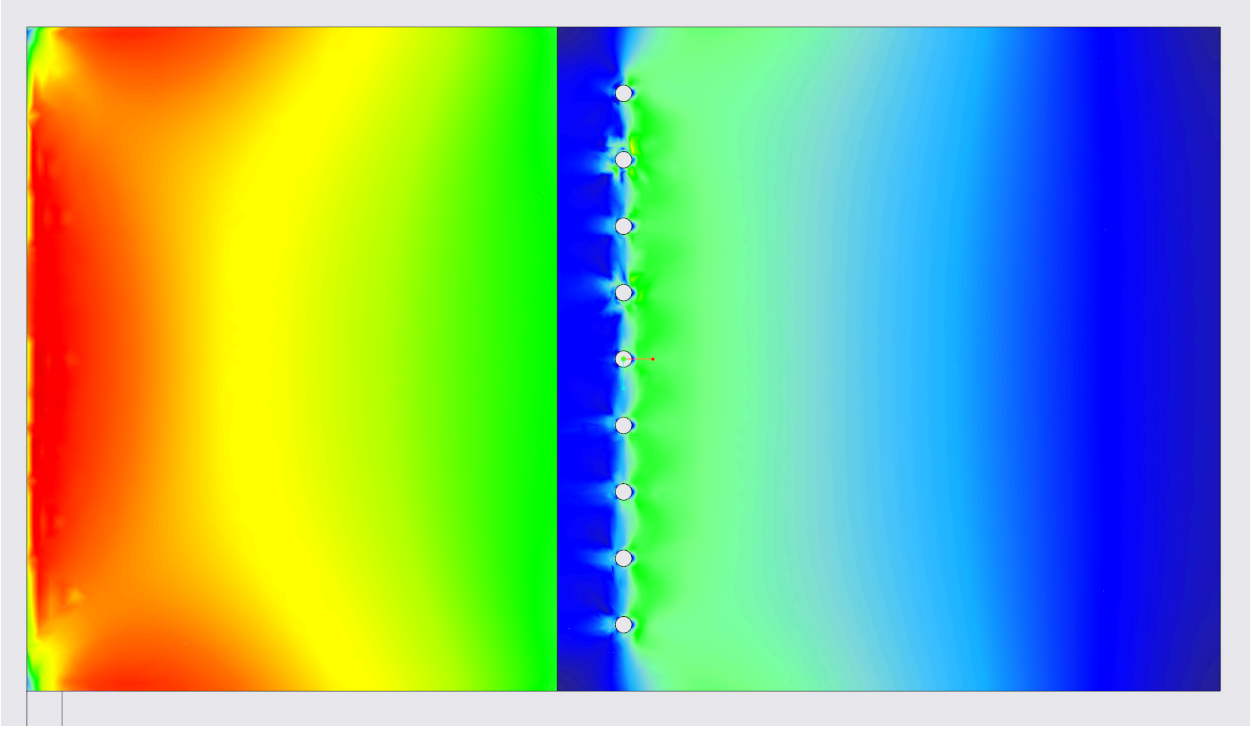

*Figure VI.D.3: Results from the 0.5” margin, 0.5” spacing test. Note the lack of the previous stress concentration near the middle fastener.*

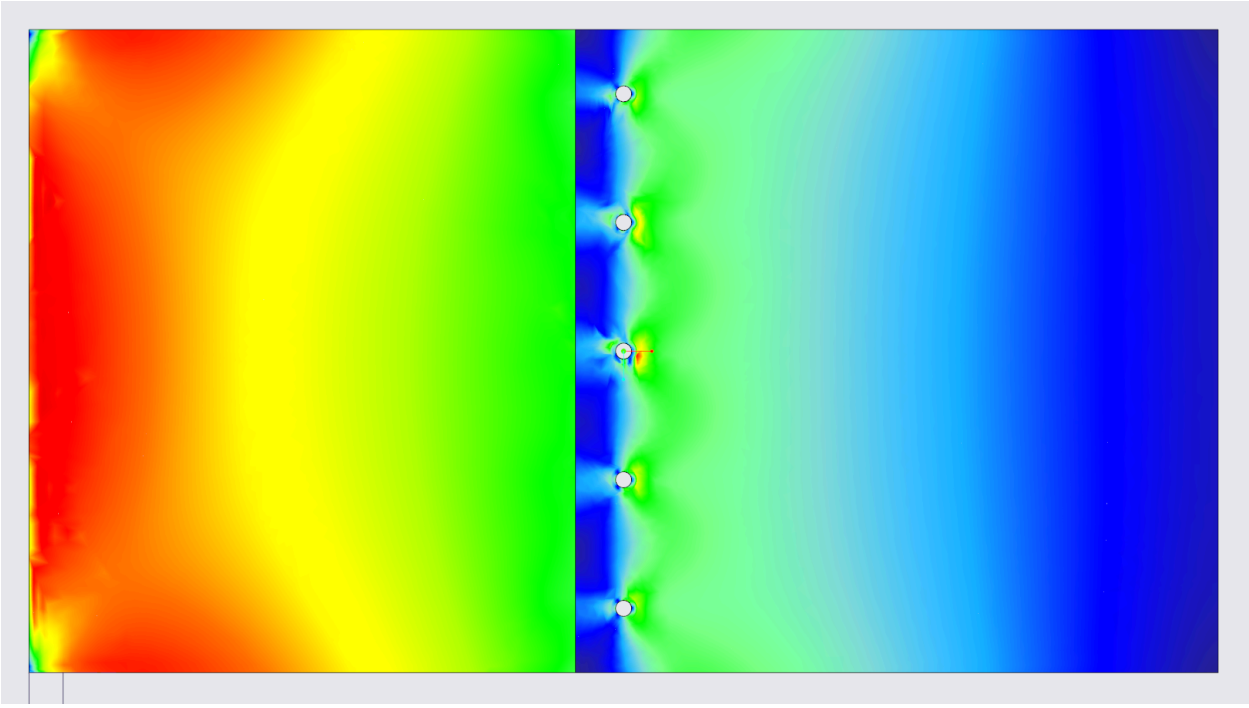

*Figure VI.D.4: Results from the 0.375” margin, 1” spacing test. A smaller margin creates a high stress concentration near the central fastener.*



*Figure VI.F.1. Final wing design mounted on the testing rig.*

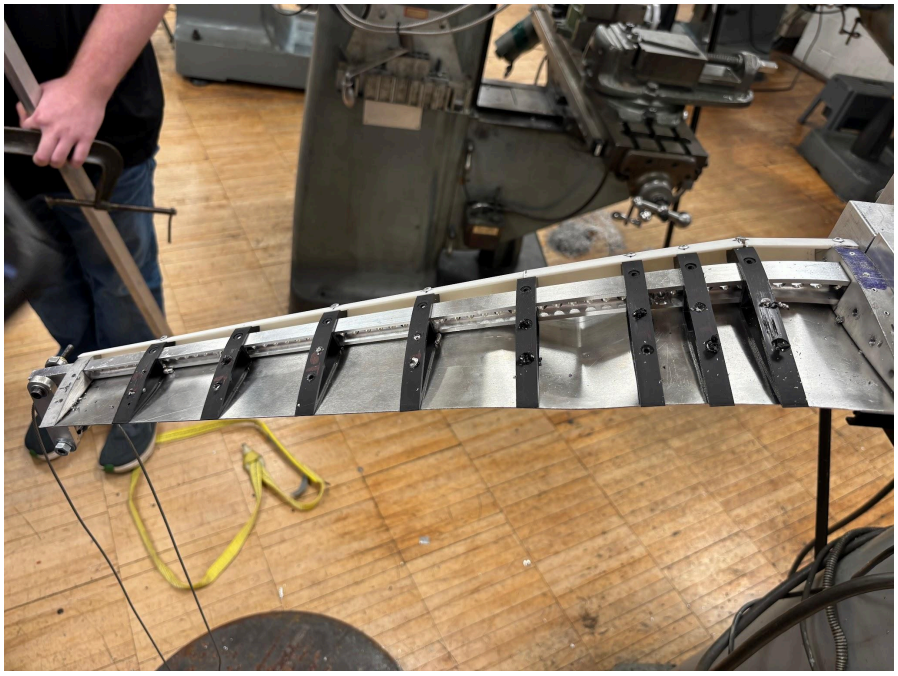

*Figure VI.F.2 Permanently deformed wing post-testing.*